Characterization of the Role of Rac3 in Neuronal Function

Thesis

UNRESTRICTED

Sara Gualdoni

Characterization of the role of Rac3 in neuronal function

Degree of Doctor of Philosophy
in
Molecular and Cellular Biology

June 2008

Sponsoring Establishment:

Vita-Salute San Raffaele University

Milan, Italy

Submission date: 20 May 2008
Date of award: 28 August 2008

Director of Studies:

Prof. Ivan de Curtis

External supervisor:

Dr. Vania M. Braga

CONTENTS

DECLARATION

This thesis has been written by myself and it has never been submitted for a degree or any other qualification at this University or another institution.

All the results presented here were obtained by myself except for the following: Gabriele Ciceri made the morphological analysis described in Fig. 3.35. Corbetta Sara conducted the morphological analysis and the immunofluorescence on hippocampal slices shown in Fig. 3.36-3.39.

The results described in Fig. 3.5-3.21 have been published (Gualdoni et al., 2007, Normal levels of Rac1 are important for dendritic but not axonal development in hippocampal neurons. Biol Cell 99, 455-64). The results described in Fig 3.1 have been published (Corbetta et al., 2008, Hyperactivity and novelty-induced hyperreactivity in mice lacking Rac3. Behav Brain Res 186, 246-55). The results described in Fig 3.2 + Fig 3.22-3.26 + Fig 3.29-3.46 have been included in the following manuscript (Gualdoni and Corbetta et al., Essential role for Rac1 and Rac3 GTPases in neuronal development).

ABSTRACT

A major goal in neurobiology is to study the mechanisms by which neurites navigate towards their targets to establish functional synapses. While a large amount of information is available on the extra cellular signals driving neuritogenesis and synaptogenesis, major gaps exist in the comprehension of the intracellular events.

Rho family GTPases regulate the dynamic of the actin cytoskeleton and plays a crucial role in regulating neuronal development. In particular, Rac has been implicated in axon elongation and guidance, in dendritic growth and in the regulation of dendritic spines formation and plasticity. There are three Rac genes in mammals: Rac1, Rac2 and Rac3, sharing about 90% protein identity, all participating in several functions, including actin dynamics and adhesion (Hall, 1998). Rac1 is ubiquitous, while Rac2 is specific to the hematopoietic lineage and Rac3 is developmentally regulated in the vertebrate brain (Corbetta et al., 2005), with the highest expression during neurite branching and synaptogenesis (Bolis et al., 2003). The co-expression of Rac1 and Rac3 in the vertebrate nervous system suggests that they are needed to solve individual developmental and maintenance issues in the nervous system.

The aim of my work is to analyse the function of Rac1 and Rac3 during nervous system development. I took advantage of both *in vitro* and *in vivo* approaches to answer this question. Comparison between wild-type and Rac3-/- hippocampal neurons showed no differences in neuritogenesis and synaptogenesis processes. On the other hand, Rac1 depletion by RNAi in both wild-type and Rac3-/- hippocampal neurons during early stage of neuronal development showed specific alteration of the dendritic development without affecting axonal outgrowth. Reduced Rac1 levels impaired growth cone dynamics and F-actin levels in both neurites and growth cones. These results show that endogenous Rac1 rather than Rac3 activity is essential for early dendritic development, but not required for the initial establishment of neuronal polarity and axonal development. Depletion of either

Rac1 or Rac3 during later stages of *in vitro* neuronal development did not severe dendritic spines morphogenesis, while double depletion strongly impaired the formation and maturation of dendritic spines. All together these *in vitro* results reinforce the hypothesis that Rac1 and Rac3 are both important for neuronal development underlying a specific role for Rac3 in later events of neuronal development.

We next evaluated the effects of the depletion of Rac1 and Rac3 *in vivo*. I generated mice with conditional deletion of Rac1 in neurons (Rac1N), by crossing Rac1Flox/Flox mice (Walmsley et al., 2003) with transgenic Synapsin-Cre mice (Zhu et al., 2001) and double Rac1N/Rac3-/- mice.

As Rac3-/-, also Rac1N developed normally and was fertile. Both Rac3-/- and Rac1N did not reveal major abnormalities in the brain cytoarchitecture, cell layering or alteration in the general organization of dendrites and synapses. Double Rac1N/Rac3-/- mice died around 13 days after birth (P13) and showed strong neurological defects. Morphological analysis revealed evident alterations in the hippocampus. The abnormalities in the organization of the hippocampus may be correlated with the frequent spontaneous epileptic seizures developing after P7 in these mice. We found that double depletion of Rac1 and Rac3 induced an increase of WAVE1 (Ser310) and PAK1 (Thr423) phosphorylation, and reduced the total levels of RhoA. All together the data obtained in this thesis show for the first time that both Rac1 and Rac3 are important for neuronal development, while mutation of each gene leads to viable animals with no evident anatomical defects due to partial compensatory effects.

ABBREVIATIONS

Arp2/3	actin-related protein
ATP	adenosine triphosphate
ADP	adenosine diphosphate
AMPA	α-amino-3-hydroxy-5-methyl-4-isoxazole propionate
Cdc42	cell division cycle 42
Cdk5	cyclin-dependent kinase 5
CRIB	Cdc42/Rac-interactive binding
DIV	days *in vitro*
F-actin	filamentous actin
F/F	flox/flox
G-actin	globular actin
GABA	γ-aminobutyric acid
GADPH	glyceraldehyde-3-phosphate dehydrogenase
GAP	GTPase activating protein
GDI	GDP dissociation inhibitor
GDP	guanosine diphosphate
GEF	guanine nucleotide exchange factor
GIT	G-protein-coupled receptor kinase-interacting
GTP	guanosine triphosphate
IRSp53	insulin receptor substrate of 53KDa
LTD	long-term depression
LTP	long-term potentiation
MAP	microtubule associated proteins
MT	microtubule

NMDA	N-methyl-D-aspartate
P7	postnatal day 7
PAK	p21-activated kinase
PSD	post-synaptic density
Rac1	Ras-related C3 botulinum toxin substrate 1
Rac1N	Rac1 null
RhoA	Ras homologous member A
siRNA	small interfering RNA
Syn	Synapsin
WASP	Wiskott-Aldrich syndrome protein
WAVE	WASP family Verprolin-homologous family
WT	wild-type

LIST OF FIGURES

1 INTRODUCTION

In the nervous system neurons establish neuronal circuits that are necessary to process the complex information. Stimuli arriving to the brain are integrated and various responses are generated by connecting individual circuits to form complex neuronal networks (Cline, 2003; Sur and Leamey, 2001; Zhang and Poo, 2001).

To establish correct functional circuits newly born neurons migrate from their place of origin to reach their final destination. Then neurons extend dendrites and axon to create synaptic contacts with their targets (Cline, 2001; Hatten, 1999; Scott and Luo, 2001).

Thus, during the development of the nervous system the understanding of the molecular mechanisms involved in the processes of neuronal differentiation and neuronal morphogenesis has a fundamental relevance.

1.1 The life of neurons

1.1.1 Neuronal migration

During the formation of the central nervous system (CNS) cell migration is an important step that allows young neurons to move towards the surface to develop the correct structure and shape of the neural tube. Migrating neurons have to travel long distances, up to centimetres in the primates (Hatten, 1999). During their journey the cells have to acquire spatial information and respond to guidance cues to reach their correct position and to establish functional neuronal circuits.

After the definition of the anterior-posterior (AP) axis the newly formed neural tube has to undergo to the subdivision into vesicles. Domains characterized by specific transcription factors markers will define the forebrain (Rubenstein and Beachy, 1998), midbrain, cerebellum (Joyner, 1996), hindbrain (Guthrie, 1996) and spinal cord (Lee and Jessell,

1999). Later on neurons begin to acquire either ventral or dorsal identity, for the formation of the dorso-ventral axis (DV).

The acquisition of a dorso-ventral identity is crucial for the correct establishment of the brain regions. Cells in the dorsal region form laminar structures while cells in the ventral region form nonlaminar structures. Forebrain domains, hippocampus, olfactory bulbs and cerebellar cortex originate from dorsal laminar structures of the neural tube (Hatten, 1999). Although neuronal migration occurs in the whole developing nervous system, it has been well studied in the forebrain and in the cerebellum.

Two modes of neuronal migration have been identified during cortical development: radial migration and the more recently identified tangential migration.

The main feature of radial migration is that neurons generated in the germinal zone move orthogonal to the surface of the brain, along radially oriented glial cells. On the contrary, cells migrating tangentially move parallel to the surface of the brain along axons or other neurons. An example of neuronal radial migration is the one occurring during the development of cerebral cortex in the dorsal forebrain (Nadarajah et al., 2002). Newly generated post-mitotic neurons leave the proliferative ventricular zone (VZ) to form the preplate (PP) layer at the surface of the cortex layers. This layer is subsequently divided in the superficial marginal zone (MZ) and in the inner subplate zone (SP) by a continuous arrival of cortical neurons from the VZ that will form the II-VI layers of the cerebral cortex following an inside-out sequence. Neurons that are generated earlier will form the inner layers of the cortex, while later cells will pass the existing layers to stop and accumulate in the more superficial layers.

In the cerebral cortex the intermediate zone (IZ) divides the SP from the VZ and is enriched in afferent and efferent axons of neurons. In a second step another proliferative zone, called sub-ventricular zone (SVZ), will form between the IZ and the VZ (figure 1.1).

There are two different modes of radial movement: somal translocation during the early phases of corticogenesis and glia-guided locomotion during later stages of cerebral cortex

formation (Nadarajah et al., 2003).The cells that navigate using somal translocation usually have an initial bipolar morphology with a long thin radial basal neurite connected with the pial surface and a short transient trailing process. The cell moving toward the surface describes a continuous movement resulting in a fast rate of migration. As soon as the cell leaves the ventricular zone the trailing neurite is lost, the cell acquires a typical unipolar morphology with its radial process becoming shorter and thicker upon soma translocation. On the contrary, cells that migrate using glia-guided locomotion have a shorter radially orientated neurite that is not attached with the pial surface. When the soma moves forward, the leading process keeps constant its length. This movement results in a slower average rate, since the cells alternate phases of advancement with phases of stationary periods.

The majority of cortical excitatory pyramidal neurons, the projection cells of the cerebral cortex, use the radial migration to leave the germinal VZ and form the cortical layers. By contrast cortical inhibitory interneurons use tangential migration to leave their origin in the ventral telencephalon and reach the correct layers in the cortex (Anderson et al., 1997; Tan et al., 1998).

During tangential migration GABA (γ-aminobutyric acid) positive interneurons have to migrate from the ganglionic eminence of the ventral telencephalon, where they originated (Anderson et al., 1997), to the dorsal developing cerebral cortex crossing domains with high density of cells (figure 1.1). Specifically their migratory routes are modulated by different attractive or repulsive guidance cues, resulting in the formation of tangentially oriented marginal and intermediate zones migratory routes.

Both the tangential and the radial migration share common cellular mechanisms for cell movement. Three steps unify migrating cells: the extension of the leading process to explore the environment and receive directional cues; the nucleokinesis, the movement of the nucleus towards the leading edge; the retraction of the trailing process (Nadarajah and Parnavelas, 2002). The cytoskeleton plays crucial roles in these steps. In particular, actin dynamics are required for extension and retraction of the cellular protrusions.

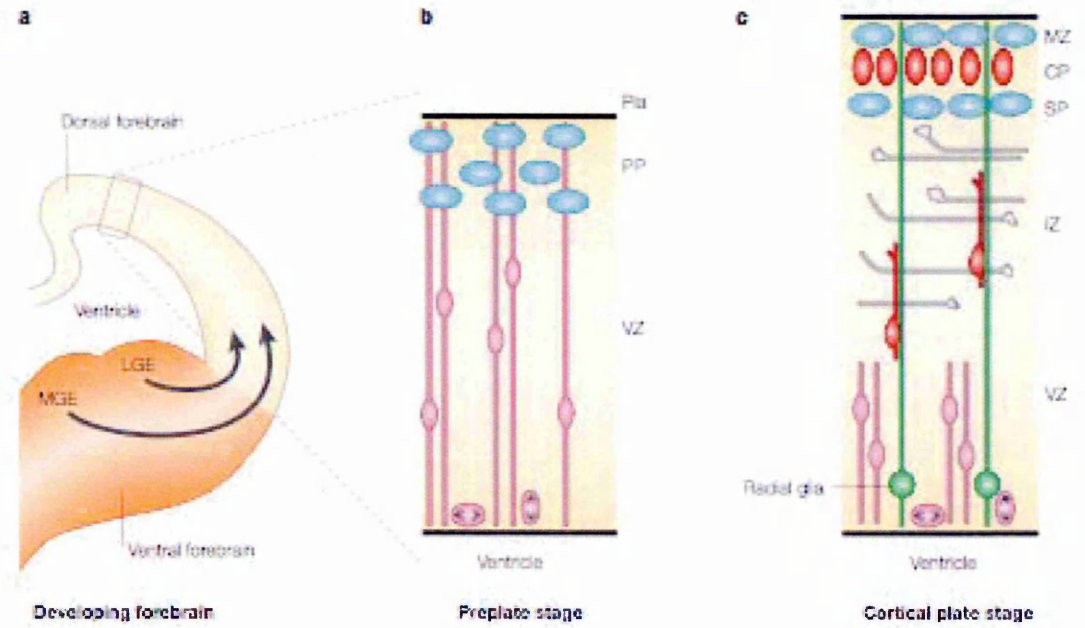

From Bagirathy Nadarajah and John G.Parnavelas, Nature Reviews Neuroscience, 2002

Figure 1.1 Cerebral cortex development. (a) Scheme of a section of the developing forebrain. (b,c) Enlargements of the frame selected in (a) showing different stages of neocortical development. (a) Interneurons originate in the lateral ganglionic eminence (LGE) and medial ganglionic eminence (MGE) and migrate to the neocortex following tangential migratory routes (arrows). (b) Preplate stage; postmitotic neurons move out of the ventricular zone (VZ) to form the preplate (PP). (c) Cortical plate stage; pyramidal neurons migrate, guided by radial glia, through the intermediate zone (IZ) to reach the PP and form the cortical plate (CP) between the outer marginal zone (MZ) and inner subplate (SP).

1.1.2 Neuronal differentiation

Neurons in the developing nervous system acquire a variety of different morphologies. The process that orchestrates neuronal morphogenesis to generate an intricate fully functional cell can be seen as series of different phases. The first phase is the budding from the neuronal sphere of what will become a neurite (second phase). The third phase consists in neurite differentiation to acquire either dendritic or axonal identity (da Silva and Dotti, 2002; Luo, 2002). The three phases just described are common to the neuronal differentiation of neuronal populations with distinct final morphologies. For example the sprouting of the first neurite is vital during *in vivo* cortical neurons differentiation, since it is important for the migration of newly born neurons from the VZ to their final destination.

Specifically, neurons from a rhomboid-like shape in the VZ acquire a bipolar appearance, with a thick neurite towards the cortical plate and a long thinner neurite towards the VZ. The axonal fate of cortical neurons *in vivo* is already determined at the bipolar stage (Calderon de Anda et al., 2008).

The use of primary neuronal cultures has became a great tool, since neurons can reproduce *in vitro* the differentiation process observed *in vivo*, to investigate the intracellular changes during neuronal differentiation. The development of hippocampal neurons *in vitro* represents one of the better-characterized system (Bartlett and Banker, 1984a; Bartlett and Banker, 1984b; Dotti et al., 1988).

1.1.2.1 Neuritogenesis

Initially, after the cell has attached to the substratum, the budding process breaks the round symmetry of the neuron, leading to lamellipodia, a veil-like structure containing a mesh network of filamentous actin (F-actin) (Smith, 1994), formation (stage1). Then the first neurite emerges followed by the generation of subsequent other small neurites, displaying high motility (stage 2). At stage 2, neurites extend and retract quickly for short distances maintaining the cells in a symmetrical morphology. The growth cone is the specialized migratory structure that leads such processes. It is composed of a central core rich in microtubules, mitochondria, and a variety of organelles. From the central domain a lamellipodium projects with long thin finger-like filopodia, containing linear bundles of actin filaments (Smith, 1994), extending from its leading edge. Filopodia function as sensors for exploring the environment. The growth cone directs neuritic extension by either favouring both attachment and consequent growth (in the case of positive cues), or by inducing neuritic retraction (in the case of inhibitory signal) (Dent and Gertler, 2003).

1.1.2.2 Neuronal Polarization

The symmetrical morphology of neurons at stage 2 is kept since all the neurites extend at about the same rate. At a certain point symmetry is broken because one of the neurites elongates faster than the others becoming the axon (stage 3). Recent data indicate a direct correlation between the formation of the first neurite and the axon specification (Calderon de Anda et al., 2008). Cells at this stage are defined polarized, since they have lost the symmetrical morphology (stage 3). The shift between stage 2 and stage 3 includes neuronal polarization (Bradke and Dotti, 2000). The process of axonal guidance plays a fundamental role because it allows the elongating axon to respond quickly to positive or negative cues in order to choose the correct direction of migration (Gallo and Letourneau, 2004). During stage 3 the axon continue to extend at fast rate, while the other neurites undergo to little elongation.

Neurons progress then to stage 4, when non-axonal processes mature and acquire the branching features of dendrites. At the end of this stage neurons have two distinct functional domains: the somato-dendritic and the axonal domain. Dendrites unlike axons don't migrate very long distances throughout the nervous system, but they branch intensively to form the dendritic tree that has unique morphologies depending on the neuronal type (Cline, 2001; Wong and Ghosh, 2002). With further development, the density of the neuronal network increases, the dendritic trees become more complex and branched, local structural changes occur to form post-synaptic specializations at the tip of small dendritic protrusions, known as dendritic spines. Dendritic spines are highly specialized subcellular structures, up to few μm in length, localized at the post-synaptic region of the most of the excitatory synapses in the brain.

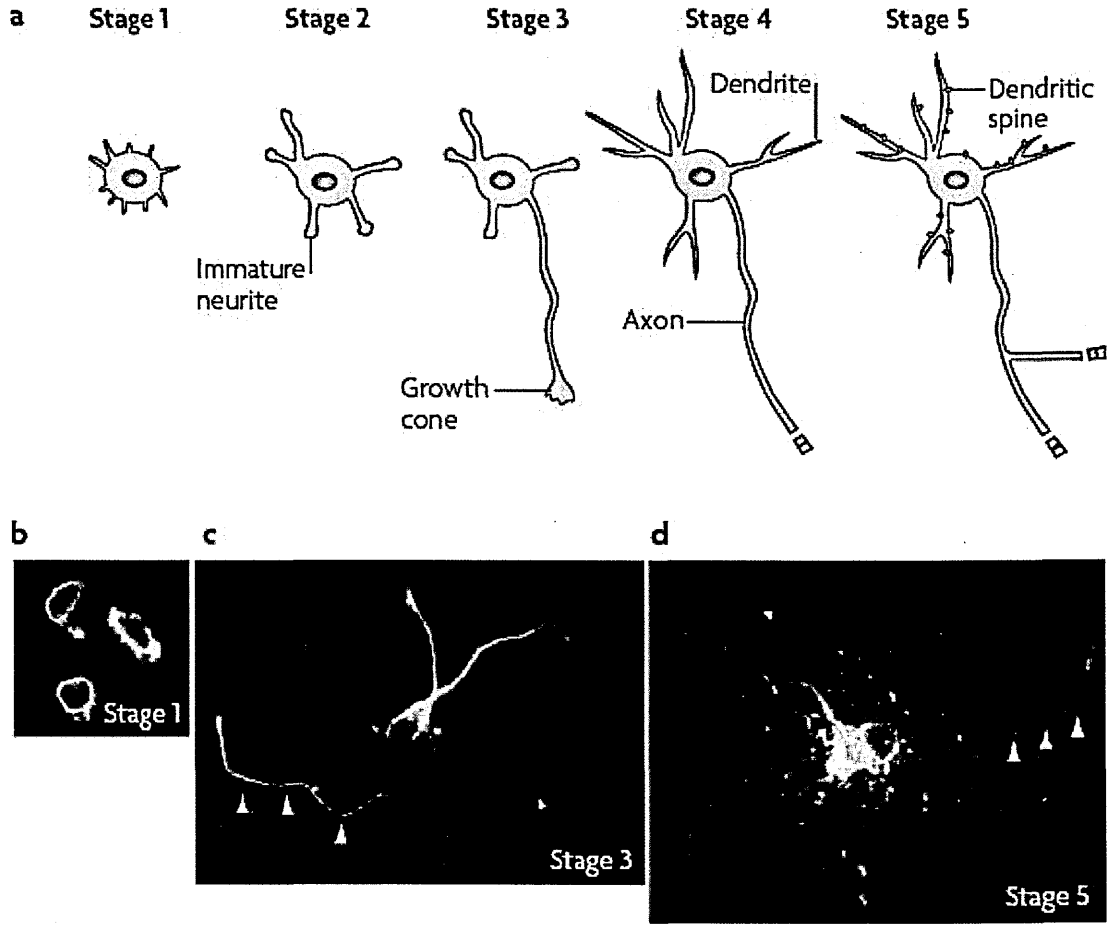

From (Aimura and Kaibuchi, 2007)

Figure 1.2 Neuronal morphology during *in vitro* neuronal differentiation. (a) Schematic representation of neuronal polarization in cultured hippocampal neurons. After the cell has attached to the substratum, the budding process breaks the round symmetry of the neuron, leading to lamellopodia like protrusions (Stage1). These protrusions develop into several immature neurites (Stage2). At a certain point symmetry is broken because one of the neurites elongates faster than the others becoming the axon (stage 3). Non-axonal processes mature and acquire the branching features of dendrites (stage 4). With further development neurons form synaptic contacts through dendritic spines and axon terminals (stage 5). (b-d) Immunofluorescence analysis on neurons of stages 1,3 and 5. The arrowheads indicate the axon. Actin filaments are shown in red and the microtubules in green. The blue staining in (d) represents synapsin 1 at the presynaptic terminal.

1.1.2.3 Synaptogenesis

The definition of functional neuronal circuits in the developing nervous system requires the correct establishment of millions of synapses, specialized cell-cell connections, to mediate

signal transmission between neurons. Not only the neurotransmitter release targeting specific post-synaptic ion channel receptors is important for neuronal communication, but also the interaction between membrane-bound signaling adhesion molecules at the pre- and post-synaptic sites (Waites et al., 2005). For example, the direct binding of the pre-synaptic neurexins to the postsynaptic neuroligins, or the pre-synaptic ephrins to their postsynaptic Eph partners mediate trans-cellular bidirectional signaling during synaptogenesis and synapse modulation (Dalva et al., 2007).

During development, once axons have reached their final destination, they undergo branching of their terminals towards the targets. Subsequently growth cones collapse and pre-synaptic terminals form. Axons not only branch and form synapses at their tips but also they establish lateral branches along all their length (Acebes and Ferrus, 2000; Scott and Luo, 2001). Filopodia extending from the dendritic shafts get in contact with the axon causing the recruitment, via vesicular packets, of pre-synaptic proteins at the newly forming synaptic sites (Ahmari et al., 2000). In parallel, proteins accumulate in discrete puncta at the active zone, within a dense matrix into the dendritic spine called post-synaptic density (PSD) (Bresler et al., 2004).

Both the intrinsic cellular mechanisms that give rise to a first "rough draft" of the circuit and the later dynamic processes of learning- and memory- related plasticity are the crucial players for creating functional neuronal networks. Dendritic spines play an important role during these processes. Two kinds of spine motility are required for the formation and a correct functioning of neuronal circuits: the first during development, coinciding with the transition from filopodia to mature spines, and the second during later phases, upon stimulation. Specifically, during early phases of synaptogenesis, immature dendrites produce long, thin motile filopodia to search active pre-synaptic partners and establish synaptic contacts. These filopodia-like protrusions are converted later into spines that develop to form mature and stable mushroom-like spines, typically with a large head connected to the dendrite by a narrow neck. Dendritic protrusions that don't form contacts

with pre-synaptic sites lack the post-synaptic proteins-enriched puncta in their head and become unstable undergoing retraction and elimination. Thus, the extension of filopodia towards the active zone in axon allows the stabilization of dendritic spines. This is a crucial step during the development of the synaptic contact.

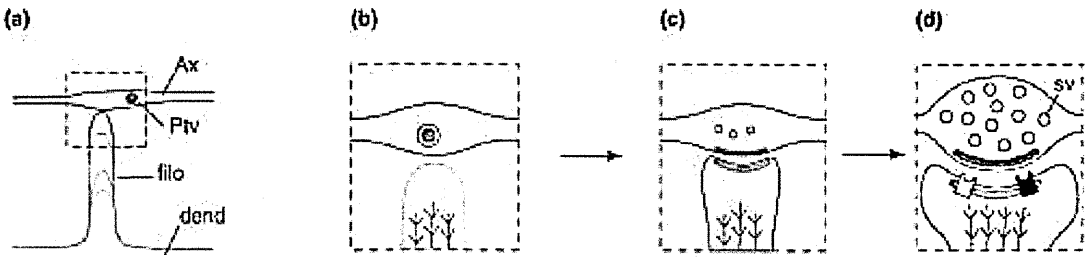

From (Matus, 2005)

Figure 1.3 Synapse development. (a) Growing dendrite (dend) extends and retracts (gray lines) filopodia (filo) towards the axon (ax) containing presynaptic transport vesicles (ptv). The frame selected is shown at higher mignification in b-d. (b-c) Ptv carries complexes of structural proteins at the presynaptic membrane site (blue). At the postsynaptic site, proteins accumulate at the active zone in the PSD (red). Herringbone lines represent actin filments. (d) Accumulation of synaptic vesicles (sv) in the presynaptic bouton induces spine maturation. NMDA (black box) and AMPA receptors (white box) are recruited at the postsynaptic plasma membrane.

1.1.2.4 Synaptic Plasticity

The morphogenesis process is not ultimate once the first synapses appear. During and after synaptogenesis neurons can refine and optimize their morphology in a constant dynamic process, by growing and retracting neurites, by modulating the number of synapses and by reshaping existing synaptic contacts (stage 5). This morphological fine-tuning allows neurons to respond and adapt to different extracellular stimuli (Cline, 2003). The activity-dependent regulation of the dynamic and the morphology of spines is a key factor for processing information at synapses. There is a strong relationship between plasticity and synaptic transmission, since it has been demonstrated that synaptic activity may induce the

formation of new spines and modulate the shape of existing spines (Jourdain et al., 2003). Plasticity is induced during memory formation and is believed to be necessary and sufficient for the storage of information in specific areas of the brain where plasticity takes place (Martin et al., 2000). Hippocampal activity and synaptic plasticity of hippocampal pyramidal cells are essential for learning and memory (Morris et al., 1986; Neves et al., 2008; Tsien et al., 1996).

LTP (long-term potentiation) is a well-studied model for synaptic plasticity identified in the hippocampus (Bliss and Gardner-Medwin, 1973; Bliss and Lomo, 1973), where high-frequency stimulation of afferent fibers induces a long-term potentiation of synaptic transmission. LTD (long-term depression) is another example of activity-dependent plasticity (Dudek and Bear, 1992), in which low-frequency electrical stimulation induces a weakening of synaptic transmission. During LTP and LTD actin-mediated spine remodeling has been observed. In particular, LTP induces formation of new spines, increases the head size, favors actin polymerization and filamentous actin, and promotes the clustering and activation of AMPA (α-amino-3-hydroxy-5-methyl-4-isoxazole propionate) and NMDA (N-methyl-D-aspartate) glutamate receptors at the post-synaptic membranes (Fukazawa et al., 2003; Matsuzaki et al., 2004; Okamoto et al., 2004). On the contrary, LTD induces actin depolymerization causing spine retraction and sometimes spine elimination.

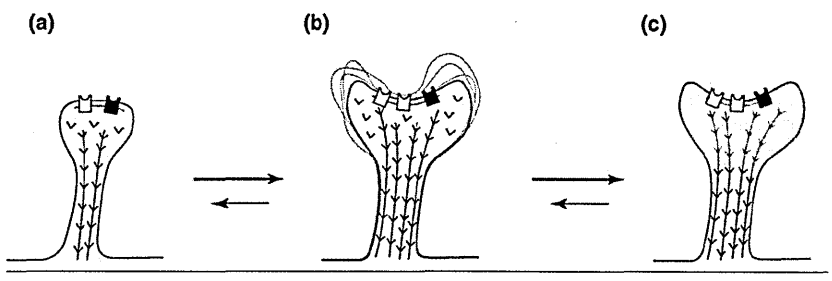

from (Matus, 2005)

Figure 1.4 Synapses plasticity. (a,b) LTP stimulation induces increases in actin polymerization and spine head size. At the plasma membrane clustering and activation of AMPA (white boxes) and NMDA receptors (black box) occurs. The spine head is highly motile (gray outlines). Herringbone lines represent actin filments and v-shape actin monomers. (b,c) Continuous stimulation of NMDA receptors results in blockade of spine motility and accumulation of actin binding proteins (green) at the spine head.

In summary, the morphogenetic process is important to define specialized cell compartments (dendrites, axon, soma) and to confer the correct directionality in the neuronal circuits. Input, integration and propagation of signals are thus mediated by specialized cellular structures. Moreover, signal transmission is controlled by the modulation of synaptic vesicles exocytosis and recycling at the synaptic terminal, which regulate neurotransmitter release.

1.2 Cytoskeletal changes during neuronal differentiation

Cellular events that characterize the change in shape and structure of a cell during differentiation are based on cytoskeletal and membrane modification. The generation of a protrusion like a filopodium or a lamellopodium at the leading edge of a migrating cell requires a dynamic cytoskeletal rearrangement and addition of new membrane in the involved area (Raftopoulou and Hall, 2004). During neuronal morphogenesis the regulation of the membrane organization and cytoskeleton dynamics are thus crucial. For example, growth cones, presynaptic terminals and dendritic spines are modulated by the interplay between cytoskeletal and membrane dynamics.

1.2.1 Microtubules and microtubule associated proteins

Changes in membrane organization depend also on microtubules (MTs) cytoskeleton. Intracellular transport plays a relevant role during neuronal morphogenesis, where

microtubules and microtubule-associated motor proteins direct vesicular transport (Hirokawa and Takemura, 2005). MTs are made of linear protofilaments of α and β tubulin that polarize in an ordered conformation that confers to MTs an intrinsic polarity characterized by a dynamic plus end and a relatively stable minus to the MTs (Desai and Mitchison, 1997). Immature neurons have MTs with a mixed polarity, while polarized neurons have the MTs in the axon and in distal dendrites with a plus-end pointing away from the cell body; proximal dendritic MTs have a mixed polarization (Baas et al., 1989). MTs polarization is very important for the directional transport of vesicles in neurons. Molecular motors like kinesin and dynein move along MTs. Specifically, proteins of the kinesin family (KIFs) move towards the plus-end, promoting transport from the cell body to the distal axon (anterograde transport), while dyneins promote the transport from the dendritic and axonal extremities to the cell body (retrograde transport) (Hirokawa, 1998).

The organization of MTs in dendrites and axon differs also in term of MTs associated proteins (MAPs). MAPs control MT dynamics, with MTs in mature dendrites being more stable. MTs are associated to different axon- (e.g. tau) and dendrite- (e.g. MAP2) specific MAPs that crosslink them.

MTs exert tension forces and provide structural stability as neurons differentiate. For example, when the axon is formed MTs generate dense parallel arrays providing a structural rigidity to the fast-elongating neurite, while MTs bundles in the growth cone either loop or spread out, depending on whether the growth cone is stationary or is moving (Dent and Gertler, 2003; Dent and Kalil, 2001). Furthermore, MT dynamics are necessary to re-shape differentiated mature neurons, as during axon retraction and pruning (Gallo and Letourneau, 1999).

1.2.2 Actin

Actin plays a central role during neuronal differentiation because it regulates membrane dynamics and the spatio-temporal modulation of MTs. F-actin is composed of 10 nm thick helical polymers made of two filaments of actin monomers of 43 KDa that due to their globular structure are defined G-actin. Actin monomers exist as ATP-actin, ADP-Pi-actin and ADP-actin. Actin polymerization is favoured by ATP-actin addition at the barbed end (fast growing end) of the filament, whereas ADP-actin dissociation is favoured at the pointed end (slow growing end) (Pollard and Borisy, 2003). Between these two forms the intermediate ADP-Pi-actin is generated by hydrolysis of the ATP. After ATP-actin is incorporated into filaments, ATP is slowly hydrolysed. The dissociated ADP actin monomers can undergo exchange of ADP for ATP, creating a reserve pool for polymerization. Polymerized actin may give rise to different structural forms such as bundles, arcs or meshworks.

The actin cytoskeleton plays a variety of roles during neuronal differentiation. Actin dynamics and actin turnover are tightly regulated during this process.

Initially, when the symmetry of the neuronal sphere is broken, the sprouting bud contains filopodia and lamellipodia that later will originate neurites (Dotti et al., 1988). These actin-based structures are also present in developing neurites, where they drive motility at the edge of the growth cones, and act as sensors for extracellular cues. Specifically, during neuritogenesis, microtubule-directed events follow actin-based formation of filopodia and lamellipodia. Then, MTs stabilize the neurite to allow further elongation (Dehmelt and Halpain, 2004). For example, actin and MT dynamics are essential for the movement of the growth cones towards a chemoattractant. Once actin polymerization has produced new filopodia and lamellipodia, MTs start to invade the growth cone up to the actin-rich peripheral region. The interaction between proteins at the tips of MTs and actin associated

proteins allows MTs to be further stabilized and to extend, thus contributing to growth cone migration (Schaefer et al., 2002; Zhou et al., 2002).

During synaptogenesis, filopodia forming along dendrites are the pioneering structures that will give rise to dendritic spines, where actin is enriched to allow morphological changes upon incoming synaptic signals (Matus, 2000; Tada and Sheng, 2006). Experiments in primary hippocampal neurons have shown the importance of actin during synaptogenesis. The use of the actin polymerization inhibitor latrunculin prevents synapse formation by disrupting both pre- and post-synaptic terminals (Zhang and Benson, 2001). In addition, abnormalities in spine morphology and density have been observed *in vivo*, in patients affected by mental retardation associated to mutations in genes encoding for proteins that regulates the actin cytoskeleton (Purpura, 1974; Ramakers, 2002). Actin exert crucial functions also in the organization of presynaptic terminals, where actin filaments function as scaffold for synaptic vesicle clusters and for recruiting vesicles from a reserve pool to a readily releasable pool of vesicles (Dillon and Goda, 2005).

1.3 Rho GTPases

The family of Rho GTPases belongs to the Ras superfamily of small (around 21 KDa) GTPases. Rho GTPases are found in all eukaryotic organisms, from yeast to primates (Jiang and Ramachandran, 2006), where they play crucial roles in different biological processes including cell adhesion, migration, cytokenisis, cell cycle progression, transformation and neuronal development (Etienne-Manneville and Hall, 2002; Evers et al., 2000; Jaffe and Hall, 2005; Malliri and Collard, 2003; Nobes and Hall, 1999; Raftopoulou and Hall, 2004; Sahai and Marshall, 2002; Threadgill et al., 1997). Rho GTPases control the cell morphology by modulating the actin cytoskeleton and membrane dynamics (Bader et al., 2004; Egea et al., 2006; Hall, 1998; Symons and Rusk, 2003).

The most studied Rho GTPases are Rac1 (Ras-related C3 botulinum toxin substrate 1), Cdc42 (cell division cycle 42) and RhoA (Ras homologous member A). On the other hand there are 22 different proteins belonging to this family, each with specific cellular functions and classified in 6 subfamilies: Rho, Rac, Cdc42, Rnd, RhoBTB and RhoT/Miro (Bustelo et al., 2007). In classic studies on fibroblasts, the expression of constitutively active Rac and Cdc42 mutants (proteins that remain active in the absence of upstream activating signals) induce the formation of protrusion to generate lamellipodia and filopodia respectively. On the other side RhoA activation leads to the generation of stress fibres and focal adhesions (Heo and Meyer, 2003; Kozma et al., 1995; Nobes and Hall, 1995; Ridley and Hall, 1992; Ridley et al., 1992). Lamellipodia, filopodia and stress fibres are actin-containing structures playing important roles during the migration of non-neuronal and neuronal cells.

Cdc42 has been correlated to filopodia formation while Rac to lamellipodia formation, although recently filopodia have been identified in Cdc42 null fibroblast. A plausible hypothesis is that the lack of Cdc42 could be compensated by other Rho GTPases acting in filopodia formation (Czuchra et al., 2005).

Stress fibers (bundles of myosin-containing actin filaments linked to focal adhesions at the ventral surface of the cell) form, upon Rho activation to stabilize the cell on the matrix and to promote acto-myosin contractility for the translocation of the cell during migration by inducing retraction of the rear of the cell. These processes are mediated by an increasing acto-myosin contraction of the ventral stress fibres (Pellegrin and Mellor, 2007). Recent studies have shown the localization of RhoA in lamellipodia and membrane ruffles at the leading edge of a cell, even though its role there is still unclear (Pertz et al., 2006).

1.3.1 Structure of Rho GTPases

Figure 1.5 Scheme of the Rho GTPases

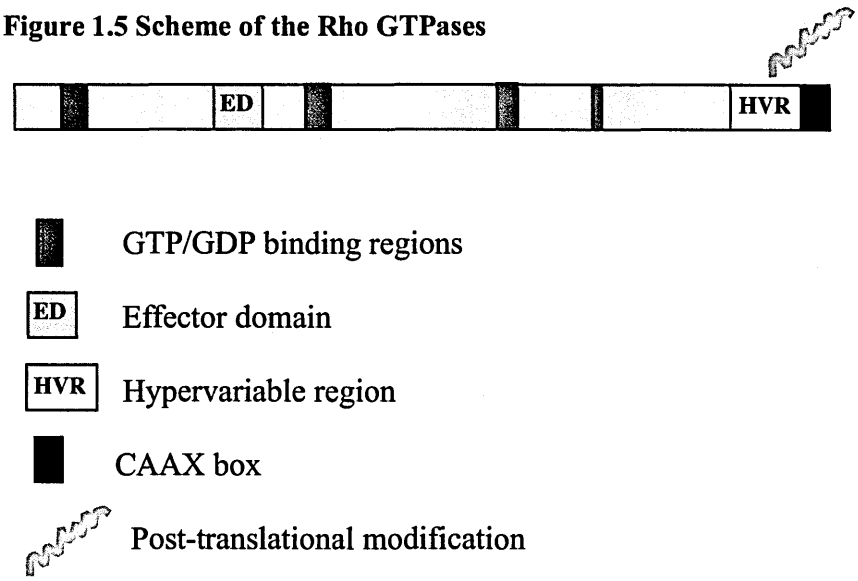

Modified from (Ridley, 2006).

The 22 Rho GTPases share high homology in the primary aminoacidic sequences, but also specific differences at the N- and C-terminus. All members of the family share specific domains crucial for their function. In particular, Rho GTPases have the nucleotide-, the Mg^{2+}- binding pockets and two switch regions that, depending on the GDP or GTP binding, change conformation to interact with target proteins. Mg^{2+} is required for stabilizing the binding with the specific guanine nucleotide (Rossman et al., 2005; Worthylake et al., 2000). The C-terminal CAAX sequence, composed of a cystein, two aliphatic aminoacids and a variable aminoacid, next to the hypervariable region undergoes post-translational modifications on the cystein by linking a lipidic group. The last 3 aminoacid (AAX) are cleaved and the C-teminus is methylated (Ridley, 2006).

1.3.2 Regulation of Rho GTPases

Most of the Rho family GTPases can bind a guanine nucleotide and are regulated by cycling between a GDP-bound inactive state and a GTP-bound active state that allows

them to interact with downstream effectors. A complex set of regulators controls the switch between these conformational states. GEFs (guanine nucleotide exchange factors) activate GTPases by stimulating the release of GDP for the exchange with GTP (Schmidt and Hall, 2002). The first identified Rho GEF was Dbl (diffuse B-cell-lymphoma) (Hart et al., 1991). Over 60 GEF are now known in the human genome. They all share a region of homology consisting in a DH (dbl-homology) domain flanked by a PH (pleckstrin-homology) domain. To date, different studies have been performed to characterize the three dimensional structure of DH and PH domains associated with distinct GTPases (Rossman et al., 2002; Snyder et al., 2002; Worthylake et al., 2000). This analysis allows characterizing specific functions for these domains. The DH domain is responsible for exchanging the GDP to GTP by inducing an intermediate nucleotide- and Mg^{2+}- free conformation. The PH domain, binding phosphoinositides, is able to recruit GEF proteins to the plasma membrane and in some cases to interact with downstream effectors of Rho GTPases. For example the PH domain of Trio interacts with the actin filaments cross-linker filamin (Bellanger et al., 2000).

GAPs (GTPase-activating proteins) inactivate the GTPases by enhancing the rate of GTP hydrolysis, converting them to the inactive GDP-bound form (Bernards and Settleman, 2004). The first Rho GAP was discovered in the 1989 (Garrett et al., 1989) and to date more than 70 GAP proteins have been identified, all containing the RhoGAP catalytic domain.

The GDI (guanine nucleotide dissociation inhibitor) proteins are the third class of regulators. They prevent the exchange of GDP to GTP and the binding of the GTPases to the membrane by capping their lipidic tail (DerMardirossian and Bokoch, 2005).

Rho GTPases undergo specific post-translational modifications at the C-terminus that are essential for their binding to the membranes and their consecutive activation. Mainly, they are characterized by prenylation (farnesylation or geranylgeranylation) with some exceptions where palmitoylation takes place. For example, Rac proteins are

geranylgeranylated (Joyce and Cox, 2003) while Rho proteins can either be geranylgeranylated or both prenylated and palmitoylated (Adamson et al., 1992). These post-translational modifications are believed to contribute to the specific intracellular membrane localization. RhoA for example is targeted to the plasma membrane, while RhoB can also be localized at endosomal compartments (Adamson et al., 1992; Ridley, 2006).

1.3.3 Regulation of the actin cytoskeleton by Rho GTPases

Modification of the actin cytoskeleton is driven by the work of a complex set of actin binding proteins (ABP) (Pollard and Borisy, 2003). These include proteins that bind/sequester actin monomers as profilin; proteins that disassemble the filaments as ADF (actin depolymerizing factor)/cofilin; proteins that nucleate actin as Arp2/3 (actin-related protein) and WASP (Wiskott-Aldrich syndrome protein)/WAVE (WASP family Verprolin-homologous family); proteins that cap the barbed (plus) end of actin filament as gelsolin or the pointed (minus) end as tropomodulin; proteins that inhibit barbed end capping as DRFs (Diaphanous-related formins) and Ena/Vasp; proteins that stabilize filaments by bundling and cross-linking as fascin and α-actinin; proteins that anchor F-actin to the membranes as cortactin, vinculin and spectrin.

The Rho GTPases orchestrate the process of polymerization/depolymerization of actin filaments by activating or inactivating several actin binding proteins. For example, WASP/WAVE proteins and DRFs are two classes of downstream effectors of Rho GTPases that promote actin polymerization by adopting different mechanisms. WASP (Derry et al., 1994) and N-WASP (Neural-WASP) (Miki et al., 1996) proteins are direct downstream effectors of Cdc42 while Scar/WAVEs (Miki et al., 1998a; Miki et al., 1998b; Suetsugu et al., 1999) belong to the Rac signalling pathways. They activate the Arp2/3 complex, one of the main actin nucleator that stimulates actin polymerization from an

already existing actin filament to form a branching filament network (Takenawa and Miki, 2001). WASP/N-WASP and WAVEs are activated by different mechanisms. The WASP proteins exist as auto-inhibited monomers (Kim et al., 2000). They interact through their CRIB (Cdc42/Rac-interactive binding) domain with active Cdc42. This binding induces a conformational change that allows the interaction of WASP with the Arp2/3 complex to start actin polymerization (Stradal et al., 2004). WASP activation can be achieved also by other mechanisms including protein phosphorylation (Cory et al., 2003), or the interaction with SH3-domain containing proteins (Takenawa and Miki, 2001).

Unlike WASP, WAVE proteins don't have a CRIB domain to bind directly Rho GTPases, but are regulated through other mechanisms. WAVEs are part of a multi-protein complex including Nap125 (Nck-associated protein), PIR121 (a p53-inducible protein), Abi2 (Abl interactor 2) and the heat-shock protein HSPC300. According to a recently proposed model, Rac induces the dissociation of the inhibitory subunits Nap125, Abi2 and PIR121 from the WAVE-HSPC300 subunits that can activate the Arp2/3 complex to stimulate actin polymerization (Eden et al., 2002). In contrast, other data from *in vitro* and *in vivo* studies show that Rac activation does not lead to the dissociation of the complex. In this model, the WAVE complex may instead function as a positive regulator that is recruited where actin polymerization is active, such as lamellipodia or membrane ruffles (Innocenti et al., 2004; Steffen et al., 2004). Other regulatory mechanisms specific for each WAVE protein have been described. For example, Cdk5 (cyclin-dependent kinase 5)-mediated phosphorylation of WAVE1 (enriched in the brain) inhibits its ability to activate the Arp2/3 complex and actin polymerization (Kim et al., 2006). The binding of WAVE2 (the ubiquitous form) to activated Rac through the Rac downstream effector IRSp53 (insulin receptor substrate of 53KDa) induces initiation of actin filaments assembly (Miki and Takenawa, 2002; Miki et al., 2000).

The DRF proteins are effectors belonging to a second class of actin nucleating proteins. They promote actin polymerization in non-branching actin filaments by binding two actin

monomers. They bind the barbed end of the filaments to promote linear elongation (Kovar et al., 2006). Work in neurons with constitutively active and dominant negative mutants has shown the role of formins in axon elongation (Arakawa et al., 2003).

Rho GTPases regulate actin dynamics also by signalling to the actin-depolymerazing factor ADF/Cofilin (DesMarais et al., 2005). Cofilin plays a crucial role during lamellipodia formation by severing actin filaments to generate new free actin ends for binding of the Arp2/3 complex. Moreover cofilin increases the turnover of the actin monomers at the pointed end (minus) of existing filaments (Pollard and Borisy, 2003). Phosphorylation of cofilin on serine 3 by LIM kinase leads to its inactivation and therefore to the stabilization of actin filaments (Huang et al., 2006; Yang et al., 1998). Rho GTPases signal to LIM kinase through the Rac/Cdc42 effector PAK (p21-activated kinase) (Edwards et al., 1999) and the Rho kinase ROCK (Maekawa et al., 1999). Both PAK and ROCK activate LIM kinase by phosphorylating it.

PAKs are a family of serine/threonine protein kinases. Six members of the PAK family (PAK1-6) have been identified (Bokoch, 2003). In the inactive state they form homodimers in which the regulatory domain of one PAK inhibits the catalytic domain of the other. Upon activation by Rho GTPases, PAKs undergo a conformational change that releases the N-terminal auto-inhibitory domain from the C-terminal kinase domain, resulting in PAK auto-phosphorylation and activation (Bokoch, 2003; Buchwald et al., 2001). The phosphorylation of threonine 423 in the catalytic domain of PAK1 is necessary to release the autoinhibition. The regulatory mechanism of PAK activity is controlled also by cdk5 and its neuron-specific regulatory subunit p35, a Rac-GTP interactor. In particular, work in neurons has shown that cdk5 can specifically phosphorylate PAK1 on the threonine 212, thus decreasing PAK activity and affecting neuronal morphology (Nikolic et al., 1998; Rashid et al., 2001). Therefore Rac GTPases can modulate PAK activity by directly activating it, and at the mean time by limiting the duration of its activation through p35/cdk5.

One of the downstream effectors of Rho is ROCK that phosphorylates different proteins involved in regulating actin dynamics and cell contractility, like LIM kinase and MLC (myosin light chain) (Amano et al., 1996; Riento and Ridley, 2003). The function of Rho has always been linked to stress fiber formation and acto-myosin contraction, anyway recent data show active RhoA localizing in lamellipodia and in membrane ruffles (Kurokawa and Matsuda, 2005; Pertz et al., 2006). Even though the precise role of RhoA at the leading edge is still not completely clear, it is hypothesized that it may signal to the formin Dia 1 to promote actin polymerization.

1.3.4 The Rac GTPase family

Three Rac genes encoding Rac1, Rac2 and Rac3 proteins have been identified in vertebrates (Didsbury et al., 1989; Haataja et al., 1997; Malosio et al., 1997). Their aminoacid sequences share about 90% protein identity, but they are spatially and temporally differently regulated. Rac1 is ubiquitously expressed (Moll et al., 1991), Rac2 is specifically expressed in hematopoietic cells (Shirsat et al., 1990) and Rac3 has predominant expression in the developing nervous system (Haataja et al., 1997; Malosio et al., 1997).

Rac2-null mice develop normally and are fertile. Histopathological analysis of non-hematopoietic organs does not show gross alterations, although neutrophils isolated from Rac2 knock-out mice have deficits in multiple functions, including cytoskeletal remodelling and superoxide production, with significant consequences for leukocyte trafficking and host defense (Roberts et al., 1999).

1.3.4.1 Rac3: the neurospecific Rac GTPase

Rac3 is the least characterized the Rac. It is likely that the gene for Rac3 did first appear in

vertebrates, since an ortholog of Rac3 has not been found in less complex chordates (Philips et al., 2003), insects (Hariharan et al., 1995), or nematodes (Lundquist et al., 2001). It has the strongest homology to Rac1, with the major divergence at the C-terminal hypervariable region (residues 180 to 192). This region undergoes post-translational modification believed to be important for the specific intracellular localization and for the interaction with target proteins (Joyce and Cox, 2003; Kinsella et al., 1991). Few studies have tried to address the specific role of Rac1 and Rac3 during neuronal development (Albertinazzi et al., 1998; Hajdo-Milasinovic et al., 2007). Specifically, over-expression of Rac3 (chRac1B) in chicken retinal neurons strongly enhances neurite outgrowth compared to Rac1 over-expression (Albertinazzi et al., 1998). In contrast, recent data showed opposite effects of Rac3. Rac3 over-expression in neuroblastoma cells causes severe morphological changes by inducing rounding of these cells. On the other hand, down-regulation of Rac3 by shRNA leads to consistent cell spreading and outgrowth of neurite-like protrusions, while down-regulation of Rac1 resembles the same phenotype induced by Rac3 over-expression (Hajdo-Milasinovic et al., 2007). The molecular mechanisms that drive Rac3 function is thus still to be elucidate, since contradictory data have originated by using different cell systems.

So far, with the exception of some endogenous Rac3 protein identified in primary lymphomas from Bcr/Abl P190 transgenic mice (Cho et al., 2005), the Rac3 protein has been detected exclusively in neural tissue. Analysis of Rac3 expression in developing chick has revealed that the transcript for avian Rac3 (chRac1B) is specifically expressed in the developing peripheral and central nervous system (Malosio et al., 1997), where it is co-expressed with Rac1. Further analyses have shown that the levels of Rac3 transcript are developmentally regulated both in avian and mouse brain, with a peak of expression at seven days after birth (in mouse), corresponding to the time of intense neurites branching and synaptogenesis (Albertinazzi et al., 1998; Bolis et al., 2003). It is reasonable to hypothesize that this gene would contribute in the organization of the brain of more

evolved animals by turning on later during development. In human the highest level of Rac3 mRNA is found in brain (Haataja et al., 1997).

Recent data obtained in our laboratory have shown that Rac1 and Rac3 have partially different expression patterns during neuronal development. In situ analysis on mouse brain has shown that Rac3 is widely and specifically expressed in the developing nervous system and that the restricted expression pattern of Rac3 differs substantially from that of Rac1 and Rac2, suggesting specific roles for each gene (Corbetta et al., 2005). In E13 (embryonic day 13) mouse embryos, Rac3 mRNA is expressed in area of the brain including cerebellum, mesencephalon and pretectum, medulla oblungata, and the inner layer of the developing retina. A strong expression is also detected in dorsal root ganglia, and in the ventral part of the spinal cord. At P7 (postnatal day 7), the time of the highest expression of Rac3, the in situ analysis has revealed high levels of Rac3 mRNA in several regions of P7 mouse brain. Rac3 is particularly abundant in the hippocampus, with a strong signal in the CA1-CA3 region and a much weaker signal in the dentate gyrus. In the cerebral cortex, Rac3 is enriched in the pyramidal neurons of the developing fifth layer, with a lower expression level in the second and third layers. In addition, Rac3 mRNA is evident in several nuclei of the thalamus, in the amygdala, in the pons, mesencephalon and olfactory bulbs. In the cerebellum, the highest expression level is detected in the deep cerebellar nuclei and in scattered cells in the internal granular layer, while Purkinje cells show low expression levels. All territories in which the gene is expressed contain projection neurons involved in long and complex neuronal networks. From this analysis, white matter regions do not show Rac3 expression, suggesting that the gene is not expressed in oligodendrocytes (Corbetta et al., 2005).

Different studies have shown that Rac1 is ubiquitously expressed in the adult rat brain and in the developing mouse brain (Bolis et al., 2003; Tanabe et al., 2000). Recent data from our laboratory have shown that Rac1 transcript is expressed in all the region of hippocampus including the CA1-CA3 and dentate gyrus.

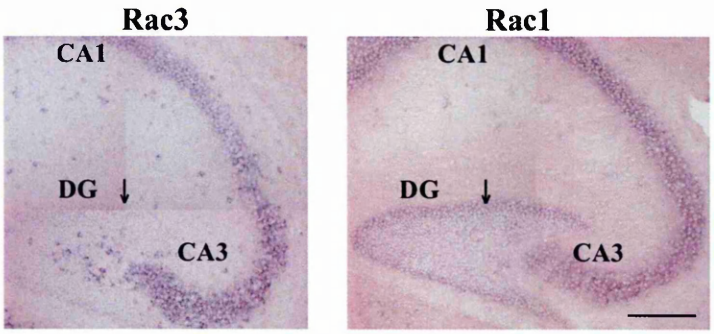

From Corbetta et al., 2005.

Figure 1.6 Expression of Rac1 and Rac3 mRNA in P7 mouse hippocampus. In situ hybridization on P7 mouse hippocampus parasagittal sections from wild-type mice, using Rac3 or Rac1 antisense probes. Arrows indicate an evident difference in labeling in the dentate gyrus between Rac3 and Rac1. Bars: 200 μm

Further studies are necessary to identify morphological and functional differences in the fine organization of the neuronal networks. The combination of in vivo and in vitro analysis is required to establish possible deficits in neuronal development.

1.3.5 Rho GTPases in neuronal differentiation

Studies in different organisms, including *C.elegans*, flies and vertebrates have helped to characterize the *in vivo* function of Rho GTPases. These proteins seem to play distinct roles during the development of the nervous system, even though functional redundancy within the family must also be considered.

1.3.5.1 Rho GTPases during neuronal migration and neuritogenesis

Rho GTPases play important roles in the first phases of a neuronal life, since they regulate neuroblast cytokinesis (Di Cunto et al., 2000) and migration of newly born neurons from the ventricular zone (Chae et al., 1997). As already described previously, neuronal

migration in the neocortex occurs with an inside-out mechanism. Rac signalling is crucial in controlling this event, since mice mutant for p35, the neurospecific cdk5 regulatory subunit, show a reversed pattern of migration (Chae et al., 1997).

Up to now, most of the effects mediated by the Rho GTPases have been studied using overexpressed mutants that may interfere with the function of other related GTPases. More recently, a number of studies have addressed more directly the function of the endogenous GTPases.

Work in the nematode *C.elegans* has shown that expression of activating Rac mutant (Mig-2) leads to defects in neuronal migration, while deletion of the same gene produces animals with a weaker phenotype, suggesting that different Rho GTPases might interplay to properly coordinate neuronal migration (Zipkin et al., 1997).

Inactivation of one of the three RAC-related genes encoding for Rac GTPases Mig-2, CeRac-2 and CeRac-1/CED-10 has a mild effect, while double or triple inactivation leads to both axon outgrowth and dendrites fasciculation defects (Wu et al., 2002).

In *Drosophila* the expression of constitutively active V12dRac1 and V12dCdc42 mutants or dominant negative N17dRac1 causes axon elongation and guidance defects, as well as abnormalities in the morphology of dendrites in different neuronal types (Allen et al., 2000; Lee et al., 2003; Luo et al., 1994). These data indicate that the effect of these mutants depends on the specific neuronal environment. As observed in worms, also in flies the three *Drosophila* Rac-related proteins (dRac-1, dRac-2 and Mtl) have redundant roles during axon elongation and guidance. In particular, the progressive loss of the three Rac-related proteins causes first defects in axon branching, then in guidance and at last in neurite growth (Hakeda-Suzuki et al., 2002; Ng et al., 2002). These results indicate that growth, guidance and branching require increasing amounts of GTPase activity in vivo. While Rac and Cdc42 promote neurite growth and dynamic behaviours, RhoA acts as a negative regulator of neurite growth, since neurons lacking RhoA overextend the dendrites

and constitutively active RhoA dramatically reduces dendritic arborisation (Lee et al., 2000).

Studies in the vertebrate *Xenopus* have shown that Rac1, Cdc42 and RhoA are crucial during neuritogenesis. Overexpression and activation of Rac and Cdc42 stimulate dendritogenesis, while constitutively active RhoA leads to reduction in dendritic arborisation, as observed in *C.Elegans*. Moreover overexpression of the three GTPases causes guidance errors (Li et al., 2000; Ruchhoeft et al., 1999).

Deletion of Rac1 in mouse leads to embryonic lethality. The Rac1-deficient embryos show a high degree of cell death in the space between the embryonic ectoderm and endoderm at the primitive streak stage, and die before embryonic day 9.5. Analysis of the primary epiblast culture isolated from Rac1-deficient embryos indicates a main role for Rac1 in lamellipodia formation, cell adhesion, and cell migration in vivo, suggesting that Rac1-mediated cell adhesion is essential for the formation of three germ layers during gastrulation (Sugihara et al., 1998). Transgenic mice overexpressing constitutively active V12Rac1 in vivo have confirmed the function of Rac1 during axon elongation and dendritic maturation (Luo et al., 1996). Recently, conditional deletion of Rac1 in mouse VZ progenitors has suggested a role of Rac1 in axon guidance rather than axonal formation, since axonal outgrowth is not affected in Rac1/Foxg1-Cre knockout embryos, while corpus callosal and hippocampal commissural axons fail to cross the midline (Chen et al., 2007).

Knockout mice for Rac3, the neurospecific Rac GTPase, develop normally and don't show gross morphological alterations in the brain, possibly due to a compensation by Rac1 (Corbetta et al., 2005). On the other hand Rac3 knockout mice display reduced behavioural flexibility, showing hyperactive behaviour and hyper-reactivity to the presentation of new stimuli, suggesting a role of Rac3 during the formation or function of neuronal circuits important for cognitive functions (Corbetta et al., 2008; Corbetta et al., 2005). Ablation of Cdc42 in the brain of mice leads to different abnormalities, including defects in axonal

formation, indicating a specific role for Cdc42 in neuronal polarity and axonal determination (Garvalov et al., 2007).

Several studies in cultured neurons have contributed to the definition of the role of Rho GTPases during neuronal differentiation. Inhibition of Rho GTPases with toxin B in primary hippocampal neurons leads to actin destabilization in growth cones and consequent generation of multiple axons (Bradke and Dotti, 1999). These results underline a role of Rho GTPases in neuronal polarization. However, since toxin B targets different members of this family, it is unclear which Rho GTPase directs polarization. Studies on neuronal cell lines show that RhoA activation inhibits neurite extension, while RhoA inactivation results in the inhibition of neurite retraction induced by extracellular stimuli (Hirose et al., 1998; Kozma et al., 1997). Subsequent studies have provided further support to the idea that Rac and Cdc42 are positive morphogenetic regulators while RhoA is a negative regulator of neuritic growth and axon guidance (Ahnert-Hilger et al., 2004; Albertinazzi et al., 1998; Brown et al., 2000; Hu et al., 2001; Leeuwen et al., 1997; Nakayama et al., 2000).

The hypothesis of a crosstalk between Rac, Cdc42 and Rho for the regulation of neuritogenesis has been supported also by *in vivo* studies. Constitutively active Rac induces an hyper-activation of endogenous RhoA, while constitutively active RhoA induces Rac1 inactivation (Li et al., 2002). Recent data suggest that Rac1 and Cdc42 may regulate neuritic growth by using different mechanisms. Specifically, cultured hippocampal neurons from Cdc42 knockout mice show alterations in axonal growth, confirming in vivo studies. Cdc42 knockout neurons sprout neurites that develop as dendrites, indicating a specific role of Cdc42 in axon specification and in the establishment of neuronal polarity (Garvalov et al., 2007). The role of Rac during dendritic and axonal specification is still unclear.

1.3.5.2 Rho GTPases during synaptogenesis and synaptic plasticity

Rho GTPases play a critical role also in later stages of neuronal development, during dendritic spine morphogenesis. Up to now, the studies aimed at characterizing the role of Rho GTPases during spine formation and maintenance have used overexpressed constitutively active and dominant negative mutants, while the precise role of the endogenous proteins *in vivo* needs further investigation. Constitutively active RhoA causes a reduction in spine density and length, while inhibition of RhoA leads to the opposite phenotype, indicating RhoA as a negative regulator of spine formation and maintenance (Nakayama et al., 2000; Tashiro et al., 2000).

In contrast, Rac1 is considered a positive regulator of the process of spine formation. Mice expressing constitutively active Rac1 in Purkinje cells show an increase number of dendritic spines (Luo et al., 1996). A similar phenotype has been reproduced also in cultured neurons expressing constitutively active Rac mutants, while dominant negative Rac mutants cause the opposite phenotype with a reduction in spine number and morphological differences (Nakayama et al., 2000; Tashiro et al., 2000). In particular inactive Rac mutants affect spinogenesis by reducing spine density and increasing their length, resulting in the formation of thin, long immature filopodia-like protrusions in young neurons, and in the reduction of spine head size in older neurons, with an overall inhibition of spine maturation (Tashiro and Yuste, 2004).

Several studies have been performed to dissect the molecular mechanisms that link neuronal stimulation to actin dynamics during the formation of dendritic spines. A well-characterized signalling pathway starts with the activation of the tyrosine kinase membrane receptor EphB at the post-synaptic site upon binding of its ephrin ligand on the axonal membrane. Ephrin-induced receptor activation leads to activation of the Rho GEF kalirin that activates Rac, with subsequent activation of PAK (Penzes et al., 2003). Active PAK can phosphorylate LIM kinase, which inactivates cofilin and inhibits actin depolymerization, thus resulting in spine formation. Gross hippocampal spine

abnormalities are observed in EphB1, EphB2 and EphB3 double and triple knock-out mice, with a reduction in the expression levels of both AMPA and NMDA glutamate receptors (Henkemeyer et al., 2003). Transgenic mice expressing a peptide inhibitor of PAK in the forebrain show altered spine morphology, with a reduction in spine density and increased head size (Hayashi et al., 2004). Moreover, treatment of cultured hippocampal neurons with PAK inhibitory domain results in the reduction of the ephrin-specific effects on spines formation (Penzes et al., 2003). Accordingly, also LIMK1 knockout mice show abnormal spine morphology: spines have larger heads and thicker necks compared to control mice (Meng et al., 2002).

Some Rho GTPase-interacting proteins function as scaffolds by localizing signalling molecules at neuronal cell-cell interaction sites. In this direction, GIT proteins (G-protein-coupled receptor kinase-interacting proteins) assemble complexes to target regulators of the actin cytoskeleton like the Rac GEF PIX and the Rac/Cdc42 effector PAK at spines (Zhang et al., 2003). Expression of dominant negative GIT1 constructs in cultured hippocampal neurons causes an increase in the number of dendritic protrusions concomitant with a decrease of mature mushroom-like shaped spines and synapses.

AIM OF THE WORK:

Some controversies in the current literature, concerning the function of GTPases on different aspects of neuronal development, have been probably originated by the attempt to unify data from different models, as *C.elegans*, flies and vertebrates in a common scheme. Up to now, most of the effects mediated by the Rho GTPases have been studied using over-expressed mutants that may interfere with the function of other related GTPases.

In addition, the majority of previous works studied the role of the Rac proteins in the development of the nervous system only by using Rac1 mutants. This approach cannot distinguish between the specific functions of each Rac isoform. This raises difficulties to reveal specific functions for the two different Rac genes expressed in vertebrate nervous system. This limitation is overcome by using isoform-specific Rac null-mutants. This work for the first time investigates the function of Rac GTPases in the development of the mammalian nervous system, by analysing the role of the neural-specific Rac3 protein and of the ubiquitously expressed Rac1 by using Rac null -mutants. The co-expression of Rac1 and Rac3 in the vertebrate nervous system suggests that they are needed to solve developmental and maintenance issues in the nervous systems of higher complexity.

The combination between *in vivo* and *in vitro* experimental approaches allows a better characterization of the role of these proteins during neuronal development.

In our laboratory, we have generated Rac3 knockout mice (Corbetta et al., 2005), conditional Rac1 knockout mice for the deletion of this gene in neurons and the double Rac3/Rac1 conditional knock-out mice. In this thesis, I thus combine the *in vitro* with the *in vivo* approaches to study the function of these proteins in neuronal development.

2 MATERIALS AND METHODS

2.1 Mice

Animal care was in accordance with institutional guidelines. SynI-Cre transgenic mice specifically expressing the viral Cre recombinase under the control of the synapsin I promoter in differentiated neurons (Zhu et al., 2001), Rac1F/F (Rac1flox/flox) mice carrying loxP sites between exons 4 and 5 of Rac1 gene (Walmsley et al., 2003), Rac3–/– mice with deletion of the Rac3 gene (Corbetta et al., 2005), and ROSA26 mice (Soriano, 1999). For the generation of mice with the specific conditional deletion of Rac1 in neurons, Rac1F/F mice were bred to SynI-Cre transgenic animals. Offsprings Rac1F/+SynI-Cre mice were crossed to Rac1F/F mice to obtain Rac1N mice (Rac1F/FRac3+/+SynI-Cre) carrying neuronal deletion of the Rac1 gene (Fig.2.1 A). For the generation of mice with inactivation of both Rac1 and Rac3 in neurons, Rac3–/– mice were bred to Rac1F/F mice to generate Rac1F/+Rac3–/+ mice. Rac1F/+Rac3–/+ mice were intercrossed to generate Rac1F/FRac3–/– mice (defined Rac3–/–). The Rac3–/– mice were mated to SynI-Cre mice to generate Rac3–/+SynI-Cre mice. These mice were crossed with Rac3–/– mice to obtain SynI-Cre/Rac3–/– mice, which were bred to Rac1F/FRac3–/– mice to generate Rac1F/+Rac3–/–SynI-Cre mice. Breeding of Rac1F/+Rac3–/–SynI-Cre and Rac1F/FRac3–/– animals was finally used to produce Rac1F/FRac3–/–SynI-Cre mice (defined Rac1N/Rac3-/-), carrying deletion of both Rac3 and Rac1 genes in neurons (Fig.2.1 B). For experiments, Rac1F/F mice were crossed with Rac1F/+SynI-Cre mice to obtain Rac1F/F and Rac1F/FSynI-Cre littermates, defined WT and Rac1N respectively in the text; while Rac1F/FRac3–/– mice were crossed with Rac1F/+SynI-Cre/Rac3–/– mice to obtain Rac1F/F/Rac3–/– and Rac1F/FSynI-Cre/Rac3–/– littermates, defined Rac3–/– and Rac1N/Rac3–/– respectively in the text.

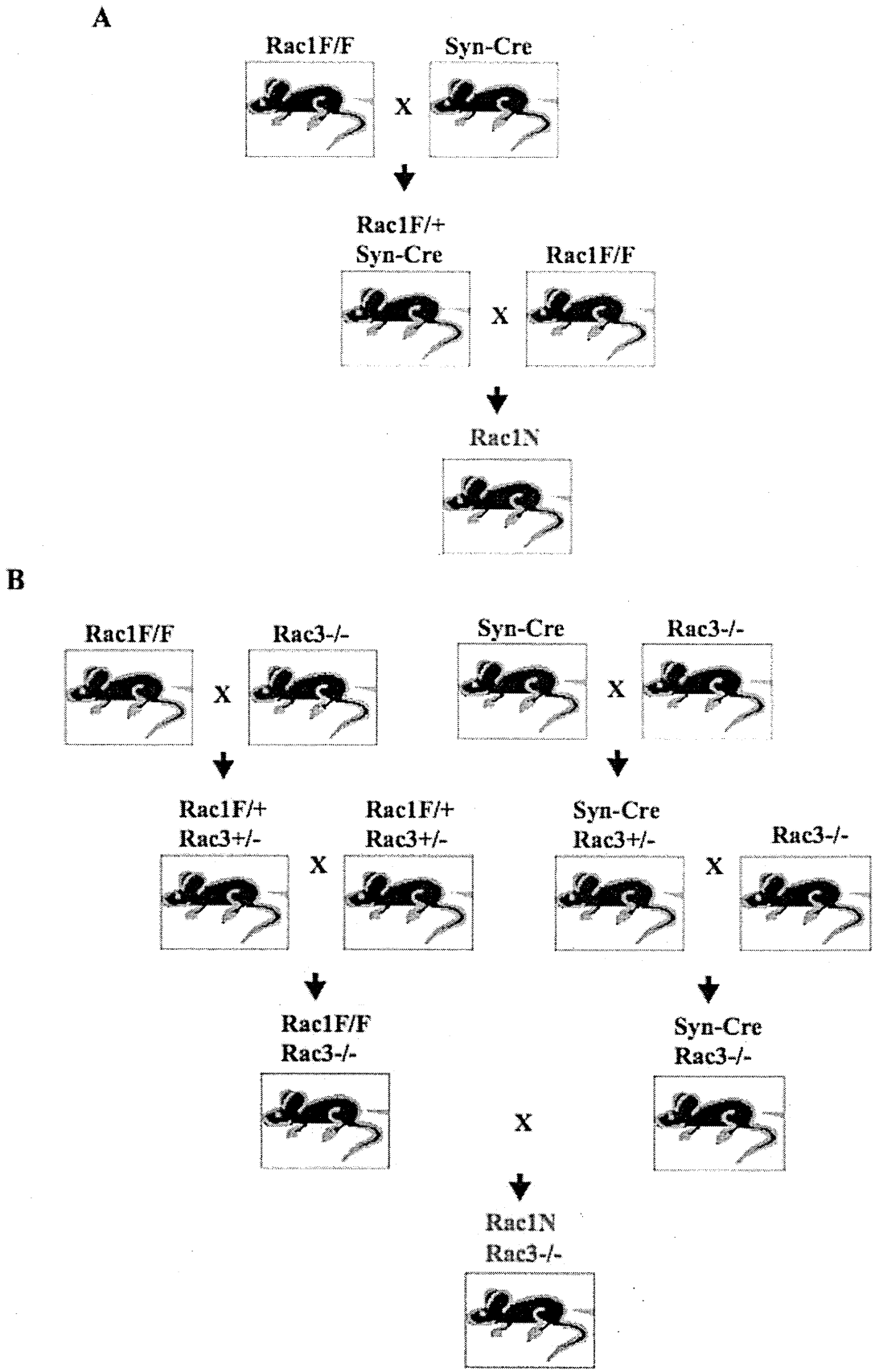

Figure 2.1 Scheme of the crosses performed to generate Rac1N and Rac1N/Rac3-/-. (A) Scheme of the crosses to generate the Rac1N (Rac1F/FSyn-Cre) mouse and (B) to generate the double Rac1N/Rac3-/- (Rac1F/F/Rac3-/-Syn-Cre) mouse.

2.2Analysis of genomic DNA

The genotypes were determined by PCR on genomic DNA from tails or different organs., Tail or organ samples were incubated overnight in lysis buffer [50 mM Tris- Cl pH=8, 100 mM EDTA, 100 mM NaCl, 1% SDS (sodium dodecyl sulfate), 1 mg/ml of proteinase K], followed by precipitation with isopropanol. Specific primers for PCR were: primers F1 (5'-CATTTCTGTGGCGTCGCCAAC-3') and R2 (5'-CACGCGGCCGAGCT GTGGTG-3') for the Rac3 wildtype allele; primer R3 (5'-TTGCTGGTGTCCAGACC AAT-3') from the lacZ gene for the Rac3 targeted allele. The 3 primers were used in a multiplex PCR with LA Taq (Takara) with the following amplification conditions: 1 min at 94°C, 30 cycles of 20 sec at 98°C and 1 min at 66°C, and 10 min at 72°C at the end of the run. Amplification products were resolved on a 1.6% agarose gel. Primers Pr1 (5'-ATTTTGTGCCAAGGACAGTGACAAGCT-3'), Pr2 (5'-GAAGGAGAAGAAGCTGAC TCCCATC-3'), and Pr3 (5'-CAGCCACAGGCAATGACA GATGTTC-3') were used for the identification of the floxed and deleted Rac1 alleles. PCR analysis with these primers was performed with GoTaq polymerase (Promega) under the following amplification conditions: 5 min at 94°C, 30 cycles of 30 sec at 94°C, 30 sec at 55°C, and 30 sec at 72°C, followed by 7 min at 72°C. For the SynI-Cre transgene we used the primers Pr4 (5'-CCAGCACCAAAGGCGGGC-3') and Pr5 (5'-TGCATCGACCGGTA ATGCAG-3') under the following conditions: 5 min at 94°C, 32 cycles of 30 sec at 94°C, 30 sec at 61°C, and 30 sec at 72°C, followed by 7 min at 72°C.

2.3Northern blot analysis

Total RNA was isolated from P13 brains and adult spleen with the RNeasy Midi kit (Qiagen). Northern blot analysis of total RNA (15 μg/lane) was performed as previously described (Lehrach et al., 1977). Blots were hybridized with a 378-bp PCR fragment corresponding to base pairs 181 to 558 of the translated Rac2 cDNA (amino acids 61 to

186), or with a 1.2-kb fragment corresponding to part of the 3' untranslated region of the Rac1 cDNA. Hybridization took place in hybridization buffer supplemented with 32P-labeled probes (1-2 x 106 cpm/ml) for 15 hours at 65°C. Following high-stringency washes at 65°C, X-ray films were exposed for 3-12 hours to the hybridized filters.

2.4 Reflexologic tests

10 animals for each genotype (WT, Rac1N, Rac3-/- and Rac1N/Rac3-/-) were tested for the following reflexologic tests at P3, P6, P9, and P12 following a well characterized protocol (Fox, 1965): righting reflex, negative geotaxis, cliff drop aversion, grasp reflex, and tail suspension. The responses in all tests except for the righting reflex were recorded using the following numerical scoring method: 0 (no response), 1 (weak response) and 2 (strong response). For the righting reflex, the maximal effect was graded as 3. The average scores for each group of mice were plotted for comparison. The weight of each animal was measured before the tests. Statistical significance was assessed by the Student's *t*-test. Differences were considered significant at a $P < 0.05$.

2.5Antibodies

The following antibodies and dilutions were used for biochemical and morphological analysis: anti-calretinin at 1:1000, and anti-tau-1 at 1:100 (Chemicon International, Temecula, CA); anti-neuronal β3-tubulin at 1:200 (Berkeley Antibody Company); anti-Cdc42 at 1:500, anti-p42-p44 MAPK at 1:1000, and anti-phospho- Thr202/Tyr204 p42-p44 MAPK at 1:1000 (Cell Signalling Technology, Danvers, MA); anti-phospho-Tyr596/Tyr602 Eph at 1:500 (Marston et al., 2003); anti-GFP at 1:400 (Molecular Probe Inc, Eugene, OR); anti-β1 integrin at 6 μg/ml (Tomaselli et al., 1988); anti-IRSp53 at 0.5 μg/ml (Choi et al., 2005); anti-Kalirin7 at 1:1000 (Penzes et al., 2000); anti-βPIX at 1:500

(Za et al., 2006); anti-Rac3 at 1:500 (Corbetta et al., 2005); anti-phospho-Ser310 WAVE1 at 1:1000 (Kim et al., 2006); anti-GluR2/3 at 1:100, anti-WAVE at 1:1000, anti-PSD95 at 1:500, anti-RhoA at 1:1000, and anti-Rac1 at 1:1000 (Upstate, Lake Placid, NY); anti-p35 at 1:1000, anti-Cdk5 at 1:1000, and anti-PAK1 at 1:1500 (Santa Cruz Biotechnology Inc, Santa Cruz, CA); anti-zinc transporter-3 (ZnT-3) at 1:200 (Palmiter et al., 1996); anti-calbindin at 1:200 (Swant, Bellinzona, Switzerland); anti- synapsin I at 1:200 (Valtorta et al., 1988); anti-paxillin at 1:1000, anti-PKL/GIT at 1:250 (BD Biosciences, San Jose, CA); anti-VAMP2 at 1:500 (Synaptic System, Göttingen, Germany); anti-tubulin at 1:2000 (Amersham Life Science, Little Chalfont, UK); anti-glyceraldehyde-3-phosphate dehydrogenase (GADPH) at 1:5000 (Biogenesis Inc, Pool, UK); anti-Cre recombinase at 1:500 (Covance, Emeryville, CA); anti-MAP2 at 1:500 (Sigma, St. Louis, MO). The anti-Liprin-α rabbit pAb was produced against thecarboxy-terminal fragment (amino acid residues 808-1202) of human Liprin-α1 fused to glutathione-S-transferase.

2.6 Biochemical analysis

All the operations were conducted at 4°C. Brains at the indicated developmental stages were extracted at with lysis buffer [1% TritonX-100, 150 mM NaCl, 1 mM Na-orthovanadate, 10mM NaF, 20 mM Tris-Cl pH=7.5, and protease inhibitors (Complete, EDTA-free, Protease Inhibitor Cocktail, from Roche)]. Lysates were transferred to new tubes and rotated for 15 min by end-over-end mixing. The insoluble fraction was removed by centrifugation for 15 min at 12,000 g. Protein determination was done using Bradford protein assay reagent from BIO-RAD.

2.6.1 Immunoprecipitation

Primary antibodies pre-adsorbed for 1 hour to 25 µl of protein A Sepharose beads (Amersham Biosciences) were added to lysates (2 mg protein/ immunoprecipitation), and incubated for 3 hours at 4°C with rotation. Immunoprecipitates were washed four times with 0.5 ml of lysis buffer with 0.5% Triton X-100.

2.6.2 Western blot analysis

Brain lysates (100 µg/lane) and immunoprecipitates were analyzed by SDS-PAGE, electrophoretically transferred to 0.2 µm PROTRAN® nitrocellulose membranes (Schleicher & Schuell BioScience GmbH, Germany) and stained with 0.2% Ponceau S in 3% TCA to visualize molecular weight standards and proteins. Filters were blocked for 1 h at RT with 5% non-fat dry milk or BSA (Roche) in 50 mM Tris-HCl, 150 mM NaCl (pH 7.5) and then incubated for 2 h in the same buffer containing the primary antibodies. After incubation with primary antibodies, filters were incubated for 1 hour with 0.2 µCi/ml of [125I]- protein A or [125I]-anti-mouse immunoglobulin (Amersham Biosciences), washed, and exposed to Amersham Hyperfilm-MP overnight.

2.6.3 Quantifications of protein levels

Films from blots were scanned with Personal Densitometer (Molecular Dynamics), and bands were quantified by ImageQuant 5 software (Molecular Dynamics). Values were compared between WT and Rac1N littermates, and between Rac3-/- and Rac1N/Rac3-/- littermates, respectively. Each value was normalized to the protein levels of an internal standard in the same lysate (tubulin or GADPH). To compare values obtained in different experiments, the variability between experiments was corrected as follows: in each

experiment, the value from each genotype was divided by the sum of the values of the two genotypes to be compared. The resulting ratios were analyzed by using the statistical program GraphPad Prism 4.0 (GraphPad software, San Diego California, USA), by two-way ANOVA analysis. Each experimental condition was repeated at least three times. Values of $P < 0.05$ were considered statistically significant.

For the determination of the relative amounts of Rac3 and Rac1 in brain, duplicate aliquots of brain lysates from wild-type mice at P7 (corresponding to the peak of Rac3 protein expression in brain) were immunoprecipitated with anti-Rac3 antibodies. Immunoprecipitates were blotted with either anti-Rac1 (recognizing both GTPases) or anti-Rac3-specific Abs. Blots were scanned, and the ratio between the values obtained with the two antibodies (anti-Rac3/anti-Rac1) was used to normalize with respect to Rac1 the values obtained by immunoblotting with anti-Rac3.

2.6.4 Synaptosomal fractions preparation

P13 mouse brains from the indicated genotype were suspended in homogenizing buffer [(10 mM Hepes-NaOH pH 7.4, 0.32 M sucrose, and protease inhibitors (Complete, EDTA-free, Protease Inhibitor Cocktail, from Roche)]. The brains were homogenized with 5 strokes in a Potter homogenizer. The homogenate (H) was centrifuged for 10 min at 1000 g. The resulting post-nuclear supernatant (S1) was separated by the nuclear pellets (P1) and centrifuged for 15 min at 10 000 g. The pellet was washed with homogenizing buffer and centrifuged once more for 15 min at 10 000 g. The resulting pellet represented the synaptosomal-enriched fraction (P2). The suspernatants from the two 10 000-g centrifugations were pooled (S2), and centrifuged for 1 h at 110 000 g in a TL-55 rotor for μ-ultracentrifuge TL-100 to separate the membrane pellet (P3) from the cytosolic fraction (S3). Synaptosomes were purified from crude membrane fraction by discontinuous sucrose density-gradient centrifugation as follow. The synaptosomal-enriched fraction (P2) was

suspended and brought to a final 0.8M sucrose and homogenized with 4 strokes in a Potter homogenizer. The homogenized was layered on a 1.2M sucrose solution [1.2 M sucrose, 10 mM Hepes-NaOH, pH 7.4, and 10 mg / ml^{-1} and protease inhibitors (Complete, EDTA-free, Protease Inhibitor Cocktail, from Roche)], and centrifuged for 20 min at 230 000 g in a SW55-Ti swinging bucket rotor for ultracentifuge L90K. The 0.8/1.2M sucrose interface was collected, suspended in the same volume of homogenizing buffer, layered onto 0.8M sucrose solution and centrifuged for 20 min at 230 000g in a SW55-Ti swinging bucket rotor for ultracentifuge L90K. The clean synaptosomes (Syn) are the pellet obtained. All fractions were analysed by sodium dodecyl sulfate (SDS)-polyacrylamide gel electrophoresis (PAGE) and immunoblotting.

2.6.5 Rac Activation assay

P7 brains from the indicated genotype were lysated in FISH buffer [(10% glycerol, 50 mM Tris pH 7.4, 100mM NaCl, 1% NP-40, 2mM $MgCl_2$ and protease inhibitors (Complete, EDTA-free, Protease Inhibitor Cocktail, from Roche)], with 5 strokes in a Potter homogenizer. The lysate was centrifuged for 10 min at 13000 rpm. The resulting supernatant was separated from the pellets and the indicated proteins amount was incubated for 1h at 4°C with 50 µl of glutathion-agarose beads (Sigma) pre-incubated with the fusion protein GST-CRIB domain, previously described (Sander et al., 1998). Briefly, Escherichia coli BL21 cells transformed with the GST–PAK-CD (CRIB domain) construct were grown at 37°C to an absorbance of 0.5. Expression of recombinant protein was induced by addition of 0.1 mM isopropylthiogalactoside for 2 h. Cells were harvested, resuspended in lysis buffer [(50 mM Tris- HCl, pH 8, 2 mM $MgCl_2$, 10% glycerol, 20% sucrose, 2 mM dithiothreitol, and protease inhibitors (Complete, EDTA-free, Protease Inhibitor Cocktail, from Roche)] and then sonicated.

Cell lysates were centrifuged for 20 min at 10000 rpm and the supernatant was incubated

with glutathione-coupled Agarose beads for 1h at 4°C. Protein bound to the beads was washed three times in lysis buffer and then equilibrated in FISH-Buffer.

The beads and lysated proteins bound to the fusion protein were washed three times in an excess of FISH-buffer and analyzed by sodium dodecyl sulfate (SDS)-polyacrylamide gel electrophoresis (PAGE) and immunoblotting.

2.7 Hippocampal neurons preparation

Primary neuronal cultures were prepared from hippocampi of embryonic day 17.5 mice from wild type and mutant mice, as described previously (Banker and Cowan, 1977).

2.7.1 Coverslips

All the procedures were done freshly before each neurons preparation.

24 mm diameter glass coverslips were placed in a coverslip rack (Thomson Scientific) in 69% nitric acid overnight, followed by 5 x 45 min washing with 2 l of MilliQ water. After the last washing coverslips were then dried on a hot plate and sterilized in the oven overnight.

Coverslips were then placed in the 3 cm diameter cell dishes. 4 small paraffin feet were then done on each coverslip with a glass Pasteur under hood, followed by poly (L-lysine)-coating (Sigma–Aldrich, Steinheim, Germany).

Poly (L-lysine)-coating: Poly (L-lysine) were diluted to 1mg/ml in filtered 0.1M Borate Buffer, pH 8.5 and filtered under hood. 500 µl/coverslip were used to completely cover their surface. Coverslips were then gently placed in the cell incubator at 37°C overnight.

Coverslips were washed 4 x 45 min with 0.5-2ml of autoclaved MilliQ water @ RT. After the last washing, 2 ml of plating medium [MEM (Life Technologies) supplemented with 10% horse serum (Hyclone, Logan, UT), 2 mM glutamine (BioWhittaker, Verviers,

Belgium), and 3.3 mM glucose] were added to each dish. These were placed in the cell incubator over-weekend.

2.7.2 Glia preparation

All the operations were performed in ice to avoid tissue degeneration.

Materials and Solutions:

P2 rats

Dissection tweezers, scissors, scalpels

6 cm diameter cell dishes

Optical fibers and dissection microscopy

15-50 ml Falcon tubes

20 ml syringes and 0.2μm pores filters

Glial medium

Dissection medium: HBSS (Hanks' Balanced Salt Solutions, w/o Ca^{++}, w/o Mg^{++})

Trypsin solution: 2.5mg/ml trypsin (Sigma–Aldrich, Steinheim, Germany) + 1mg/ml DNase (Calbiochem) in 15 ml HBSS with phenol red, w/o Ca^{++}, w/o Mg^{++} (add few μl of NaOH 0.1 N until reaching pink colour). Filter under hood.

Procedure:

P2 rat littermate was sacrificed. The head was cut off and placed in a new dish containing dissection medium. Under the microscope the skin layer was carefully removed with the tweezers. Then, by blocking the rat head with the tip of the tweezers inside the eyes, a superficial longitudinal cut along the midline of the brain cartilage was made in order to facilitate the cartilage removal. As soon as all the brain cartilage was detached, the brain was easily visible. The brain was removed and placed in a new dish-containing dissection medium. The majority of the meninges were removed. Cerebellum, olfactory bulbs,

hippocampus were removed from the hemispheres, that had to remain as clean as possible. They were then placed in a new dish-containing dissection medium.

The hemispheres were minced with the scalpels under hood and transferred in a 15 ml falcon tube. Two washes in HBSS were done before adding 7 ml of trypsin solution and incubating for 15 min @ 37°C. The supernatant were removed and diluted 1:1 in gial medium [MEM supplemented with 10% horse serum, 2 mM glutamine, penicillin, streptavidin and 34 mM glucose] in a 50 ml falcon tube. The remained pellet was incubated with other 7 ml of trypsin solution for 15 min @ 37°C. The second supernatant was add to the first supernatant and centrifuged for 10 min @ 600 rpm.

The pellet was re-suspended in 1ml/brain of glial medium and plated in 1flask/brain (75 cm^2 flask, Nunc). 24 hours later fresh glial medium was replaced, and the flasks were maintained for 1 month in culture, by changing the medium weekly.

2-3 days before the dissection of the hippocampi, 3 cm diameter cell dishes, equal to the coverslips number, were prepared from a 75 cm^2 flask of confluent glia cells, as follow. The flask containing glia cells was washed with PBS @ 37°C. Cells were then incubated with 2 ml of trypsin for 2 min in the cell incubator. Trypsin was then inactivated with 9 ml of glial medium, and 200µl of this cell suspension were plated in each cell dish. 15min-1h before the dissection of the hippocampi the glial medium was replaced with 2 ml of fresh hippocampal medium [MEM supplemented with 1% N2 supplement (Invitrogen, San Diego, CA), 2 mM glutamine, 1 mM sodium pyruvate (Sigma–Aldrich) and 4 mM glucose].

2.7.3 Dissection of hippocampi

All the operations were performed in ice to avoid tissue degeneration.

Materials and Solutions:

E17.5 mouse embryos

Dissection tweezers, scissors

6 cm diameter cell dishes

Optical fibers and dissection microscopy

15 ml Falcon tubes

5 ml syringes and 0.2μm pores filters

Hippocampal medium

Dissection medium: HBSS, w/o Ca^{++}, w/o Mg^{++}

Trypsin solution: 25mg/ml trypsin (Sigma–Aldrich, Steinheim, Germany) in HBSS with phenol red, w/o Ca^{++}, w/o Mg^{++} (add few μl of NaOH 0.1 N until reaching pink colour). Filter under hood.

Procedure:

The pregnant mouse was sacrificed in a CO^2 chamber. It was then placed with its ventral side upward. Using scissors, a superficial "V-shape" cut was made on the ventral side. The utero containing embryos was removed and placed in dissection medium. Placenta and yolk sack were removed from each embryo, the head was cut off immediately and placed in a new dish containing dissection medium. Under the microscope the skin layer was carefully removed with the tweezers. Then, by blocking the embryo head with the tip of the tweezers inside the eyes, a superficial longitudinal cut along the midline of the brain cartilage was made in order to facilitate the cartilage removal. As soon as all the brain cartilage was detached, the brain was easily visible. The brain was removed and placed in a new dish-containing dissection medium. The majority of the meninges were removed. Then the cerebral cortex from each hemisphere was slightly lifted in order to identify each hemi-hippocampus that was removed from the cerebral hemispheres and placed in a new dish-containing dissection medium.

4/5 coverslips/ embryo: for a low-density culture [short-term cultures (ST)]

2 coverslips/ embryo: for a high-density culture [long-term cultures (LT)]

The following operations were performed under hood:

Hippocampi were transferred in a 15 ml falcon tube and washed 2 times with 5-7 ml of dissection medium, depending on their number. Tryspin solution, diluted 1:10 in dissection solution, was added to the hippocampi in 3-5 ml final volume. Tryspin incubation was 15 min in the cell incubator. Trypsin was the washed 2 times with 5-7 ml of dissection medium. The hippocampi were then re-suspended in a final volume of dissection medium that was calculated as follow: 200 µl x n° total coverslips (n° coverslips for ST cultures = 4-5 x n° embryos; n° coverslips for LT cultures = 2 x n° embryos). The hippocampi were then dissociated mechanically using a 10 ml pipette, up and down for maximum 20 times. 200 µl of the cell suspension were then plated in the dishes containing the coated coverslips.

Four hours after plating, coverslips were transferred into new dishes containing glia-conditioned hippocampal medium. Cells were incubated at 37°C in 5% CO^2 humidified atmosphere for the time indicated.

2.8 Transfections

2.8.1 Lipofectamine

Hippocampal neurons were transfected at 4 DIV with either the pEGFP-N1 (1 µg) plasmid (Clontech, Mountain View, CA), or co-transfected with pEGFP-N1 (0.5 µg) and pEGFP-CRE plasmids (0.5 µg) (Rico et al., 2004) by using LipofectamineTM 2000 (Invitrogen) in hippocampal medium. Each transfection reaction was performed as follow. Lipofectamine mix (198.4 µl of hippocampal medium with 1.6 µl LipofectamineTM 2000) was prepared 7 min before being added to the DNA mix [1µg DNA (1µg/µl) in hippocampal medium to

200 µl final volume]. Lipofectamine mix was then added to DNA mix and incubated for 25 min @ RT before being added to neurons. Coverslips with hippocampal neurons were transferred in new 3 cm diameter dishes in 1.1 ml hippocampal medium. The transfection mix was then added to the neurons and left for 1 hour in the cell incubator. At the end of the incubation time, coverslips were replaced in the dishes containing glia cells and incubated for the indicated time.

2.8.2 Electroporation

Hippocampal neurons in suspension, before plating, were electroporated with siRNA oligonucleotides (0.6 µg of RNA with 2.5 µg of pEGFP-N1 /electroporation; the neurons obtained from three hippocampi were used for each electroporation), following the basic nucleofection protocol for primary mammalian neural cells (AMAXA Biosystems Gaithersburg, MD, U.S.A.). The neuronal suspension was diluted in dissection medium to 3 ml final volume/electroporation, and centrifuged @ 600 rpm for 5 min at 4°C. The supernatant was carefully removed and the pellet was re-suspended in 95 µl of electroporation mix (AMAXA) together with 5 µl of DNA+RNA mix to a final volume of 100 µl. The suspension was then transferred in the electroporation cuvette and the O-05 program was used. The cells were re-suspended in 800 µl plating medium and 200µl/ coverslip were plated. Cells were incubated at 37°C in 5% CO^2 humidified atmosphere for the time indicated.

2.9 siRNA

Rac1 and control (luciferase) siRNA duplexes were obtained from Invitrogen Ltd (Paisley, Scotland, U.K.). All siRNA candidates were evaluated and scored by the Sirna algorithm according rational design criteria (http://sfold.wadsworth.org/index.pl). The three highest scoring candidates with the lowest similarity for mouse Rac3 were selected, corresponding

to the following target sequences within the open reading frame of mouse Rac1 mRNA: rac1-1, GCATTTCCTGGAGAGTACA; rac1-2, TGTCCCAATACTCCTATCA; rac1-3:AAGCTATCCGAGCGGTTCTCTGT. As a control, the following target sequence for luciferase mRNA was used: CATCACGTACGCGGAATAC. For knockdown of Rac1, COS7 cells were either transfected with 50 nM siRNA oligonucleotides or co-transfected with 50 nM siRNA oligonucleotides with either pFLAG-Rac1 or pFLAG-Rac3 plasmid using LipofectamineTM 2000 (Invitrogen) in serum-free DMEM (Dulbecco's modified Eagle's medium). siRNA-transfected COS7 cells were incubated in growth medium [DMEM supplemented with FCIII (fetal clone III)] for 3 days before fixation, and then analysed by immunofluorescence or immunoblotting.

2.10 Immunofluorescence

After fixation of cells with 4% paraformaldehyde in 4% sucrose, 2 mM EGTA and 120 mM sodium phosphate pH=7.4, cells were washed two times in PBS and processed for immunofluorescence with the indicated antibodies. Primary antibodies and TRITC-conjugated phalloidin (Sigma–Aldrich), for F-actin staining, were diluted in GSDB solution (0.3% Triton X-100, 16% goat serum, 450 mM NaCl, 20 mM sodium phosphate pH=7.4). Primary antibodies were detected with Alexa Fluor 488/568-conjugated secondary antibodies (Molecular Probes, Eugene, OR) diluted in GSDB solution. Images were captured with a Zeiss Axiophot epifluorescence microscope (Zeiss) equipped with a C4742-95-12HR digital camera (Hamamatsu), or Axiovert S100TV microscope (Carl Zeiss AG), equipped with an ORCA II cooled CCD (charge-coupled device) camera (Hamamatsu Photonics, Hamamatsu City, Japan).

2.11 FM4-64 assay

Hippocampal neurons (14 DIV) from wild-type and Rac3 knockout mice were incubated with 10 μM FM4-64 (Molecular Probes) in depolarizing solution (KRH supplemented with 45 mM KCl) to load recycling synaptic vesicles (Pyle et al., 2000). The incubation was carried out for 30 s at room temperature. Cells were rinsed for 10 min at a flow rate of 500 μl/min with KRH containing 10 μM 6-cyano-2,3-dihydroxy-7-nitroquinoxaline and 1 μM tetrodotoxin (Tocris, Ellisville, MO, U.S.A.). Images were recorded with a Zeiss Axiovert135 microscope (Carl Zeiss) equipped with an ORCAII cooled CCD camera (Hamamatsu Photonics) and processed using Image Pro Plus 4.5 (Media Cybernetics, Silver Spring, MD, U.S.A.) and Adobe Photoshop® 8. Images of the terminals labelled with FM4-64 were acquired under constant conditions, and FM4-64 fluorescence intensity was measured within an area of 4 pixels X 4 pixels at the centre of synapse.

2.12 Time-lapse analysis

Coverslips were incubated in KRH (Krebs–Ringer–Hepes: 150 mM NaCl, 5 mM KCl, 1.2 mM MgSO4, 1.2mM KH2PO4, 2 mM CaCl2, 10 mM glucose and10 mM Hepes/NaOH, pH 7.4) in a temperature-controlled chamber at 37°C. Images were taken at 1 min intervals over 15 min with a Deltavision Widefield Microscopy System (Applied Precision, Bratislava, Slovakia), equipped with an IL-70microscope (Olympus) and a Cool SnapHQ digital camera (Roper Scientific Inc., Tucson, AZ, U.S.A.).

2.13 Morphological analysis

2.13.1 Analysis of neuritic length

Neurons were fixed at the time indicated. Images were processed using AdobePhotoshop® 8. The length of neurites, and the number of total neuritic tips, nodes and primary neurites, were measured using the public domain NIH Image software (Image J). At least 20 neurons for each condition, from two independent experiments, were used for the quantification. The data were analysed by the Student's *t* test (two-tailed distribution and two-sample unequal variance).

2.13.2 Analysis of dendritic spine morphology

Neurons were fixed at 14 DIV. Images were processed using AdobePhotoshop® 8 and the public domain NIH Image J software. For quantification, in each experiment 15-30 different 100 μm segments of primary and secondary dendrites from 7-10 neurons were analyzed for spines and protrusions. Two independent experiments were analyzed for each condition. GFP-positive dendritic protrusions were classified according to their morphology: mature spines including mushroom-shaped and stubby spines; other protrusions with no head, including short filopodia (<4 μm long), long filopodia (>4 μm long), and lamellipodia. The total protrusion density per 100 μm of dendrite was calculated by including all morphological classes of dendritic protrusions. At least 450 protrusions per condition per experiment have been considered for the quantification. The reported values represent mean values ± SEM. The data were analysed by the Student's *t* test (two-tailed distribution and two-sample unequal variance).

3 RESULTS

3.1 Rac3 during neuronal development

3.1.1 Characterization of Rac3 protein expression in mouse brain

Previous data obtained in our laboratory have shown that Rac3 is developmentally regulated both in avian and mouse brain, starting its expression around E13.5 and reaching the peak at P7 (in mouse), corresponding to the time of intense neurite branching and synaptogenesis (Bolis et al., 2003). I thus wanted to analyse the specific expression pattern of Rac3 among the different area of the mouse brain to characterise regions with higher expression. Recent work in our lab has defined the pattern of Rac3 mRNA expression in P7 mouse brain (Fig 1.3.4.1). I performed the biochemical characterization to detect the Rac3 protein in different regions of the P7 and adult mouse brain that showed higher levels of Rac3 mRNA. I used our previously characterized Rac3-specific polyclonal antibody (pAb) (Bolis et al., 2003; Corbetta et al., 2005) to immunoprecipitate the endogenous protein from lysates prepared from different areas of the mouse brain. Expression of the Rac3 protein in hippocampus, cerebellum and cerebral cortex was highest around P7 (Fig. 3.1B), while very low levels of the protein were detectable in the adult (Fig. 3.1C), supporting the hypothesis of a prominent function of Rac3 during development. As suggested by in situ hybridization analysis, glial cells were negative for the Rac3 protein, indicating a Rac3 neuronal-specific expression in the brain (Fig. 3.1B).

I then characterised the relative amount of Rac3 and Rac1 proteins in P7 mouse brain, as described in Material and Methods. At the peak of expression, Rac3 represented about 8% of total Rac in brain (Fig. 3.2). Since Rac3 distribution is more restricted than Rac1 (Corbetta et al., 2005), its expression in neurons is likely to be higher than the average percentage in the whole brain.

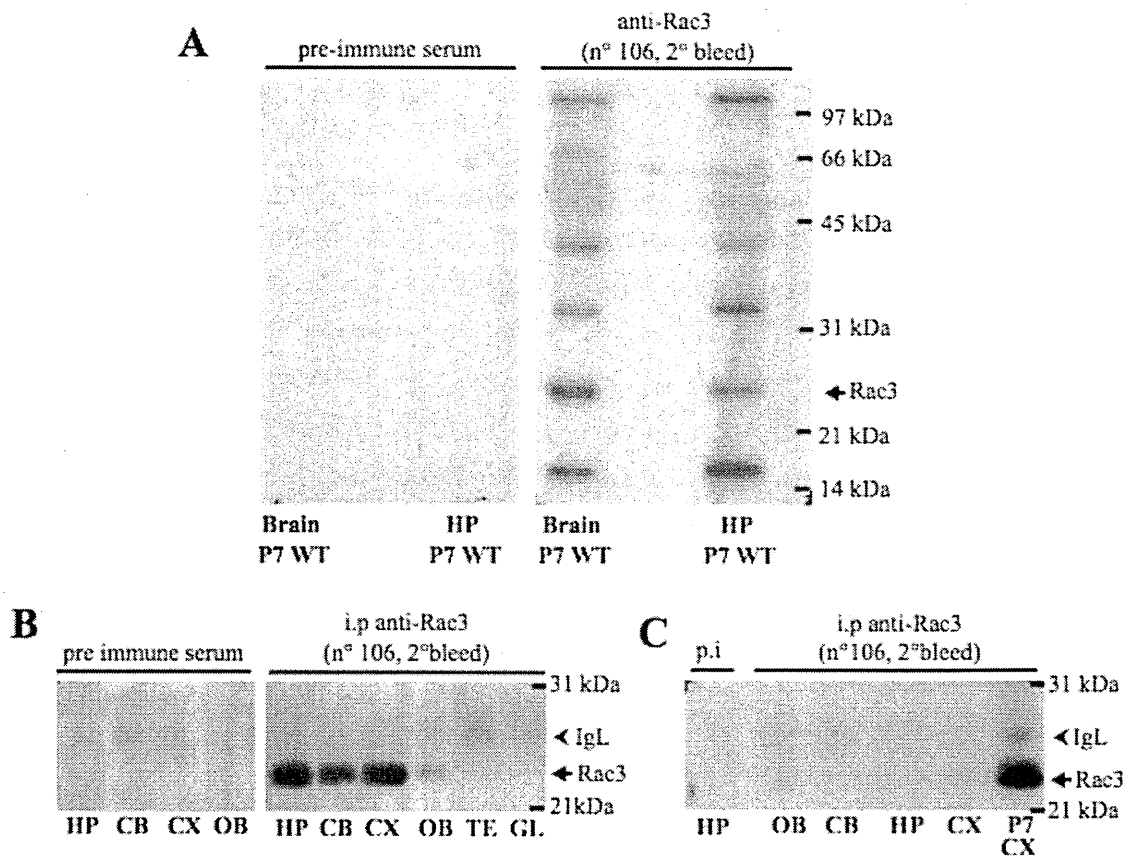

Figure 3.1 Biochemical characterization of Rac3 levels in P7 and adult wild-type brain.

(A) Rac3 protein is expressed in P7 mouse hippocampus. Immunoblotting on lysates obtained from wild-type (WT) P7 mouse total brain (positive control) and P7 mouse hippocampus using anti-Rac3 Ab [right panel, (Bolis et al., 2003; Corbetta et al., 2005)] or pre-immune serum as negative control (left panel). The band specific to Rac3 is shown (arrow). 150 μg lysate was loaded for each lane. (B,C) Rac3 protein is enriched in P7 mouse hippocampus, cerebral cortex and cerebellum. Lysates from the indicated brain regions obtained from P7 (B) and adult (C) mice (2 mg protein lysate), from P7 mouse testis (1,3 mg protein lysate), and from glial cell cultures (from P1 mice, 0,76 mg protein lysate) were immunoprecipitated with anti-Rac3 pAb (serum 106, 2° bleed), or with pre immune serum (negative control). The filter was blotted with anti-Rac1 mAb. Higher levels of the protein were found in P7 hippocampus, cerebellum and cortex, while no Rac3 was detected in glial cells. Rac3 levels were much lower in adult tissues compared to P7 tissues. The specific Rac3 band (arrow) and the IgG light chain (arrowhead) are shown. Molecular weights are indicated. HP, hippocampus; CB, cerebellum; CX, cerebral cortex; OB, olfactory bulbs; TE, testis; GL, glial cells and p.i, pre immune.

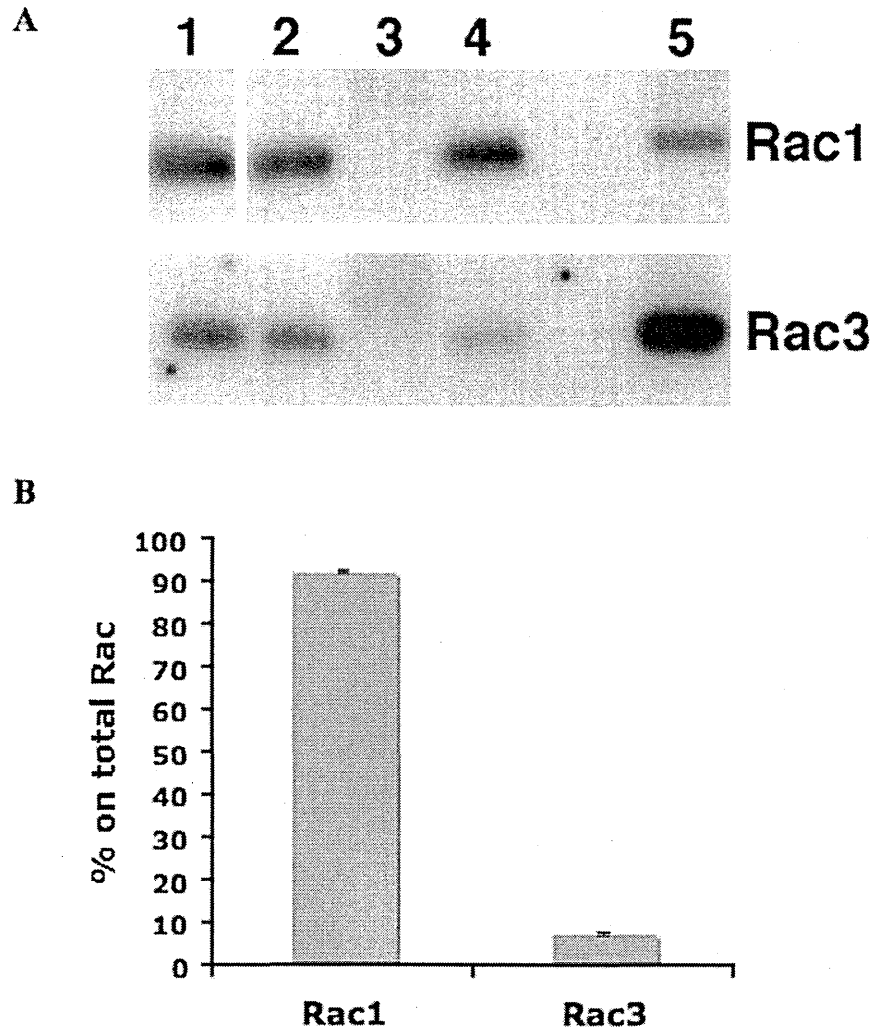

Figure 3.2 Relative amounts of Rac3 and Rac1 in P7 mouse brain. (A) Duplicate samples (upper and lower filters) from P7 brain lysates from wild-type animals were immunoprecipitated with anti-Rac3 pAb and blotted with either anti-Rac1 mAb recognizing both Rac1 and Rac3 (upper filter), or anti-Rac3-specific pAb (lower filter). In each of the two blots: lane 1, 200 μg of lysate; lanes 2 and 4, 200 μg of unbound fractions after immunoprecipitation with preimmune or immune anti-Rac3 Ab, respectively; lanes 3 and 5, immunoprecipitation from 2 mg of lysate with pre-immune serum or immune anti-Rac3 pAb, respectively. (B) Quantification on blots (see Materials and Methods) from two independent experiments shows that Rac3 and Rac1 represent about 7.6% (+/-0.4 s.d.) and 92.4% (+/-0.44 s.d.), respectively, of the total Rac in P7 mouse brain lysates.

3.1.2 The choice of the experimental system: hippocampal neuron cultures

In our laboratory we have generated the Rac3 knockout mice (Rac3-/-) (Corbetta et al., 2005). Rac3-/- animals developed normally and did not show gross morphological alterations in the brain, they were fertile and viable. The lack of a strong phenotype could possibly be due to compensation by the co-expressed Rac1 protein. In this direction, I found an increase of active Rac1 in Rac3 knockout brains (Fig. 3.3). On the other hand Rac3 knockout mice displayed abnormal behaviours, suggesting a role of Rac3 during the formation or function of neuronal circuits important for cognitive functions (Corbetta et al., 2005). I then analysed the effects of the depletion of Rac3 during *in vitro* neuronal development. Hippocampal neurons develop *in vitro* by recapitulating the developmental steps observed *in situ* (Bartlett and Banker, 1984a; Bartlett and Banker, 1984b; Dotti et al., 1988). Cultured neurons are growing in more stringent conditions as compared to the *in vivo* situation. This might enhance possible defects that could be more easily compensated by the complex environment in the animal. We have shown that Rac3 was highly expressed in the CA1-CA3 regions of the mouse hippocampus (Fig 1.3.4.1). For this reason I took advantage of the well-established system of rat hippocampal cultures (Bartlett and Banker, 1984a; Bartlett and Banker, 1984b; Dotti et al., 1988) and I adapted it to culture mouse hippocampal neurons. In brief, the hippocampi were isolated from embryonic day 17.5 (E17.5) mice, mechanically dissociated and plated onto poly-L-lysine-coated coverslips. Embryonic hippocampus is a discrete structure whose CA1-CA3 layers can be readily dissected from the brain. Hippocampal cultures are mostly composed of pyramidal neurons (90%) that develop from E15 and become postmitotic at E17.5. The dentate gyrus will develop mainly postnatally. A further advantage of this system is that the number of glial cells at this time is still low. I was therefore able to isolate an almost pure population of postmitotic neurons that will differentiate after plating. Moreover, it is possible to set up low-density hippocampal cultures that allow performing high-resolution

analysis of individual neurons by fluorescent and time-lapse microscopy.

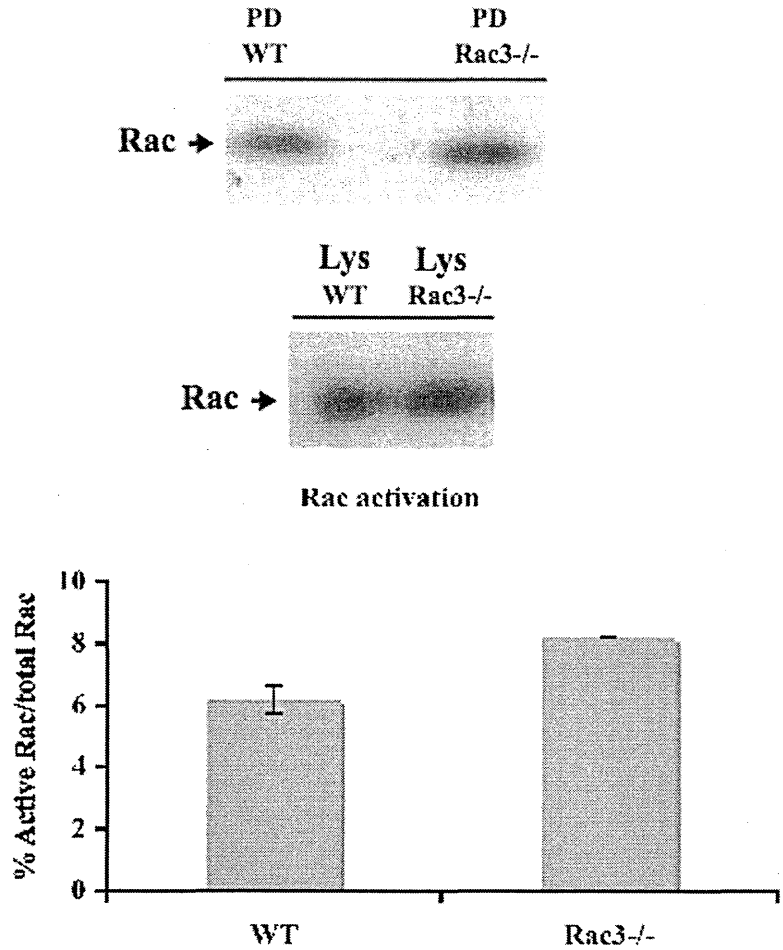

Figure 3.3 Increase of Rac activity in P7 Rac3-/- mouse brain. Rac activity was assessed by pull down assays as described in Material and Methods. Briefly, 3 mg of P7 brain lysates (Lys) from wild-type (WT) and Rac3-/- mice were incubated with GST-CRIB-bound glutathione beads. 100 μg of total lysates from each sample were loaded to evaluate total Rac levels. Immunoblotting was performed using the anti-Rac1 mAb (upper panels). Quantification shows an increased level of active GTP-Rac1 in Rac3-/- mouse brain (1.3 fold, n=2).

3.1.3 Rac3 expression in hippocampal cultures

We tried to characterize the expression of Rac3 protein in cultured hippocampal neurons by using our anti-Rac3 polyclonal antibody. Unfortunately, this antibody works specifically only by immunoprecipitation and western blotting. I therefore was not able to characterize the subcellular distribution of Rac3 by immunofluorescence on cultured neurons.

To overcome this technical problem, I conducted a biochemical analysis of the expression of Rac3. I was able to obtain 60 μg of total protein lysate from a pool of 8 independent coverslips with cultured neurons at 6 DIV. I could not detect a Rac3 positive band in this lysate, while a band for Rac3 was detected in a lysate from 100 μg of P7 mouse brain lysate (positive control) (Fig 3.4A). I re-blotted the same filter with the anti-Rac1 antibody in order to evaluate the presence of Rac1 in the lysates.

I then analysed the expression of Rac3 in hippocampi from E17.5 mice (the same stage in which we perform the dissection) by Rac3 imunoprecipitation. Using this approach I showed that Rac3 is expressed in the hippocampus of mouse embryos used for the preparation of the hippocampal cultures (Fig 3.4B).

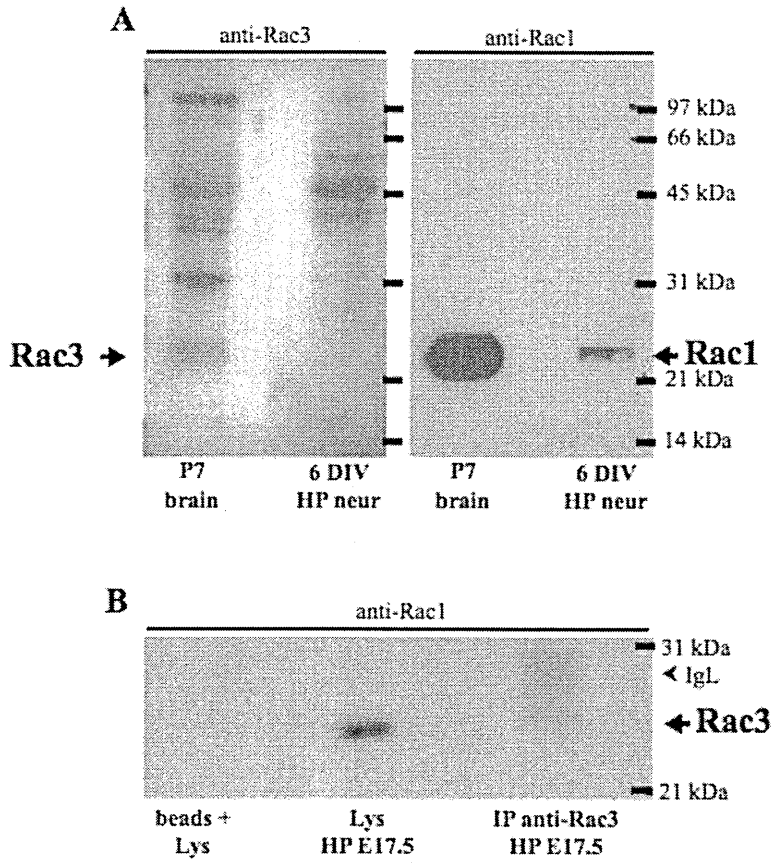

Figure 3.4 Biochemical characterization of Rac3 protein levels in developing hippocampal neurons. (A) Immunoblotting on lysates obtained from 6 DIV mouse hippocampal cultures and from P7 mouse brain using anti-Rac3 pAb (left panel). The filter was stripped and re-blotted with anti-Rac1 mAb (right panel). 60 µg of protein lysate were loaded in each lane. Molecular weights, Rac3 and Rac1 bands are indicated. Rac3 is undetectable in the lysate from 6 DIV cultures. (B) Rac3 protein is expressed in E17.5 mouse hippocampi. 1,5 mg protein lysate from E17.5 hippocampi were immunoprecipitated with anti-Rac3 pAb. The same amount of lysate was incubated with beads alone as control. 100 µg of total lysate (Lys) were loaded in the middle lane. The filter was blotted with anti-Rac1 mAb. HP, hippocampus; HP neur, hippocampal neurons.

3.1.4 Morphological analysis of Rac3-/- hippocampal neurons

Hippocampal neurons isolated from Rac3-/- mice developed normally in culture. Rac3-/- neurons did not show abnormalities both at early and later phases of in vitro development (Fig 3.5- 3.9). I conducted morphological analysis on Rac3-/- neurons at different stages. Staining of neurons at 1, 2 and 3 DIV with antibodies against cytoskeletal components showed that Rac3 depletion did not affect neuritogenesis and the establishment of neuronal polarity: Rac3-/- neurons developed normal dendrites and axons (Fig 3.5-3.7). I quantified the total neuritic length (Fig. 3.5 B), the number of total neuritic tips and the number of primary neurites per neuron (Fig. 3.5 C). I did not find differences between wild-type and Rac3-/- neurons at 1 DIV. F-actin and neuronal β-3-tubulin were not altered also at later phases of neuritogenesis, at 2, 3 and 7 DIV (Fig. 3.7). I then evaluated the effects of the depletion of Rac3 in later development, during synaptogenesis. The lack of Rac3 did not affect the formation of synaptic contacts. At 7 DIV the staining for the synaptic proteins VAMP2 (vesicle-associated membrane protein 2) and for synapsinI was enriched at the pre-synaptic boutons (Fig. 3.8). I measured the synaptic activity of Rac3-/- mature neurons (14 DIV) by analysing the uptake of the FM4-64 dye upon membrane depolarization by high extracellular K^+. Quantitative analysis of FM4-64 uptake measured at single synaptic boutons showed that the distribution of FM4-64 fluorescence intensities was similar in wild-type and Rac3-/- neurons (Fig.3.9). Given the high similarity between Rac1 and Rac3, it is possible that these GTPases have redundant functions during development, and that Rac1 could at least partially compensate for Rac3 depletion. I then tested if Rac1 was upregulated in cultured neurons. As previously reported (Kumanogoh et al., 2001), the anti-Rac1 mAb, recognizing both Rac1 and Rac3, showed a diffuse staining in the cell body and along neurites. Immunofluorescence using the Rac1 antibody did not reveal an evident increase in total Rac levels (Fig 3.10). However I could not exclude a compensatory effect due to the specific increase in the active GTP-bound form of Rac1, as

observed in the whole brain (Fig3.3).

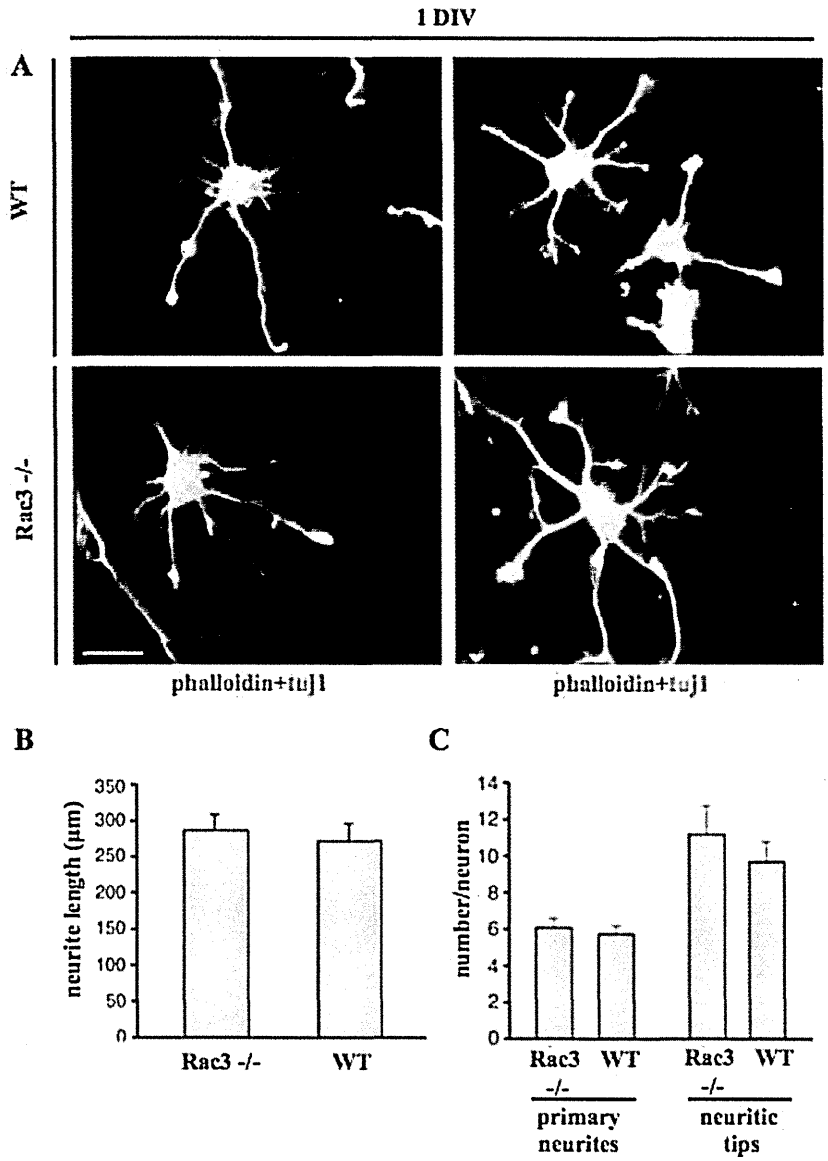

Figure 3.5 Hippocampal neurons from Rac3-/- mice reveal no major defects during early phase of neuritogenesis. (A) 1 DIV hippocampal neurons from wild-type (wt) and Rac3 knockout (Rac3-/-) embryos were stained with anti-neuronal β3-tubulin mAb (green) and phalloidin (red). (B,C) No significant differences were found between wild-type and knockout neurons for total neuritic length (axon and dendrites) (B), number of total neuritic tips and primary neurites per neuron (C). The results are expressed as the means (+/−S.E.M.) for two independent experiments. 20 neurons were analysed for each condition. Scale bar, 20 µm.

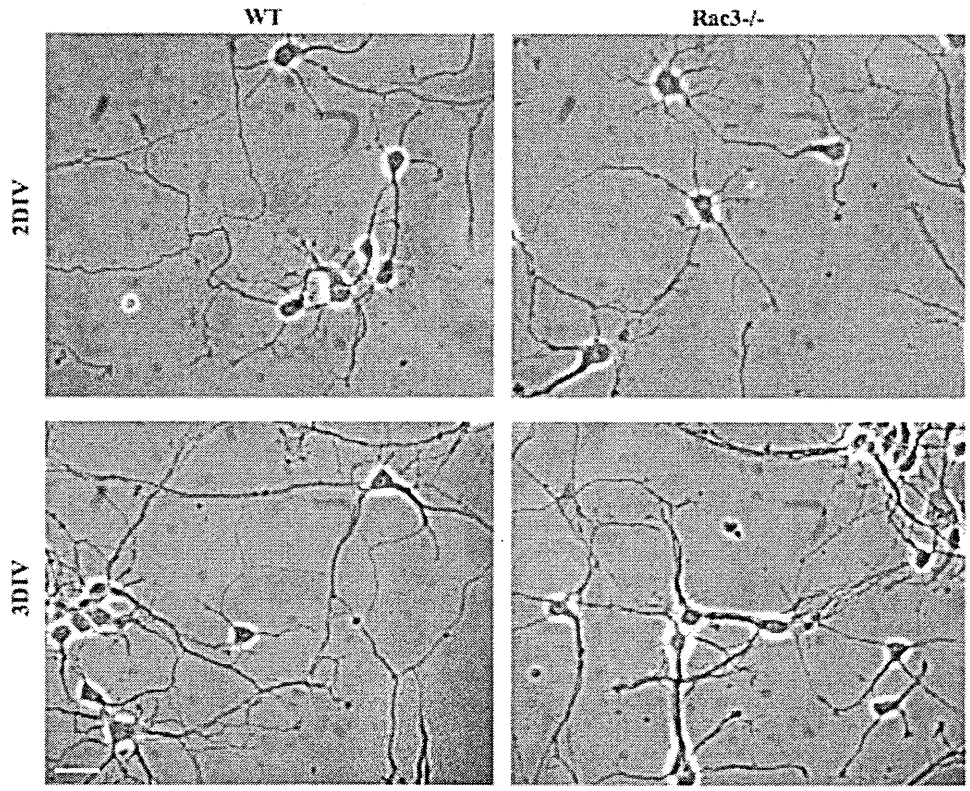

Figure 3.6 Hippocampal neurons from Rac3-/- do not show major defects during later phase of neuritogenesis. 2 DIV (upper panels) and 3 DIV (lower panels) hippocampal neurons from wild-type (WT) and Rac3 knockout (Rac3-/-) embryos were acquired using phase contrast microscopy. Scale bar, 20 μm. Rac3-/- cultures show similar neuritic network complexity as WT.

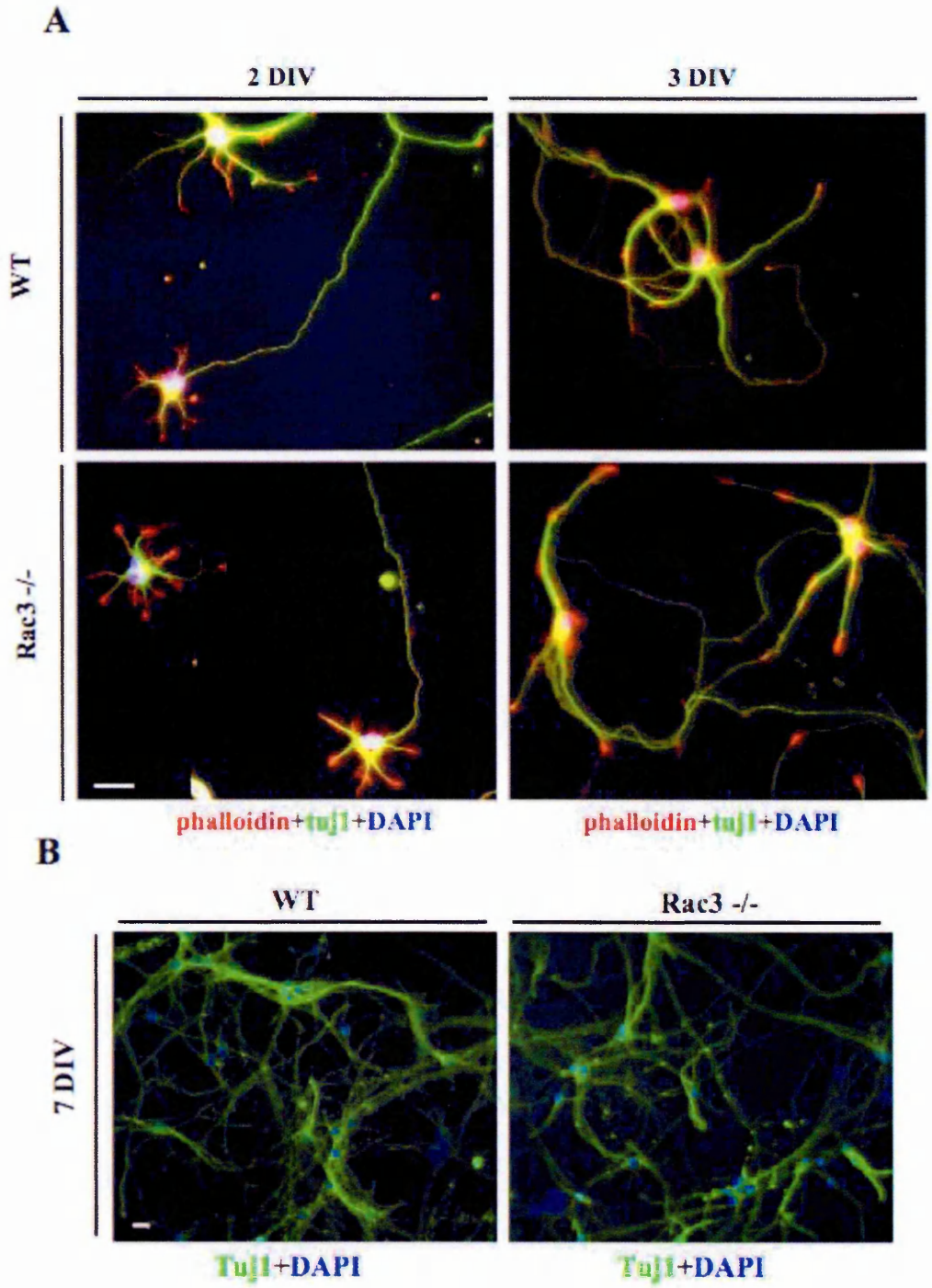

Figure 3.7 Morphological analysis of cultured hippocampal neurons from Rac3-/- mice reveals no cytoskeletal alterations during later phases of neuritogenesis. (A) 2 DIV (left panels) and 3 DIV (right panels) hippocampal neurons from wild-type (wt) and Rac3-/- embryos were stained with anti-neuronal β3-tubulin mAb (green) and phalloidin (red). Scale bar, 20 μm. (B) 7 DIV hippocampal neurons from wt and Rac3-/- embryos were stained with anti-neuronal β3-tubulin mAb (green) and DAPI (blue). Scale bar, 20 μm.

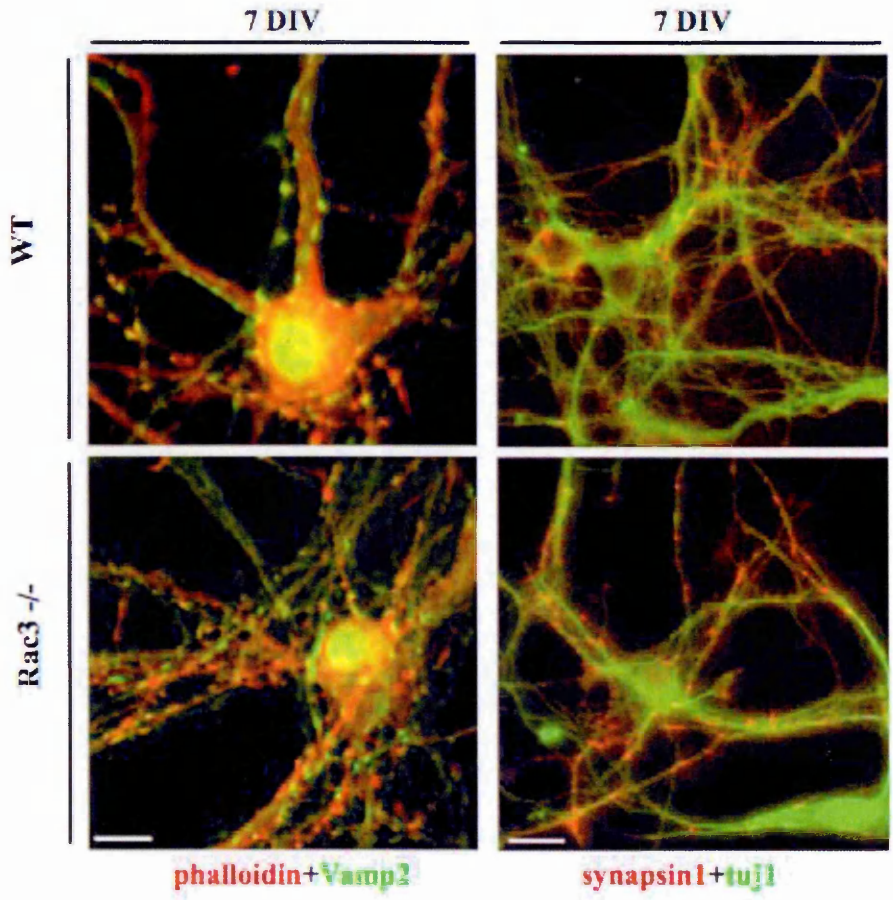

Figure 3.8 Morphological analysis of cultured hippocampal neurons from Rac3-/- mice reveals no major defects during synaptogenesis. 7 DIV hippocampal neurons from wild-type (wt) and Rac3-/- embryos were stained with anti-VAMP2 mAb (green) and phalloidin (red) (left panels) or anti-neuronal β3-tubulin mAb (green) and anti-synapsin I pAb (red) (right panels). Rac3-/- neurons show the same pattern of synapsin I- and Vamp2-positive vesicles along axonal tracts. Scale bars, 10 μm (left panels) and 20μm (right panels).

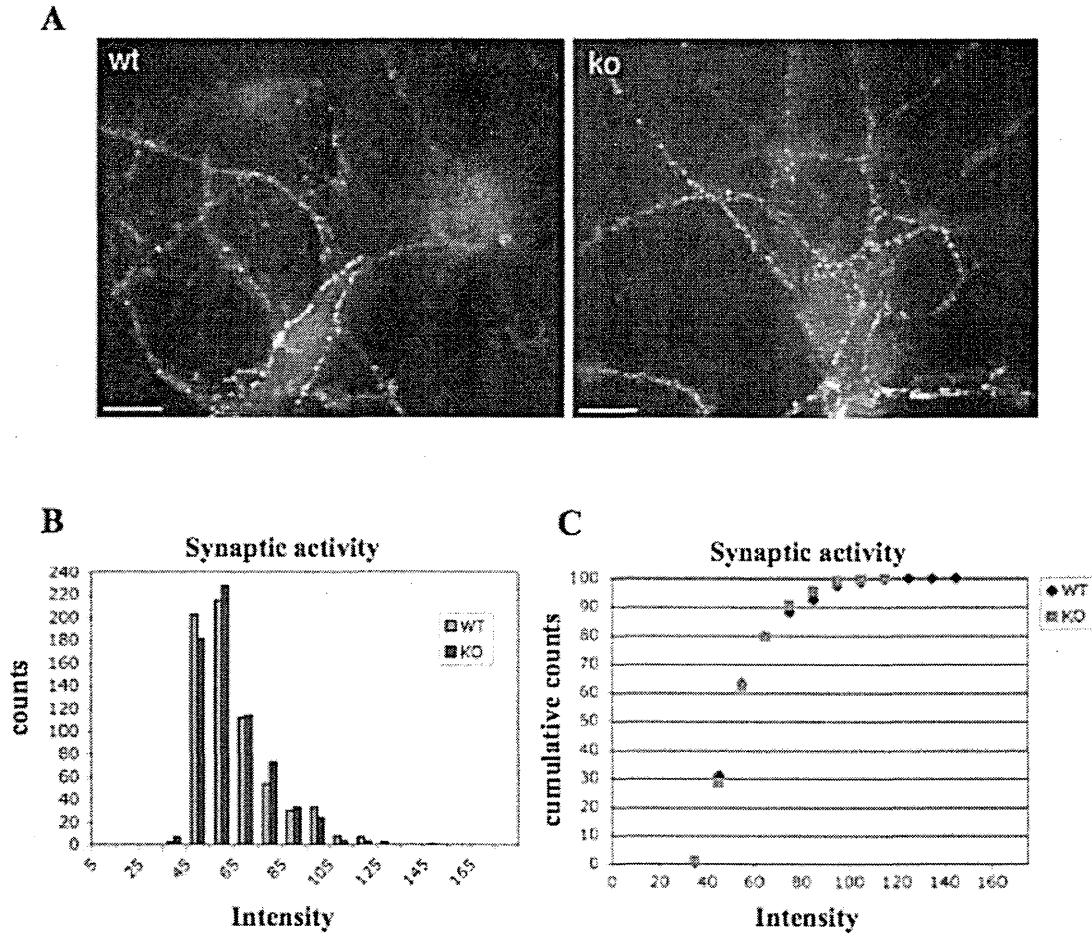

Figure 3.9 Rac3 depletion does not affect the synaptic activity of primary cultured hippocampal neurons. Wild-type (wt) and Rac3 knockout (ko) neurons after 14 DIV were loaded with FM4-64 for 30 s in depolarizing solution, followed by 10 min washing in KRH buffer. (A) FM4-64 fluorescence images. Scale bar, 10 μm. (B, C) Quantitative analysis of FM4-64 uptake measured at single synaptic boutons (667 terminals per condition, 2 independent coverslips), as described in the Materials and methods. The data are presented as histograms showing the distribution of FM4-64 fluorescence intensities (B) or as cumulative plots (C) obtained using the Origin software (Origin Lab, Northampton, MA, U.S.A.).

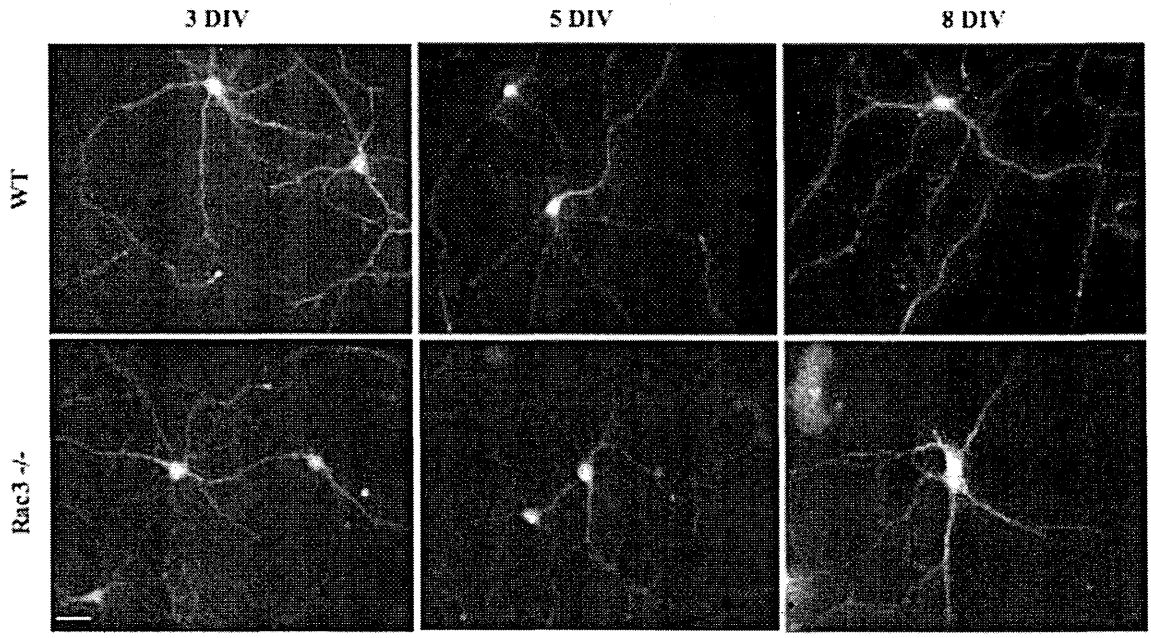

Figure 3.10 Rac1 is not evidently upregulated in Rac3-/- hippocampal neurons during *in vitro* development. 3 DIV, 5 DIV and 8 DIV hippocampal neurons from wild-type (wt) and Rac3-/- embryos were stained with anti-Rac1 mAb. Scale bar, 20 μm. No evident differences in Rac1 staining between WT and Rac3-/- neurons at different stages of *in vitro* development.

3.2 SiRNA-mediated Rac1 down-regulation

3.2.1 Characterization of the Rac1-specific siRNA oligonucleotides

I decided to down-regulate specifically the expression of the Rac1 protein during early *in vitro* development of hippocampal neurons to test the effects of Rac1 depletion on neuronal development in culture. Due to the high degree of similarity between Rac1 and Rac3 mRNA, I could identify only a limited number of Rac1-specific target sequences for siRNA that would not affect Rac3 expression. In particular I identified three mouse Rac1-specific oligonucleotides that were the least conserved in the two GTPases (Fig 3.11).

Since the efficiency of transfection of hippocampal neurons is very low, to test the three Rac1-specific siRNA oligonucleotides I generated both mouse Flag-Rac1 and mouse Flag-Rac3 constructs, and we have overexpressed them in COS7 cells together with each of the three different oligonucleotides. In this way it was possible to show biochemically and by immunofluorescence that only one of the three selected RNA duplexes specifically and efficiently down-regulated the overexpressed mouse Flag-Rac1, without affecting mouse Flag-Rac3 (Fig 3.12). I then determined the efficiency of the Rac1-1 oligonucleotide to down-regulate endogenous Rac1 in COS7 cells, both biochemically and by immunofluorescence. I used a Luciferase-specific siRNA oligonucleotide as negative control (Fig 3.13). Rac1 protein levels were strongly reduced in Rac1-1 transfected cells (83% reduced). The Rac1-1 siRNA was then used to study the effects of Rac1 depletion during hippocampal neurons development in both wild-type and Rac3-/- cells.

```
rac3            ATGCAGGCCATCAAGTGCGTGGTGGTTGGCGATGGTGCCGTGGGGAAGACGTGCCTGCTG 60
rac1            ATGCAGGCCATCAAGTGTGTGGTGGTGGGAGACGGAGCTGTTGGTAAAACCTGCCTGCTC 60
                ********************************** ** ** ** ** ** ** ** ********

rac3            ATCAGCTACACGACCAACGCCTTCCCAGGAGAATATATCCCCACAGTTTTCGACAACTAC 120
rac1            ATCAGTTACACGACCAATGCATTTCCTGGAGAGTACATCCCCACCGTCTTTGACAACTAT 120
                ***** ********** ** ** ** ***** ** ******** ** ** ********

rac3            TCAGCCAACGTGATGGTGGATGGGAAGCCAGTTAACCTGGGGCTGTGGGACACTGCTGGC 180
rac1            TCTGCCAATGTTATGGTAGATGGAAAACCAGTGAATCTGGGCCTATGGGACACAGCTGGA 180
                ** ***** ** ***** ***** ** ***** ** ***** ** ******** *****

rac3            CAGGAAGACTACGATAGGCTTCGGCCACTCTCCTATCCTCAAACAGATGTCTTTCTGATC 240
rac1            CAAGAAGATTATGACAGATTGCGTCCCCTCTCCTACCCGCAGACAGACGTGTTCTTAATT 240
                ** ***** ** ** **  * ** ** ******** ** ** ***** ** **  * **

rac3            TGCTTCTCCCTGGTGAGCCCAGCCTCCTTTGAGAATGTCCGTGCCAAGTGGTACCCAGAG 300
rac1            TGCTTTTCCCTTGTGAGTCCTGCATCATTTGAAAATGTCCGTGCAAAGTGGTATCCTGAA 300
                ***** ***** ***** ** ** ** ***** ********** ******** ** **

rac3            GTGCGGCACCACTGCCCACACACACCCATCCTTCTGGTGGGCACCAAGCTGGACCTCCGT 360
rac1            GTGCGACACCACTGTCCCAATACTCCTATCATCCTCGTGGGGACGAAGCTTGATCTTAGG 360
                ***** ******** **  * ** ** *** * ** ***** ** ***** ** **  *

rac3            GATGACAAGGATACGATTGAACGGCTGCGGGACAAGAAGCTGGCACCCATAACCTACCCC 420
rac1            GATGATAAGGACACCATTGAGAAGCTGAAGGAGAAGAAGCTGACTCCCATCACCTACCCG 420
                ***** ***** ** *****   ****  *** ********* * ***** ********

rac3            CAAGGCCTGGCCATGGCCCGAGAGATTGGTTCCGTCAAGTACCTGGAGTGCTCAGCTCTG 480
rac1            CAGGGGCTGGCCATGGCGAAAGAGATCGGTGCTGTCAAATACCTGGAGTGCTCAGCTCTC 480
                ** ** **********   ****** *** * ***** ********************

rac3            ACCCAGAGAGGTCTGAAGACAGTGTTCGACGAGGCCATCCGGGCTGTGCTCTGCCCACCT 540
rac1            ACACAGCGAGGACTCAAGACAGTGTTTGACGAAGCTATCCGAGCGGTTCTCTGTCCCCCT 540
                ** *** **** ** ********** ***** ** ***** ** ** ***** ** ***

rac3            CCAGTGAAAAAGCCAGGCAAGAAGTGCACTGTATTCTAG 579
rac1            CCTGTCAAGAAGAGGAAGAGAAAATGCCTGCTGTTGTAA 579
                ** ** ** ***      *  ** ***    * ** **
```

Figure 3.11 Rac1 siRNA oligonucleotides. Alignment of Rac1 and Rac3 coding sequences. Asterisks indicate conserved nucleotides between the two sequences. Sequences corresponding to the three Rac1-specific siRNA oligonucleotides utilized in the experiments are shown in different colors: rac1-1, red; rac1-2, pink; rac1-3, blue.

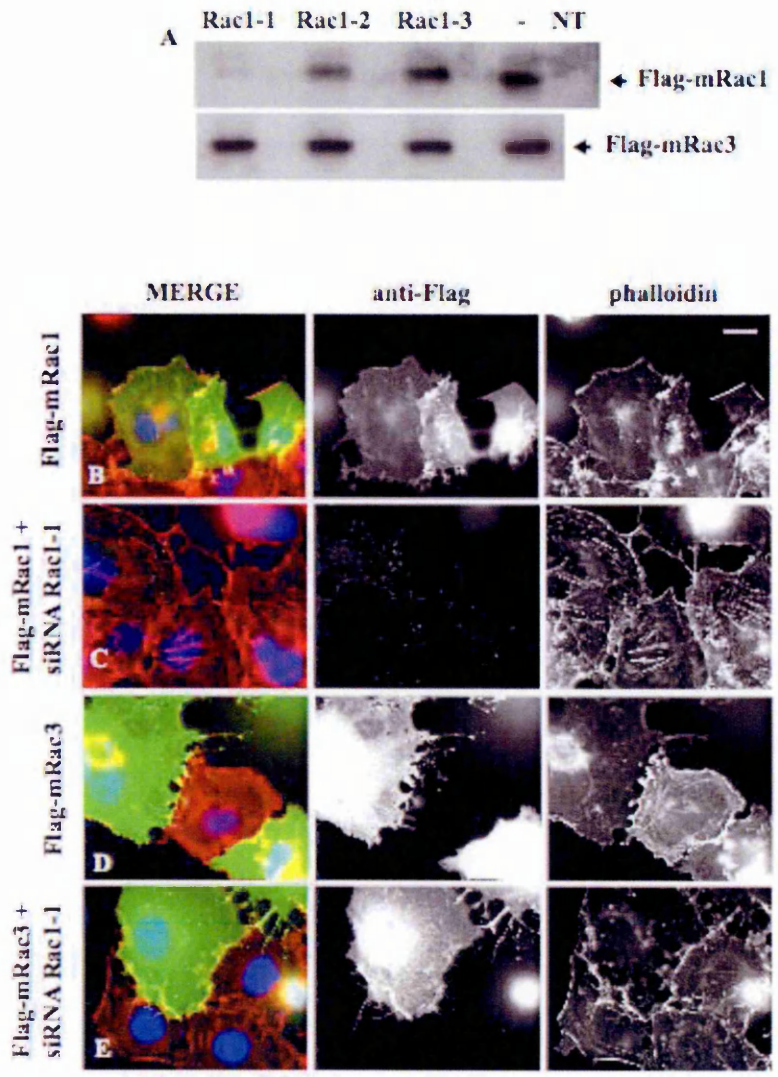

Figure 3.12 Characterization of mouse Rac1-siRNA. (A) COS7 cells were transfected using Lipofectamine™ 2000 with either pFlag-Rac1 or pFlag-Rac3 in the absence (−) or presence of 50 nM of the following Rac1-specific siRNA oligonucleotides: Rac1-1, Rac1-2 or Rac1-3. NT, lysate from non-transfected cells. 48 h after transfection, 50 µg of cell lysates were analysed by immunoblotting with anti-FLAG mAb M5. (B-F) COS7 cells were transfected using Lipofectamine™ 2000 with either pFlag-Rac1 (B-C) or pFlag-Rac3 (D-E) in the absence (B, D) or presence of 50 nM of rac1-1 siRNA oligonucleotide (C, E). 48 h after transfection cells were fixed and stained with anti-FLAG mAb M5 and phalloidin. The Rac1-1 siRNA oligonucleotide specifically reduced Flag-Rac1 levels without interfering with Flag-Rac3 levels.

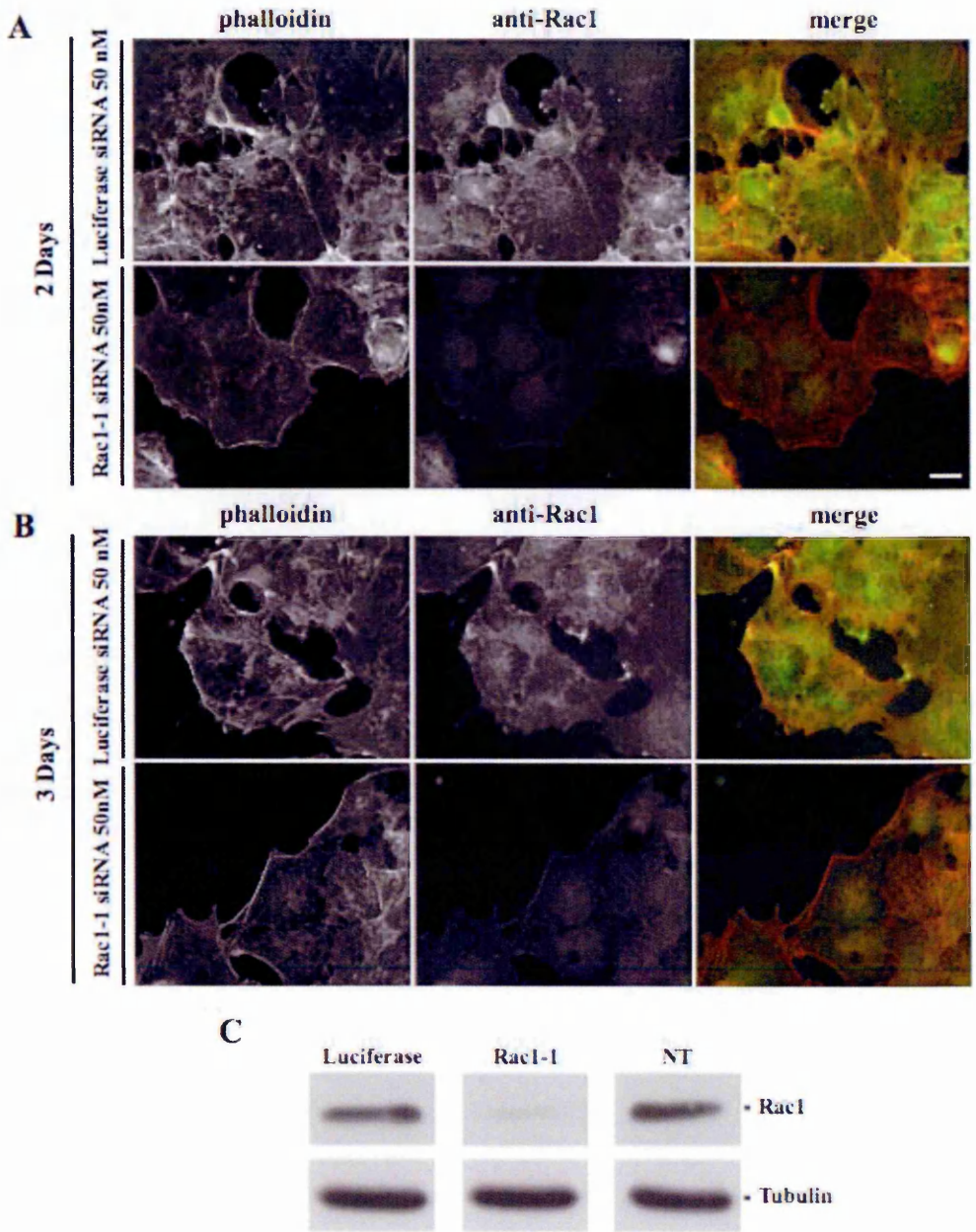

Figure 3.13 Knockdown of endogenous Rac1 protein in COS7 cells by siRNA. (A, B) COS7 cells were transfected with 50 nM of either rac1-1 or luciferase (control) specific siRNA oligonucleotides, using Lipofectamine™ 2000. 48 h (A) and 72 h (B) after transfection cells were fixed and stained with anti-Rac1 mAb (green) and phalloidin (red). Rac1-1 siRNA transfected cells show a strong reduction of Rac1 staining both at 48 and 72 hours after transfection compared to control cells. Scale bar, 20 μm. (C) COS7 cells were transfected with 50 nM of either rac1-1 or luciferase siRNAs. Non-transfected cells (NT) were analysed as additional control. 72 h after transfection, 50 μg of cell lysates were analysed by immunoblotting with anti-Rac1. Immunoblotting with the anti-tubulin mAb was used as loading control. Rac1 levels are strongly reduced in Rac1-1 siRNA-treated cells.

3.2.2 Rac1 knockdown by siRNA specifically affected dendritic development

I characterised the Rac1 monoclonal antibody (Upstate) by pre-incubating it with GST-Rac1 or GST, as negative control, before immunofluorecence, to verify the specificity of the staining in neurons. The staining of the Rac1 antibody in the cell body and in the neurites was specific, since after pre-incubation with GST-Rac1 I could not reveal any specific signal (Fig 3.14). To analyse the effect of Rac1 down-regulation during the first phases of neuritogenesis, I set up the conditions for transfecting hippocampal neurons with Rac1 siRNA by electroporation before plating. Specifically, I electroporated neurons with pEGFP either with control Luciferase or with Rac1-1 siRNA, and after 2 DIV I evaluated the levels of Rac1 proteins by immunofluorescence. Rac1 siRNA-treated cells showed a strong down-regulation of Rac1 expression (Fig 3.15). At 3 DIV, I observed a strong reduction of the dendritic tree in both wild-type and Rac3-/- hippocampal neurons transfected with siRNA, compared with control cells. Interestingly the axonal length was not affected (Fig. 3.16 A). I also showed that the polarised distribution of the microtubule-associated proteins was not disrupted in Rac1 siRNA transfected cells: MAP2 remained localised in the dendritic tree (Fig.3.17), while Tau-1 specifically identified the single long axon (Fig. 3.18), indicating that Rac1 depletion did not interfere with neuronal polarization. Quantification confirmed the specific effects of Rac1 down-regulation on dendritic length (Fig. 3.16 B), while the number of primary dendrites per cell was similar in Rac1 down-regulated and control neurons (Fig. 3.16 C). Comparison between the effects of Rac1 siRNA on neurons from Rac3-null and wild-type mice showed that, in both cases, dendrites were affected to a similar degree (41% and 52% reduction in dendrite length, respectively), whereas axons were not affected (Fig. 3.16 B). These results show that down-regulation of Rac1 specifically affected dendritic development.

I next assessed the organization of actin filaments in Rac1 siRNA-treated neurons. Staining with fluorescently conjugated phalloidin revealed that in Rac1 siRNA-targeted neurons,

the decrease of Rac signal was coupled by a decrease of F-actin in neurites and growth cones (Fig. 3.19). Time-lapse imaging in live neurons demonstrated that Rac1-mediated reduction of F-actin correlated with decreased growth cone dynamics (Fig 3.20). I quantified the behaviour of growth cones from neurons treated with Rac1-specific or control siRNA. I found a 36% decrease of the area of Rac1-depleted growth cones (Fig 3.21 B) and a 26% reduction in the dynamics of the same growth cones (Figure 3.21 C). Together, these results suggest that down-regulation of Rac1 affects early dendritic development by decreasing actin dynamics, and that this defect cannot be compensated by Rac3.

I next decided to study the effects of Rac1 and Rac3 depletion in later phases of neuronal development, when intense neurite branching and synaptogenesis occur. At these stages Rac3 shows the strongest expression during neuronal development *in vivo*. Due to the high cell mortality upon electroporation, electroporated neurons are cultured at low-density. These cultures represent a good models to perform morphological analyses during the first stages of neuronal development, but neurons at low density hardly survive for long-term studies, since the cell number is a limiting factor to establish functional neuronal networks and synapses. I tried to optimize an alternative Rac1 siRNA transfection method, by transfecting high-density neuronal cultures at 4 DIV with Lipofectamine. I could not find conditions for an efficient delivery of Rac1 RNA-oligonucleotides in these cultures. As previously reported (Wu et al., 2005) ,intracellular localization of mRNA transcripts is differently regulated. For example, RhoA mRNA localize to developing axons and growth cones where is locally translated, while Rac1 mRNA is restricted to the cell body. These differences in mRNA localization might explain of the inefficacy of delivering the small Rac1 oligonucleotides. Rac1-specific siRNA oligonucleotides have to be transported from the distal neuritic terminals to the cell body in order to target Rac1 transcript. Alternative methods would be the use of DNA-based vectors like the p-Super-based RNA interference technology, or Cre-recombinase mediated gene deletion.

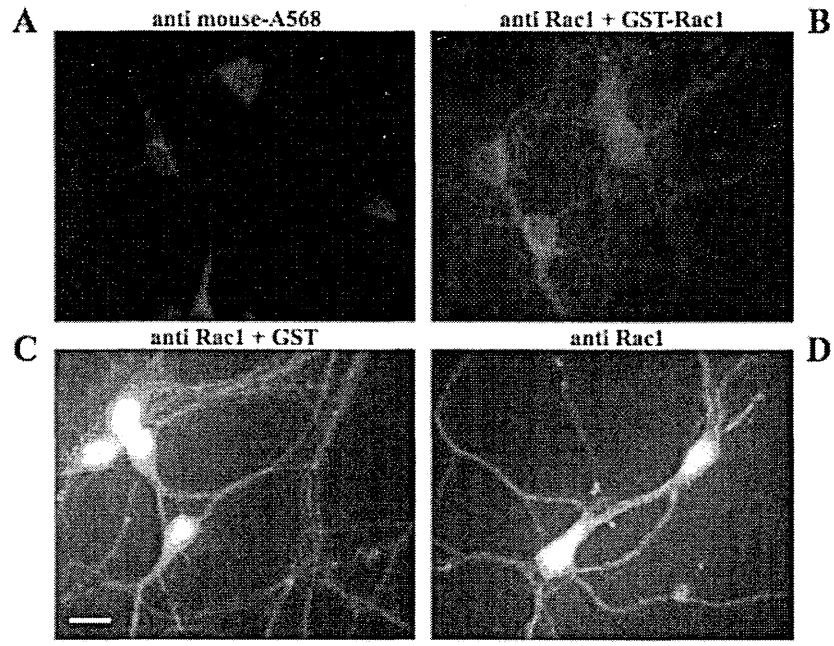

Figure 3.14 Characterization of Rac1 staining in hippocampal neurons. Hippocampal neurons from wild-type mice were fixed at 5 DIV and incubated with anti-mouse-Alexa 658 secondary antibody (A), anti-Rac1 mAb (Upstate) pre-incubated with GST-Rac1 fusion protein (B), anti-Rac1 mAb pre-incubated with GST alone (C), or anti-Rac1 mAb (D). Scale bar, 20 μm.

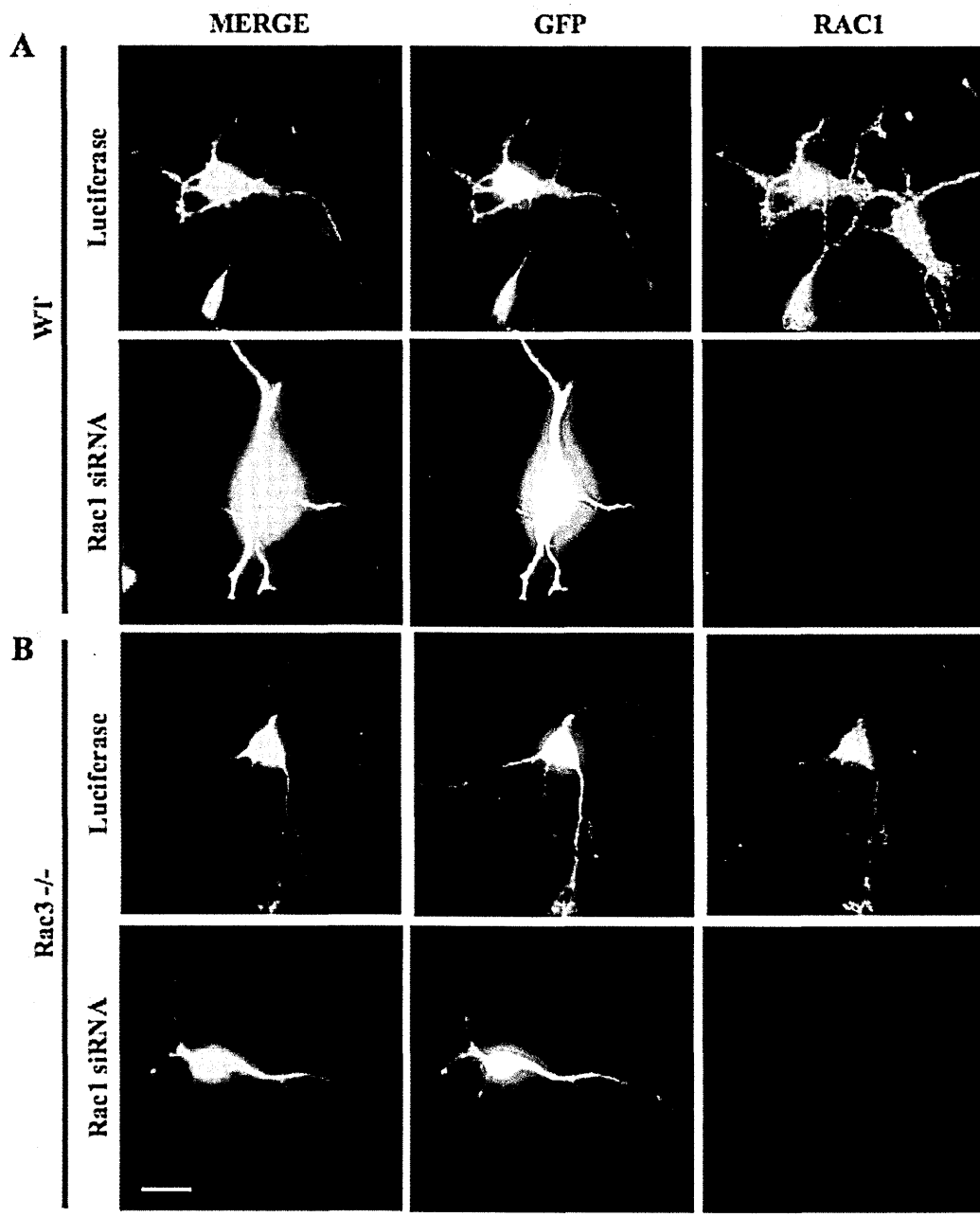

Figure 3.15 siRNA-mediated Rac1 downregulation in hippocampal neurons. Hippocampal neurons from wild-type (A) and Rac3-/- (B) embryos were electroporated before plating with pEGFP together with control (Luciferase) or Rac1-1 oligonucleotides (Rac1 siRNA). Neurons were fixed after 2 DIV and stained with anti-Rac1 mAb and anti-GFP pAb. GFP-positive neurons co-transfected with Rac1 siRNA showed a strong decrease in the intensity of Rac compared to GFP-positive control neurons. Scale bar, 20 μm.

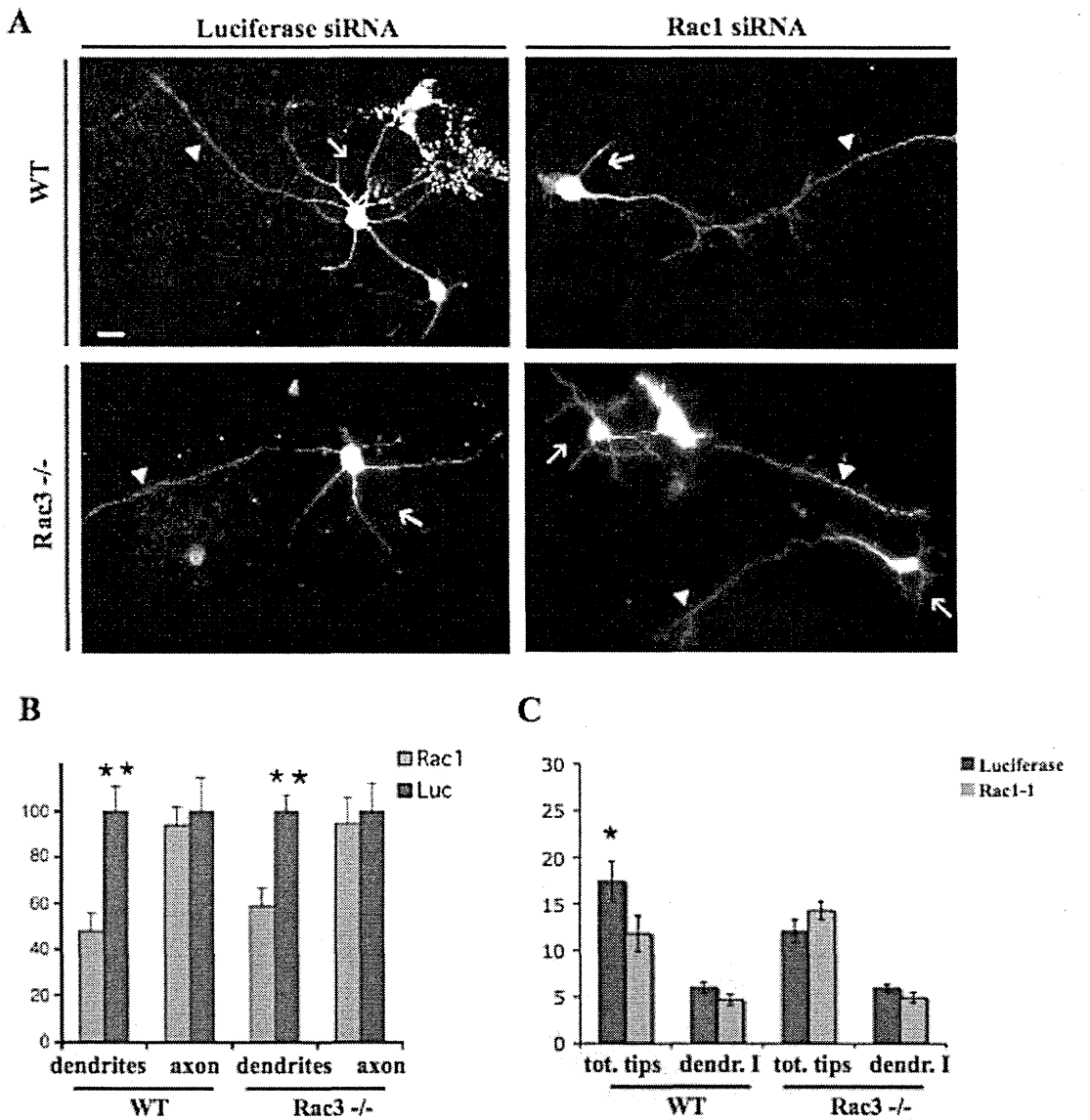

Figure 3.16 Rac1 knockdown specifically affects dendritic development. (A) Hippocampal neurons from wild-type (wt) or Rac3-/- mice were electroporated before plating with pEGFP and either Luciferase (control) or Rac1 siRNA. Neurons were fixed at 3 DIV and stained with anti-GFP pAb. SiRNA-mediated Rac1 downregulation affects dendritic (arrows) but not axonal (arrowheads) growth. Scale bar, 20 μm. (B,C) Quantification of neuronal morphology. Total dendritic and axonal length expressed as percentage of the control neurons (siRNA for Luciferase) (B), the number of primary dendrites per cell, and number of neuritic tips per cell (C). Values represent means +/−S.E.M. 22 neurons per condition. $^{**}P < 0.001$, $^{*}P < 0.05$). *P* values were obtained by the Student's *t* test (two-tailed distribution and two-sample unequal variance). Quantification was performed as detailed in the Material and Methods.

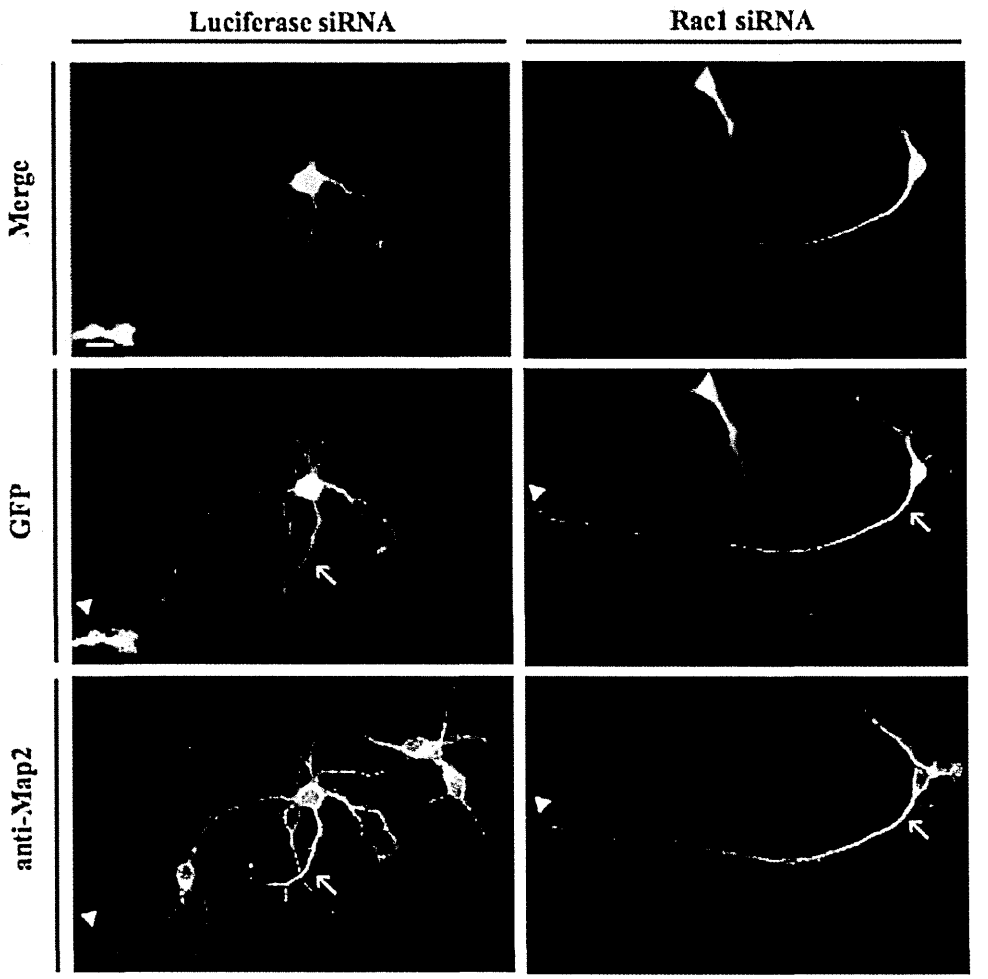

Figure 3.17 Rac1 knockdown does not affect the establishment of neuronal polarity (I). Wild-type hippocampal neurons were electroporated before plating with pEGFP and either Luciferase (control) or Rac1 siRNA. Neurons were fixed at 3 DIV, and stained with anti-GFP pAb (green) and anti-MAP2 mAb (blue). Neurons transfected with Rac1 siRNA had a normal MAP2-negative axon (arrowheads) and short MAP2-positive dendrites (arrows). Scale bar, 20 μm.

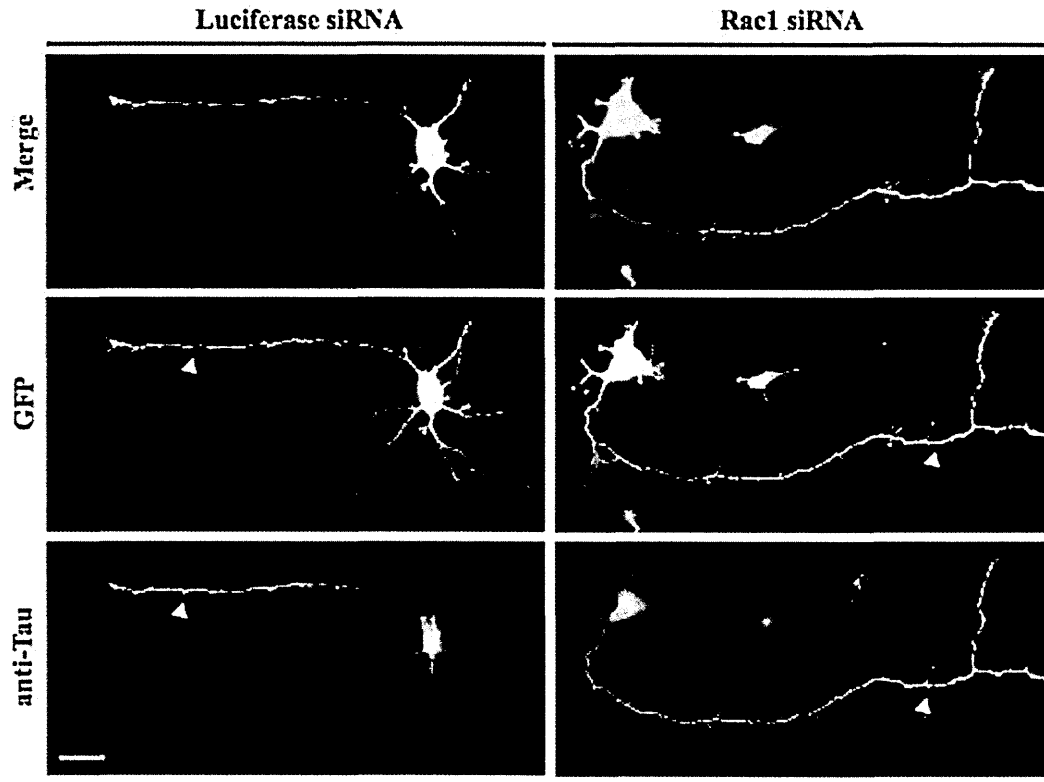

Figure 3.18 Rac1 knockdown does not affect the establishment of neuronal polarity (II). Wild-type hippocampal neurons were electroporated before plating with pEGFP-N1 and either Luciferase (control) or Rac1 siRNA. Neurons were fixed at 3 DIV and stained with anti-GFP pAb (green) and anti-Tau mAb (blue). Neurons transfected with Rac1 siRNA had a normal, long, Tau-positive axon (arrowheads). Dendrites from Rac1 siRNA-treated neurons do not show immuno-reactivity for Tau. Scale bar, 20 μm.

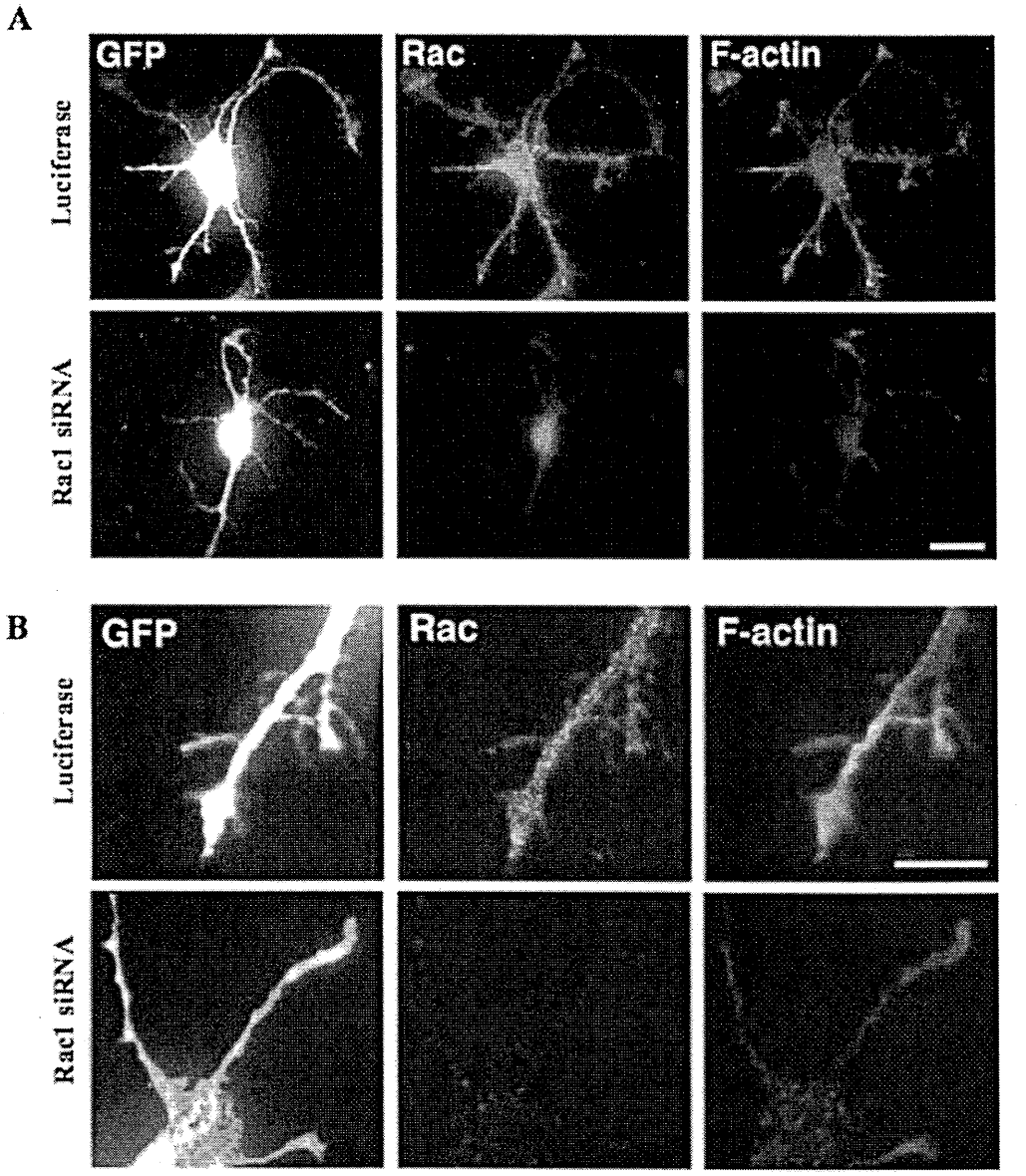

Figure 3.19 Decreased Rac1 levels induced by siRNA reduced F-actin in neurites and growth cones. Hippocampal neurons from wild-type embryos were electroporated before plating with pEGFP and either control (Luciferase) or Rac1-1 oligonucleotides (Rac1 siRNA). Neurons were fixed after 3 DIV, and stained with anti-GFP pAb, anti-Rac1 mAb and phalloidin for F-actin. GFP-positive neurons co-transfected with Rac1 siRNA showed a strong decrease in the intensity of Rac, coupled to a reduction of the levels of F-actin compared to GFP-positive control neurons. Scale bar, 20 μm (A); 10 μm (B).

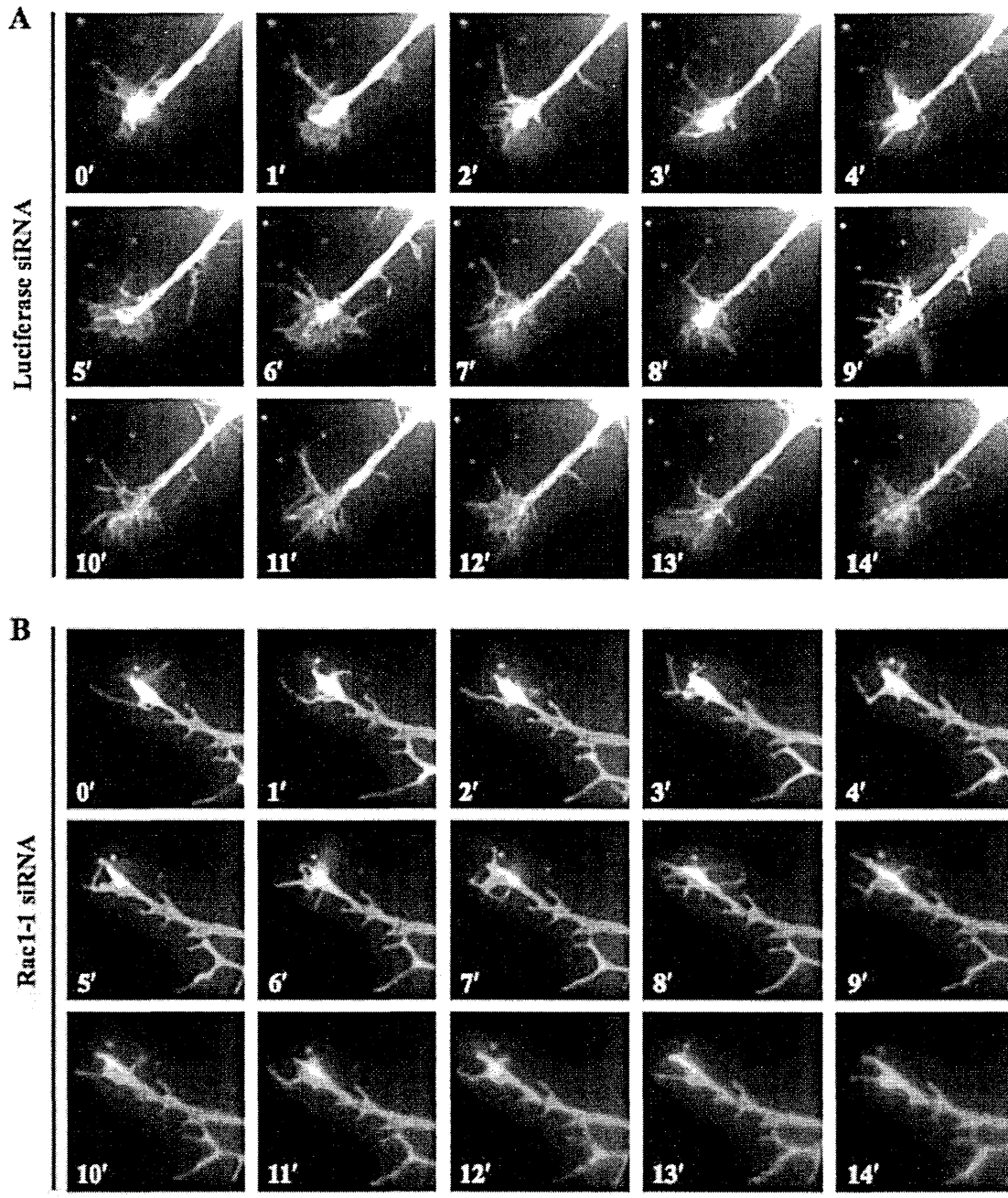

Figure 3.20 Rac1 knockdown affected growth cone dynamics (I). Time-lapse video microscopy of growth cones from 2 DIV hippocampal neurons electroporated with pEGFP and either control (Luciferase) (A) or Rac1 siRNA (B). Frames at 1 min interval, for a total of 14 minutes, are shown. Rac1 downregulation decreased growth cone dynamics, and affected growth cone morphology.

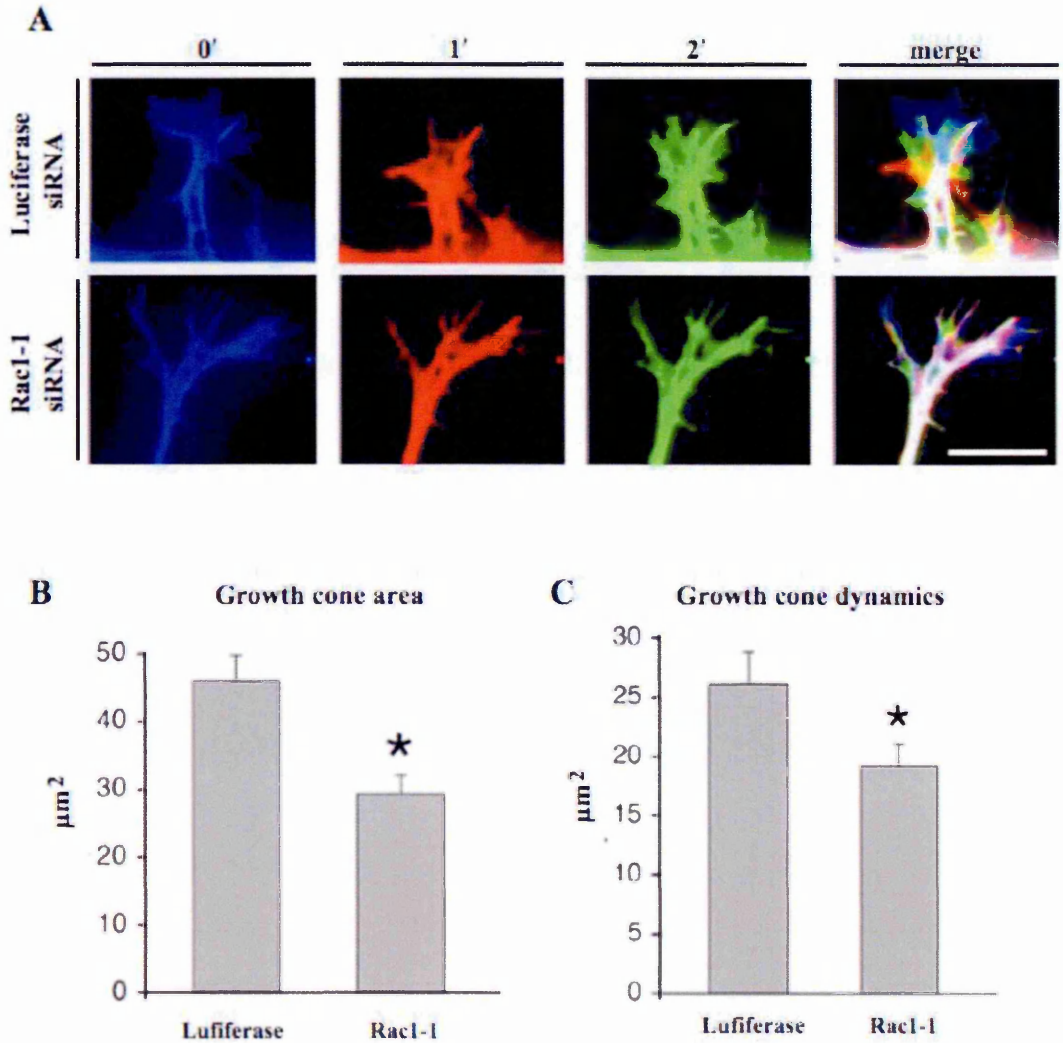

Figure 3.21 Decreased Rac1 levels induced by siRNA affected growth cone dynamics (II). (A) Dynamic behaviour of growth cones from 2 DIV hippocampal neurons electroporated with control (Luciferase) or Rac1 siRNA and pEGFP. Three frames at 1 min interval (different colors) are shown. Scale bar, 10μm. (B) The area of growth cones at 0′ (means+/−S.E.M.; n=20 for each condition; *P=0.00091) from neurons treated with control or Rac1 siRNA was measured and plotted. Rac1 siRNA-mediated downregulation significantly decreased the area of growth cones. (C) The dynamic behaviour of growth cones (means+/− S.E.M.; n=20 for each condition; *P=0.042) from neurons treated with control or Rac1 siRNA was evaluated as follows: the difference between the total area covered by a growth cone at times 0+1 min, and the fraction of remaining overlap between the areas at the two time points was calculated and plotted.

3.3 Generation and characterization of conditional Rac1 knockout (Rac1N) and double conditional Rac1/Rac3 knockout mice (Rac1N/Rac3-/-)

3.3.1 Strategy used to generate Rac1N and Rac1N/Rac3-/- mice

Given the lack of strong defects during neuronal maturation of Rac3-/- mice (Corbetta et al., 2005), we have decided to generate double Rac1/Rac3 knockout mice. Since Rac1-null mice die before E9.5 (Sugihara et al., 1998), we decided to generate mice with a conditional deletion of Rac1 in neurons. I employed mice with floxed Rac1 allele (Rac1F) obtained by Dr. Tybulewicz (Walmsley et al., 2003) and heterozygous Synapsin I Cre (Syn-Cre) transgenic mice expressing the Cre recombinase under the synapsin I promoter (Zhu et al., 2001). The aim was to characterize the effects of Rac1 depletion in neurons during late stages of neuronal development, when Rac3 expression in brain is high (Bolis et al., 2003; Corbetta et al., 2005). The Syn-Cre transgene is still off in neural precursors during early embryonic development and switches on not too late during neuronal development. Syn-Cre function is first detected at E12.5 (Zhu et al., 2001). We have analyzed the activity of the Syn-Cre transgene in Syn-Cre/ROSA26 reporter mice (Soriano, 1999). Brains from double heterozygous P8 and P13 mice were fixed and used for X-gal staining. The transgene was widely active in neurons of developing brain. Specifically, in the hippocampus Syn-Cre was active in the CA3, hilus, and external granule cell layer of the dentate gyrus, while it was almost undetectable in the CA1 and in the inner granule cell layer of the dentate gyrus (Fig. 3.22). The information obtained from this analysis is important to evaluate where to expect the Cre-mediated deletion of Rac1 in the mutant mice.

By crossing Rac1F/F with Syn-Cre mice I obtained Rac1F/+/Syn-Cre mice that I further crossed with Rac1F/F mice in order to obtain the Rac1 conditional knockout mouse [Rac1F/F/Syn-Cre (Rac1N), Fig. 3.23 A, B]. In parallel, by crossing Rac3-/- with Rac1F/F mice I obtained Rac3+/-/Rac1F/+ mice that I further crossed with each other to obtain Rac1F/F/Rac3-/- mice. By crossing Syn-Cre with Rac3-/- mice I obtained Syn-Cre/Rac3+/- mice that I further crossed with Rac3-/- mice to obtain Syn-Cre/Rac3-/- mice. Breeding of Rac1F/F/Rac3-/- with Syn-Cre/Rac3-/- mice resulted in Rac1F/+/Rac3-/-/Syn-Cre mice that I further crossed with Rac1F/F/Rac3-/- in order to obtain the double knockout mice [Rac1F/F/Syn-Cre/Rac3-/- (Rac1N/Rac3-/-)].

I confirmed Rac1 deletion by genomic PCR (Fig. 3.23 C), and by the decrease of the Rac1 transcript by northern blot analysis (Fig. 3.24 A) in total brain of both Rac1N and Rac1N/Rac3-/- mice. Incomplete ablation of Rac1 in the brain was probably due to the retention of the protein in the glial cells, and in these neurons in which Syn-Cre was not active (Fig. 3.22). Moreover, deletion of Rac1 and Rac3 was not compensated by the upregulation of the third member of the Rac family, the hematopoietic-specific Rac2, as confirmed by northern blot analysis (Fig. 3.24 B).

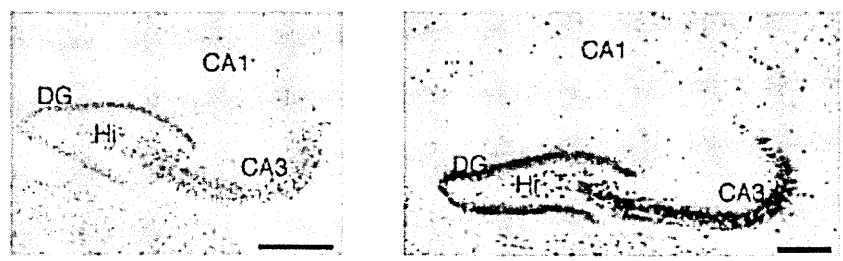

Figure 3.22 Activation of the Syn-Cre transgene. X-gal staining on P8 (left panel) and P13 (right panel) Syn-Cre/ROSA26 brain sections. In the hippocampus, Syn-Cre expression is restricted mostly to the CA3 and dentate gyrus, including the hilus, while is absent in most cells of the CA1 region. DG, dentate gyrus; Hi, hilus. Scale bars, 200 μm.

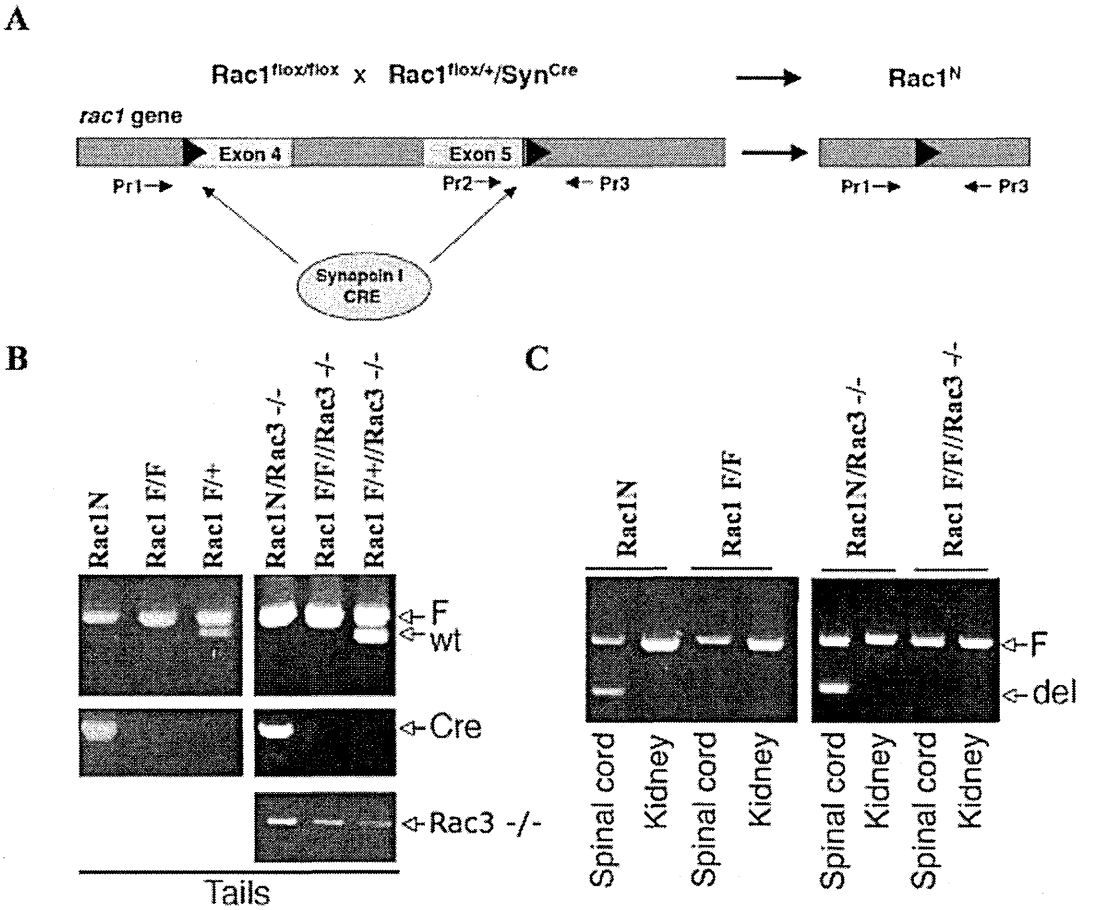

Figure 3.23 Generation of Rac1N and Rac1N/Rac3-/- mice. (A) Scheme of the Rac1 flox (F) allele before (left) and after (right) Cre-mediated recombination. (B, C) Genotyping by PCR on DNA from (B) tails and (C) spinal cord and kidney of mice with the indicated genotypes. DNAs were screened with primer 2 (Pr2) and primer 3 (Pr3) to produce a 0.33 Kb fragment from the F allele and a 0.27 Kb fragment from the wild-type allele (wt). The 0.17 Kb PCR fragment from the deleted allele (del) was obtained with primer 1 (Pr1) and Pr3 from spinal cord. Arrows indicate the specific PCR products. (B) A 0.45 Kb PCR fragment (Cre) was obtained in the syn-Cre positive transgenic mice with Pr4 and Pr5. PrF1 and PrR3 generate a 0.37 Kb fragment from the Rac3 mutant allele (Rac3-/-). Sequences of all primers are reported in the Material and Methods. Mice expressing the Cre-recombinase transgene under the synapsin-I promoter show the specific deletion in neuronal tissues of exons 4-5 of *Rac1* gene.

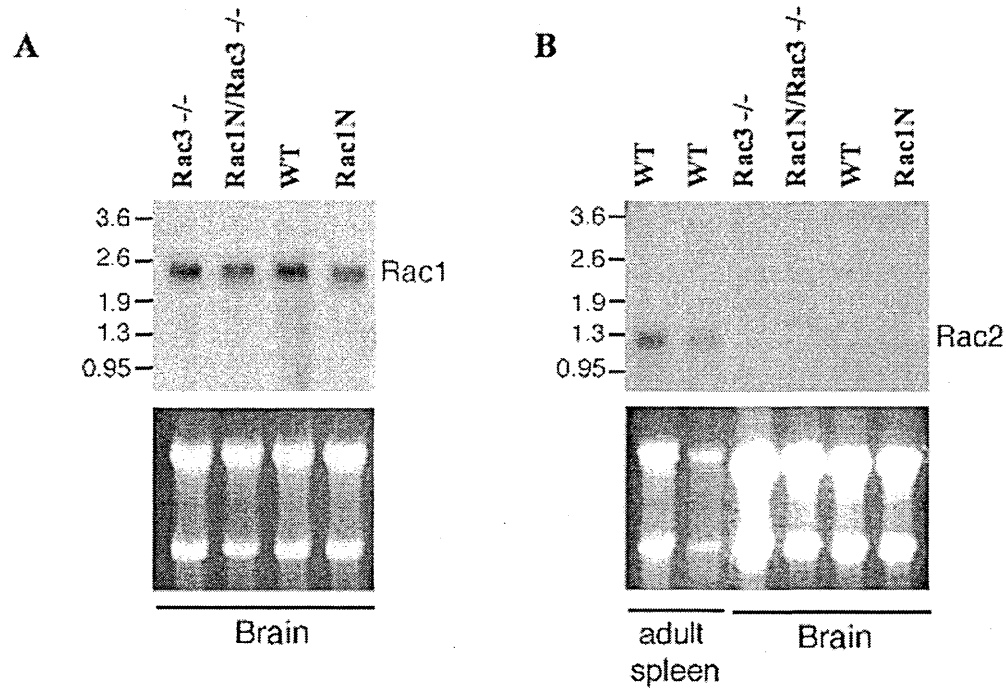

Figure 3.24 Northern blot of Rac1 and Rac2 in Rac1N and Rac1N/Rac3-/- mice. (A, B) Northern blot analysis on total RNA (15 μg per lane) extracted from P13 mouse brains of the indicated genotypes. Filters were hybridized with probes specific for Rac1 (A) or Rac2 (B). RNA from spleen was used as positive control for Rac2. Lower panels: gels used for blotting stained with ethidium bromide. Rac1N and double Rac1N/Rac3-/- mice show a reduction of Rac1 mRNA levels in total brain extract compared to their control (WT and Rac3-/- respectively). The levels of Rac2 mRNA are not changed in mutant mice.

3.3.2 Rac1N/Rac3-/- mice die around P13 and display neurological impairments

Rac1N and Rac3-/- mice developed normally, while Rac1N/Rac3-/- mice died around P13. Double knockout Rac1N/Rac3-/- showed a reduction in body growth starting around P6 (Figure 3.25 B). As a consequence, at P13 they were about half size of control animals (Figure 3.25 A, B). However, I did not find significant differences in the brain weight (P = 0.41) between double Rac1N/Rac3-/- (0.31 g ±0,023 SEM, n=5) and Rac3-/- littermates (0.28 g ±0,025 SEM, n=5).

Rac1N/Rac3-/- mice revealed muscle atrophy and neurological abnormalities assessed following a well-established procedure to test early mice reflexes. In particular, Rac1N/Rac3-/- mice displayed defects in righting reflex, negative geotaxis, and cliff drop aversion (Figure 3.26). Moreover, the double mutant mice developed spontaneous seizures starting around P7 that were more obvious and frequent at P13.

A

B

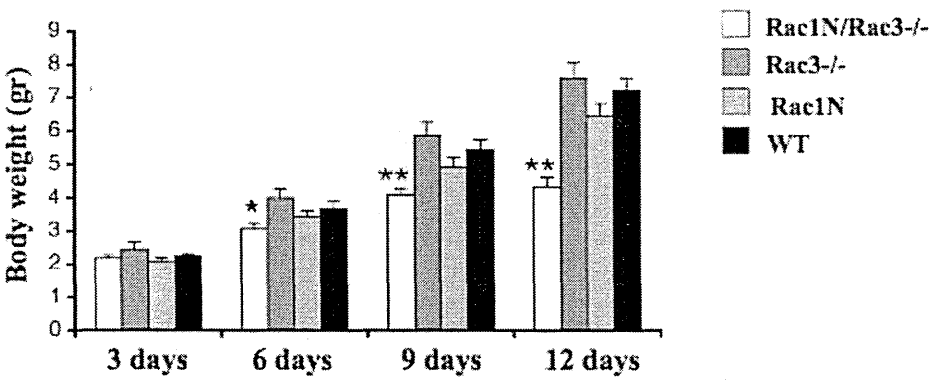

Figure 3.25 Double Rac1N/Rac3-/- mice show a reduction in the body weight. (A) Rac1N/Rac3-/- (left) and Rac3-/- (right) P13 mice. Double knock out animals are smaller in size. (B) Body weight. The body weight of 10 animals for each genotype was measured at each indicated time point. Bars are mean scores of each group. Error bars represent S.E.M. *, $P < 0.05$; **, $P < 0.005$ [as compared with control littermates (Student's *t* test)]. Double knock out mice reveal no alteration in the body weight at birth and until P6. From P6 they show a statistically significant reduction of their body weight that is more evident at P9, and at P12.

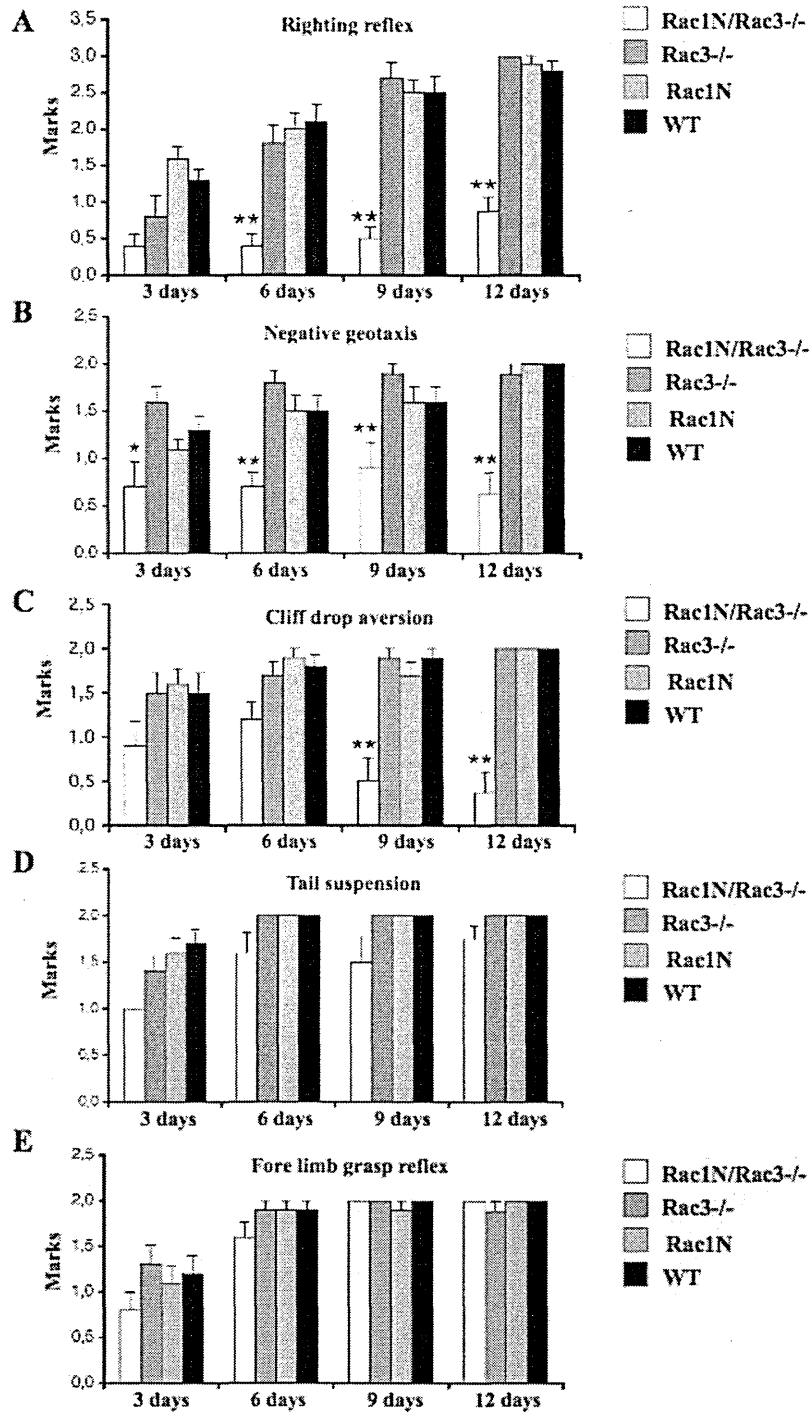

Figure 3.26 Double Rac1N/Rac3-/- mice reveal neurological impairments. The following reflexological tests were assessed as described in the Materials and Methods on 10 animals for each genotype. (A) Righting reflex, (B) negative geotaxis, (C) cliff drop aversion, (D) tail suspension and (E) fore limb grasp reflex. Bars are mean scores of each group. Error bars represent S.E.M. *, $P < 0.05$; **, $P < 0.005$ [as compared with control littermates (Student's *t* test)]. Double knockout animals display severe impairment in controlling the body orientation, starting around P6 (A-C). The sensory neuronal circuits are not affected (E).

3.3.3 Characterization of the endogenous GIT1 complex in mouse brain

In order to analyse Rac1-related signalling pathways that might be deregulated in double Rac1N/Rac3-/- mice, I characterised the endogenous GIT1 complex in wild-type mouse brain. Previous work in our laboratory has led to the identification of the GIT1/p95-APP1 complex. GIT1 is an ArfGAP of the GIT/PKL family expressed in the nervous system, as a Rac-GTP specific interactor (Di Cesare et al., 2000). It has been shown that components of the GIT1 complex modulate Rac3 function in chicken retinal neurons, by mediating Rac3-induced neuritogenesis (Albertinazzi et al., 1998). GIT1 localises both at pre- and post-synaptic sites in cultured hippocampal neurons. GIT1 is believed to regulate synaptogenesis by locally activating Rac proteins (Kim et al., 2003; Zhang et al., 2003; Zhang et al., 2005). Recent data have shown that the interaction between phosphorylated GIT1 and the SH2 domain of Grb4 is required to transduce ephrinB-induced spine formation (Segura et al., 2007). The adaptor protein GIT1 includes an amino-terminal ArfGAP domain (de Curtis, 2001), binding sites for paxillin and for the Rac/Cdc42 exchanging factor PIX/Cool that in turn can interact with PAK kinases, and for other partners. The understanding of the role of Rac1 and Rac3 during neuronal development in conjunction with the functional characterization of the GIT complex is relevant to the comprehension of the molecular alterations involved in mental retardation, since protein of this complex have been found mutated in patients with non-syndromic mental retardation (Ramakers, 2002).

I have started to characterise the endogenous GIT1 multi-protein complex in wild-type mouse brain by immunoprecipitation (Fig. 3.27 B) and by pull-down assays using GTP-activated Rac proteins (Fig. 3.27 A). Interestingly, I found that among the three PAK proteins, the 65 kDa PAK is highly enriched in the GST-Rac1 and GST-Rac3 bound complexes, preferentially interacting with GST-Rac1. Moreover, alpha-PIX (85 kDa) and the neuro-specific PAK3 (65 kDa), both implicated in mental retardation, were prominent

components of the GIT1 complex in the brain, compared to other PIX and PAK isoforms (Fig. 3.28). I further analysed the expression levels of these specific isoforms in double Rac1N/Rac3-/- brain to assess possible alterations induced by the absence of Rac proteins.

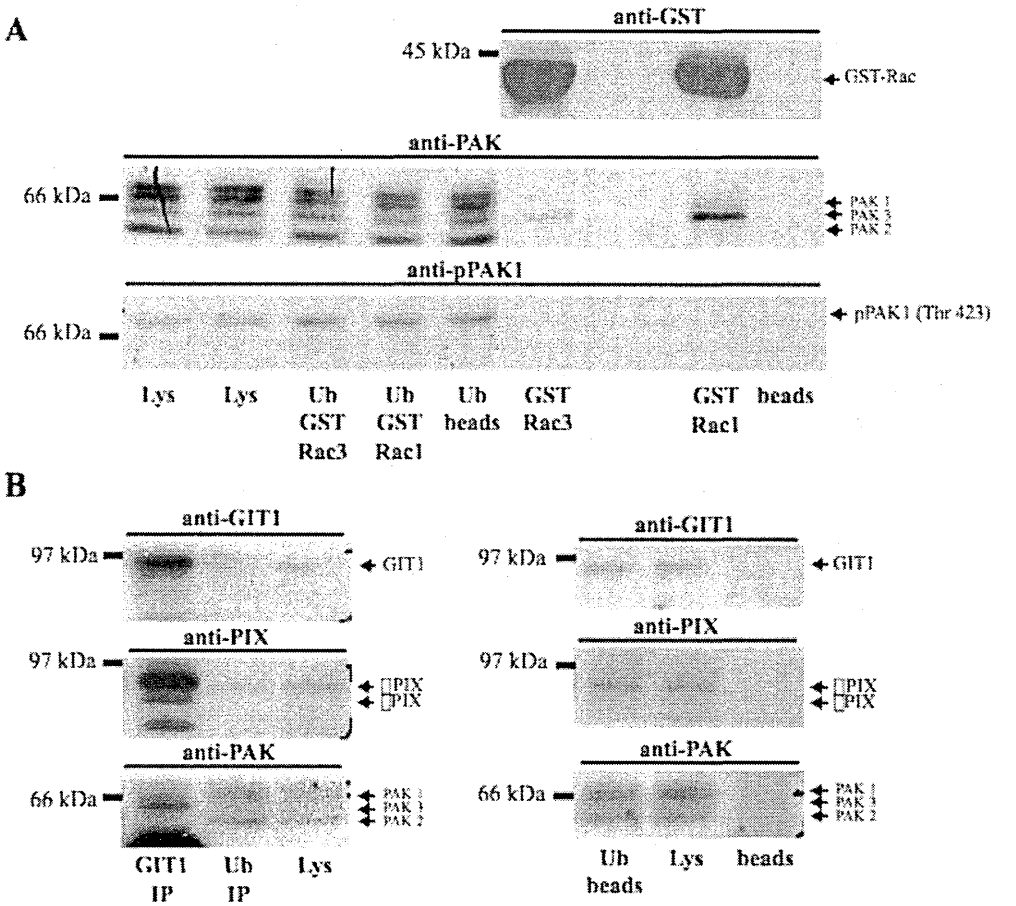

Figure 3.27 Biochemical characterization of the PAK-PIX-GIT1 complex. (A) The 65 kDa PAK specifically interacts with Rac. Equal amounts of wild type P7 mouse brain lysate (2 mg protein) were loaded on GST-Rac1 and GST-Rac3 conjugated glutathione-agarose beads activated *in vitro* with GTP-γ-S. As control, lysates were incubated with beads alone. 100 μg of brain lysate (lys) and of the unbound fraction after pull-down (Ub) were loaded. Immunoblotting with anti-GST pAb (upper panel) was used as loading control. Immunoblotting using anti-PAK pAb (middle panel) detects PAK1, PAK2 and PAK3 (68 kDa, 62 kDa and 65 kDa respectively). Immunoblotting with anti-phospho Thr423-PAK1 pAb doesn't reveal detectable active PAK1 bound to active Rac (lowest panel). (B) PAK3 specifically interacts with GIT1-PIX complex. Aliquots of 2 mg of lysate from wild-type P7 mouse brain were immunoprecipitated with anti-GIT1 pAb (serum 64, left panel). The same amount of protein was loaded on beads alone (negative control, right panel). 100 μg of brain lysate and of unbound fraction were loaded. Immunoblotting using anti-GIT1 pAb (upper panel), anti-PIX pAb (middle panel), and anti-PAK pAb (lower panel) shows the GIT1-interacting complex. Molecular weights are indicated.

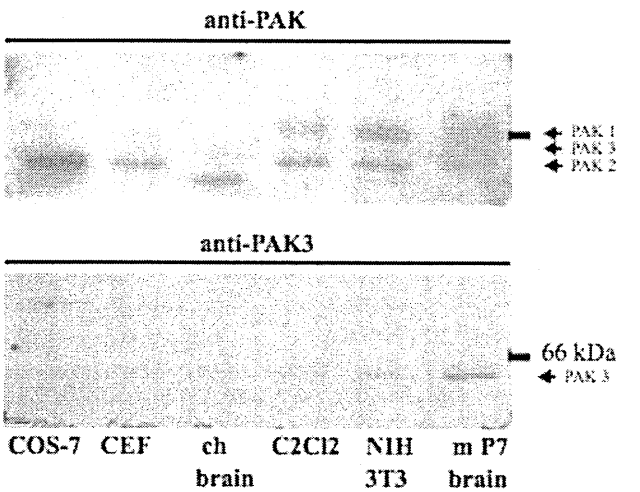

Figure 3.28 Characterization of the 65 kDa PAK isoform. The 65 kDa PAK is the neuro-specific PAK3. Cell lysates derived from non-neural murine (NIH3T3 and C2Cl2), chicken (CEF) and monkey (COS7) cells, from embryonic avian brain (ch. brain), and from P7 mouse brain (m P7 brain) were analysed by immunoblotting using the anti-PAK pAb (upper panel) and the anti-PAK3 specific pAb (lower panel). The 65 kDa PAK isoform corresponds to PAK3 and it is highly expressed in neuronal tissues. Molecular weights are indicated.

3.3.4 Increased WAVE1 phosphorylation in Rac1N/Rac3-/- brain

I next investigated which Rac-dependent signalling pathways may have been disrupted following deletion of the Rac genes, by analyzing the expression of several proteins related to Rac function. In this analysis I compared only pairs from the same litter: wild type with Rac1N littermates and Rac3-/- with Rac1N/Rac3-/- mice. I first examined by immunoblotting the expression levels of other Rho GTPases in P13 brain. I could not detect significant differences in the total levels of Cdc42 and Rac3 (Figure 3.29 B), while I found 1.3-fold decreased levels of RhoA expression in double mutant mice (Figure 3.29 A), probably due to a compensatory effect mediated by RhoA.

To identify Rac1-related signalling pathways that might be deregulated in knockout mice, I analysed by immunoblotting the expression and activation levels of Rac1 effectors or regulators in double Rac1N/Rac3-/- P13 total mouse brain (Figure 3.30, 3.33, 3.34) and in synaptosomal fractions (Figure 3.31, 3.32). I was unable to detect consistent differences between control and mutant mice in the total levels of the proteins analysed including, the GIT/Pix-PAK complex, Rac GEFs as Kalirin7, Rac effectors as IRSp53, WAVE, the cdk5 and its neuronal-specific regulatory subunit, the synapses specific proteins as the SNAREs Vamp2 (vesicles associated membrane protein 2), synaptophysin and synapsin or the post-synaptic protein PSD95, and in the phosphorylated form of the membrane Ephrin receptor (Figure 3.30-3.32).

Interestingly, however, although the expression of WAVE1 was normal, I observed a significant over 3-fold increase ($P < 0.04$) of WAVE1 phosphorylation on Ser310 in the brain of Rac1N/Rac3-/- mice compared to their Rac3-/- control. I observed only a slight increase (1.2 fold) of phosphorylated WAVE1 in the brain of Rac1N compared to the WT (Figure 3.33). It has been reported that phosphorylation of WAVE1 on Ser 310 by Cdk5 inhibits its ability to regulate Arp2/3 complex-dependent actin polymerization (Kim et al., 2006). These results indicate that Arp2/3/WAVE- dependent actin polymerization may be

altered in the central nervous system of double mutant mice.

I then investigated whether the lack of Rac had an effect on its effector PAK. As recently reported (Sananbenesi et al., 2007), inhibition of Rac1 leads to the reduction at the membrane of the levels of phosphorylated PAK on Thr 212, a site phosphorylated by p35/cdk5, and to the increase of PAK1 activity (increase of phopshorylated PAK on Thr 423). Accordingly, I found a slight increase (1.8 fold, border line significance) in PAK1 phosphorylation on Thr 423, in brain of double Rac1N/Rac3-/- mice compared to Rac3-/- mice, while I did not find any difference between Rac1N and WT mice (Figure 3.34).

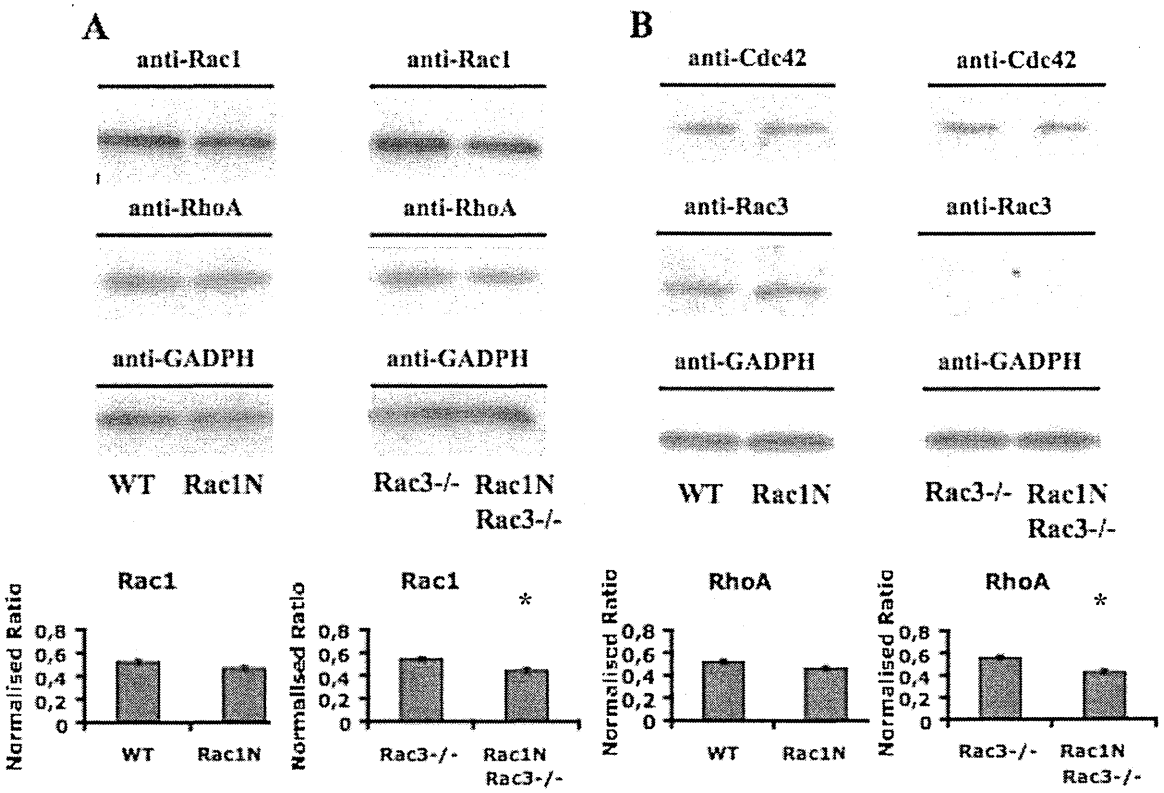

Figure 3.29 Analysis of GTPase levels in WT, RacIN, Rac3-/- and double RacIN/Rac3-/- mice brain. (A) Rac1 and RhoA are down regulated in P13 brain from double RacIN/Rac3-/- mouse. 100 µg of protein total lysate from each type of P13 brain were analysed by immunoblotting using the anti-Rac1 mAb and the anti-RhoA mAb. Immunoblotting using the anti-GADPH mAb was used as loading control. Rac1 protein levels were significantly reduced (1.2-fold) in the brain of double RacIN/Rac3-/- mice compared to Rac3-/- mice from the same littermates (*P < 0.04; n=7). No significant differences were observed between RacIN mice compared to WT mice from the same littermates. RhoA protein levels were significantly reduced (1.3-fold) in the brain of double RacIN/Rac3-/- mice compared to Rac3-/- mice from the same littermates (*P < 0.04; n=5). No significant differences were observed between RacIN mice compared to WT mice. Quantification was performed as described in Material and Methods. Each bar represents the averaged ratio between the values of each genotype with the sum of the values of the two genotypes to be compared (+/−S.E.M.).

(B) The protein levels of Cdc42 and Rac3 were not affected in P13 brain from double RacIN/Rac3-/- mouse. 100 µg of protein lysate from each type of P13 brain were analysed by immunoblotting using the anti-Cdc42 pAb and the anti-Rac3 pAb. Immunoblotting using the anti-GADPH mAb was used as loading control.

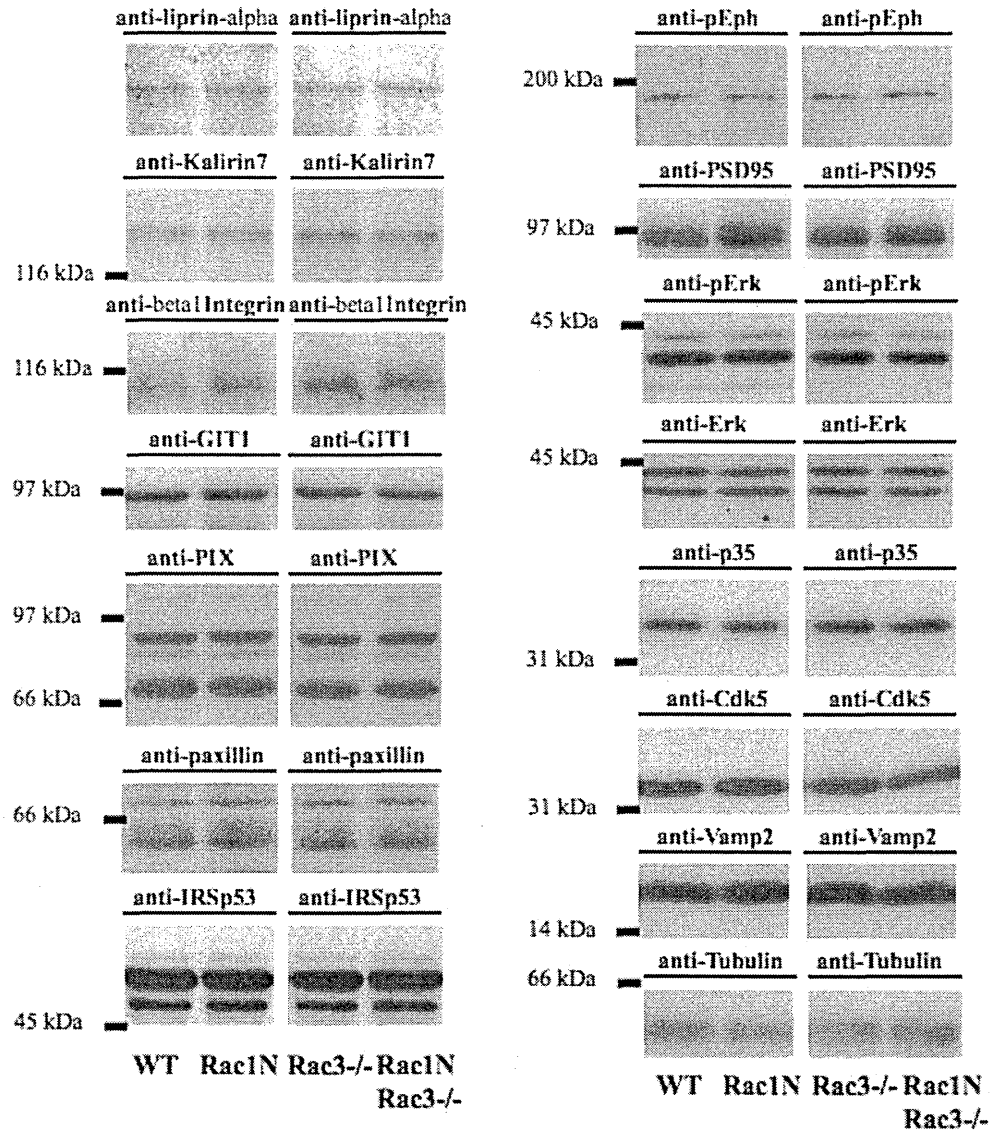

Figure 3.30 Biochemical analysis of proteins linked to Rac signaling pathways in WT, Rac1N, Rac3-/- and double Rac1N/Rac3-/- mice brain. No differences in the total levels or in the phosphorylation levels of the indicated proteins between Rac1N and WT, or between Rac1N/Rac3-/- and Rac3-/- brains. 100 μg of protein lysate from each type of P13 brain were analysed by immunoblotting using the following antibodies: anti-liprin-α pAb, anti kalirin7 pAb, anti-β1 integrin pAb, anti-p95PKL/GIT mAb, anti-β-PIX pAb, anti-paxillin mAb, anti-IRSp53 pAb, anti-phospho Eph pAb (Tyr596/Tyr602), anti-PSD95 mAb, anti-phospho p42-p44 MAPK mAb (Thr202/Tyr204), anti-p42-p44 MAPK pAb, anti-p35 pAb, anti-Cdk5 pAb, anti-Vamp2 mAb. The anti-tubulin mAb was used as loading control. Molecular weights are indicated.

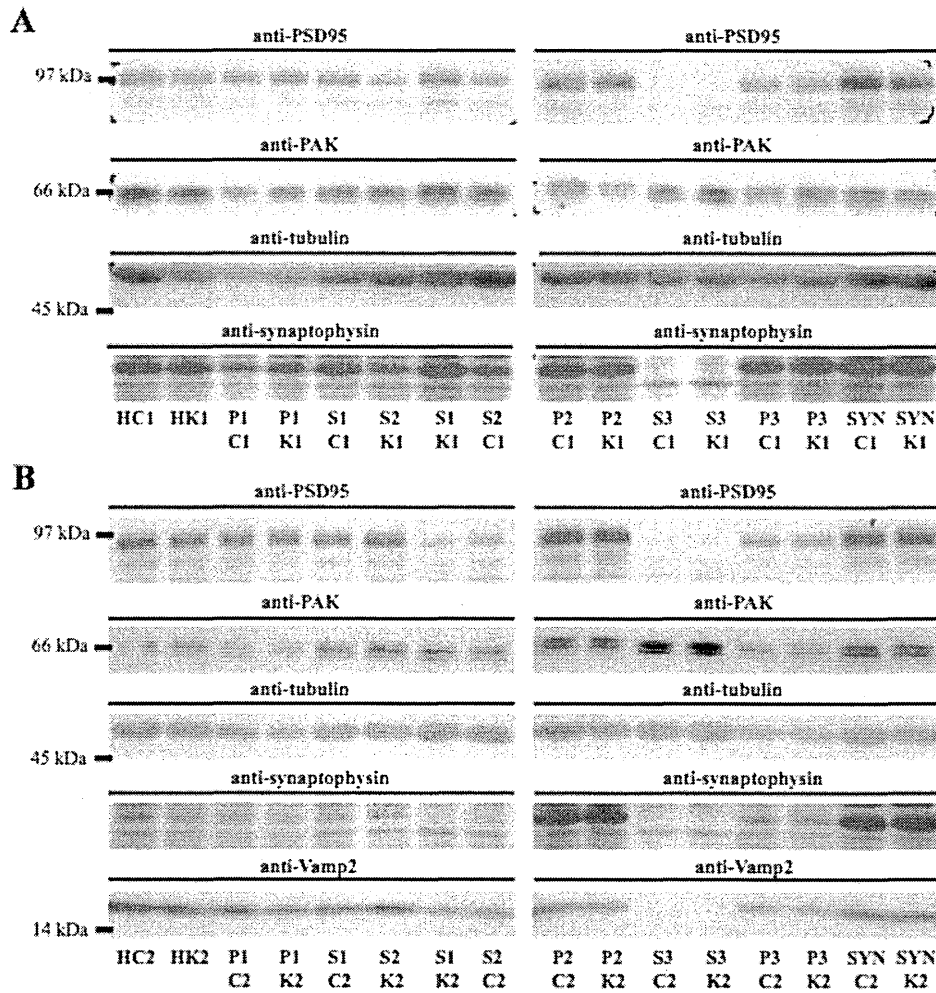

Figure 3.31 Biochemical analysis of the synaptosomal fractions from WT, Rac1N, Rac3-/- and double Rac1N/Rac3-/- mice (I). (A,B) No differences in the levels of the indicated proteins between Rac1N and WT (A), or Rac1N/Rac3-/- and Rac3-/- (B) brain fractions. 100 μg of each fraction (prepared as described in Materials and Methods) from P13 WT (C1), Rac1N (K1), Rac3-/- (C2) and Rac1N/Rac3-/- (K2) brain were analysed by immunoblotting using the anti-PSD95 mAb, anti-PAK pAb, anti-synaptophysin mAb and anti-Vamp2 mAb. The anti-tubulin mAb was used as loading control. Molecular weights are indicated. H, homogenate; P1, nuclear pellet; S1, post-nuclear supernatant1; P2, crude synaptosomal-enriched fraction; S2, supernatant-2 (membranes and cytosolic fractions); P3, membrane pellet; S3, cytosolic fraction; SYN, clean synaptosomal fraction.

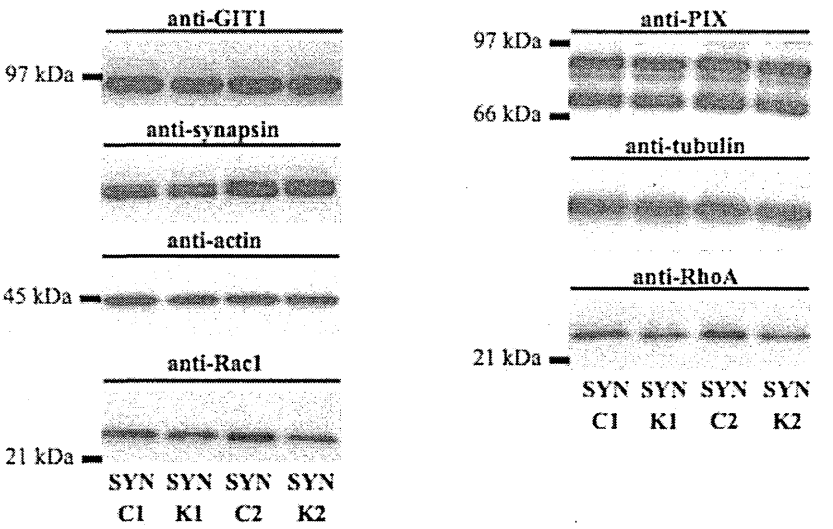

Figure 3.32 Biochemical analysis of the synaptosomal fractions from WT, Rac1N, Rac3-/- and double Rac1N/Rac3-/- mice (II). Rac1 and RhoA levels are reduced in Rac1N and Rac1N/Rac3-/- synaptosmal fractions compared to WT and Rac3-/- respectively. The levels of the other indicated proteins are comparable. 100 μg of clean synaptosomal fraction (SYN) from P13 WT (C1), Rac1N (K1), Rac3-/- (C2) and Rac1N/Rac3-/- (K2) brains were analysed by immunoblotting using the anti-GIT mAb, anti-synapsin pAb, anti-Rac1 mAb, anti-PIX pAb and anti-RhoA mAb. The anti-tubulin and anti-actin mAbs were used as loading control. Molecular weights are indicated.

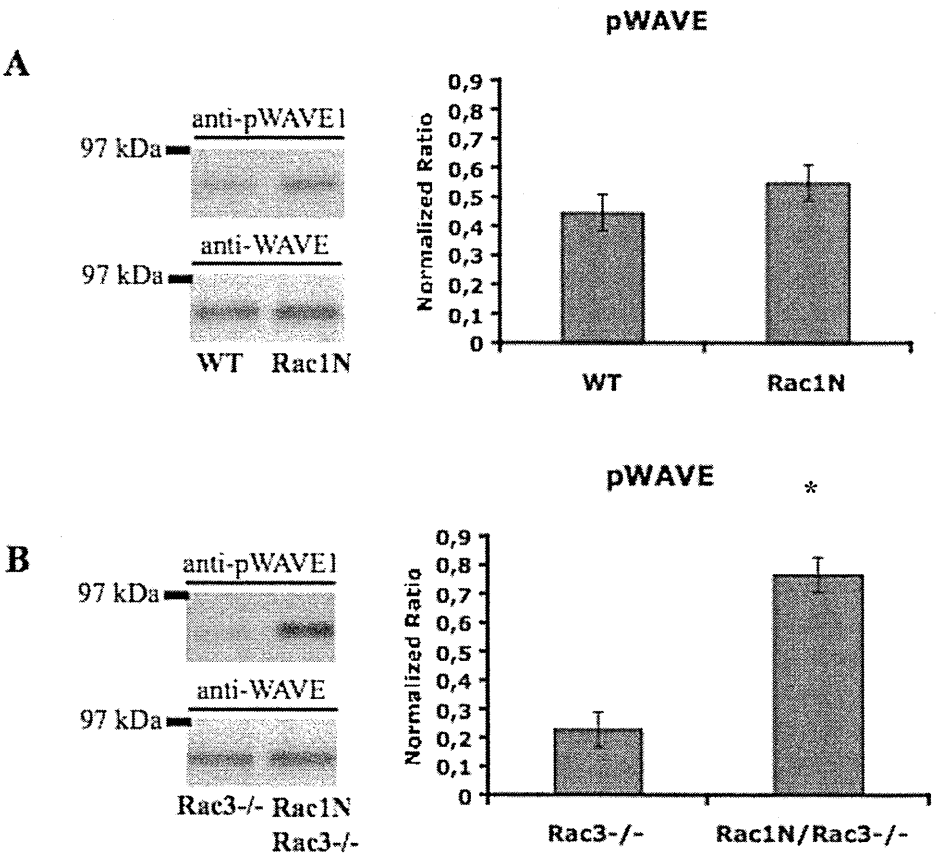

Figure 3.33 Increased phosphorylation of WAVE1 in double Rac1N/Rac3-/- brains. (B) WAVE1 phosphorylation on Ser310 is increased (over 3-folds) in the brain of double Rac1N/Rac3-/- mice compared to Rac3-/- mice (*P < 0.04; n=4). (A) No statistically significant differences were observed between Rac1N and WT brains. (A,B) 100 µg of protein total lysate from each type of P13 brain were analysed by immunoblotting using anti-phospho-Ser310-WAVE1 pAb. Immunoblotting using anti-WAVE pAb was used to look at the total WAVE. Molecular weights are indicated. Quantification was performed as described in Material and Methods. Each bar represents the averaged ratio between the values of each genotype with the sum of the values of the two genotypes to be compared (+/−S.E.M.).

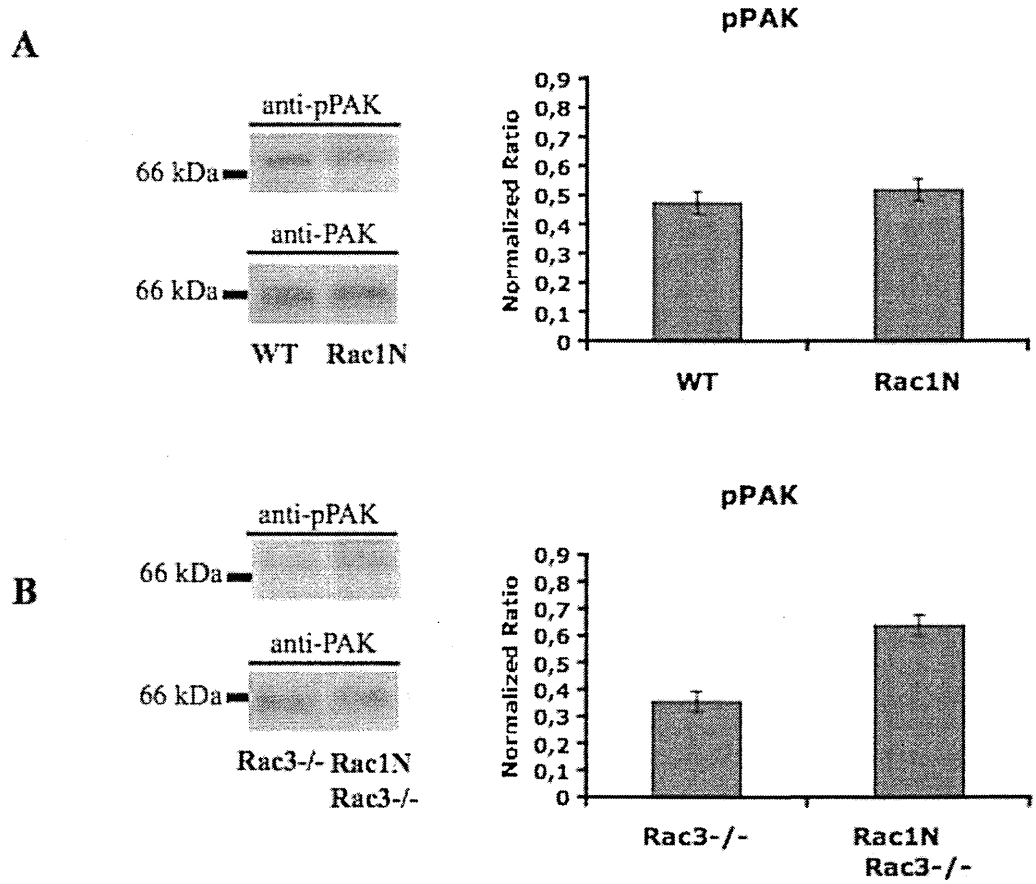

Figure 3.34 Increased phosphorylation of PAK1 in double RacIN/Rac3-/- brains. (B) PAK1 phosphorylation on Thr423 is slightly increased (1.8-fold) in the brain of double RacIN/Rac3-/- mice compared to Rac3-/- mice (P = 0.059; n=4; border line). (A) No differences were observed between RacIN mice compared to WT mice. (A,B) 100 µg of protein total lysate from each type of P13 brain were analysed by immunoblotting using anti-phosphoThr423-PAK1 pAb. Immunoblotting using anti-PAK1 pAb (recognizing PAK1/2/3 isoforms) was used to look at the total PAK. Molecular weights are indicated. (B) Quantification was performed as described in Material and Methods. Each bar represents the averaged ratio between the values of each genotype with the sum of the values of the two genotypes to be compared (+/−S.E.M.).

3.3.5 Rac1N/Rac3-/- mice show specific defects in the dorsal hilus

We performed morphological analysis of brains from mutant mice to look for anatomical correlates of the observed phenotypes. We found that the dorsal hippocampal hilus was strikingly thinner in P13 double Rac1N/Rac3-/- mice, when compared to WT and single mutant mice (Fig. 3.35). The reduced thickness of the dorsal hilus was paralleled by a strong decrease in the number of large GluR2/3 (glutamate receptor subunits 2 and 3)-positive mossy cells (Fig. 3.36), the major excitatory neurons of the hilus involved in a range of physiological and pathological conditions (Ratzliff et al., 2002; Sloviter, 1987). Moreover, in contrast to what observed in the dorsal hilus, we did not find any differences in the thickness of the ventral hilus (Fig. 3.35) in P13 double mutant animals.

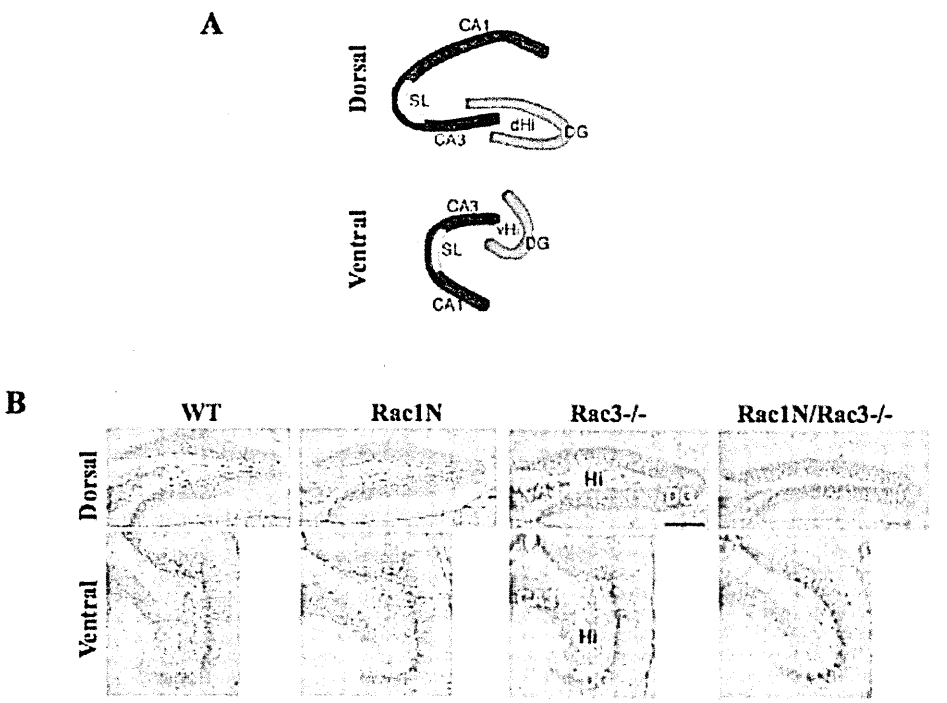

Figure 3.35 Dorsal hilus is reduced in double Rac1N/Rac3-/- hippocampus. (A) Scheme of the dorsal and ventral hippocampus. DG, dentate gyrus; dHi, dorsal hilus; vHi, ventral hilus; SL, stratum lucidum. (B) Nissl staining on sections of dorsal (upper) and ventral (lower) dentate gyrus from P13 WT, Rac1N, Rac3-/- and double Rac1N/Rac3-/- mice showed reduced thickness of the dorsal hilus in the hippocampus of double Rac1N/Rac3-/- mice. Scale bar, 200μm.

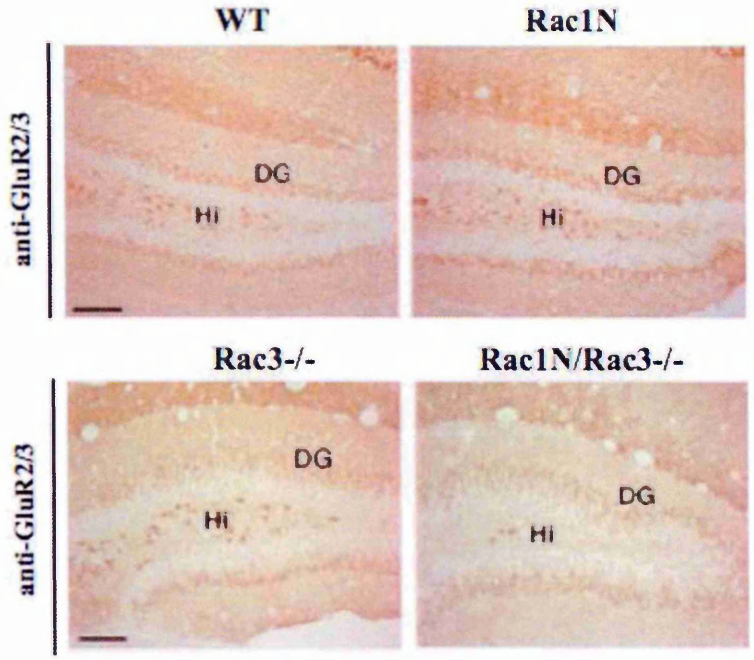

Figure 3.36 P13 double Rac1N/Rac3-/- mice show a reduced number of GluR2/3-positive mossy cells in dorsal hilus. Immunohistochemistry on P13 brain sections stained with anti-GluR2/3 Ab. GluR2/3-positive cells are strongly reduced in the dentate hilus of P13 Rac1N/Rac3-/- mice compared to Rac3-/-, WT, and Rac1N mice. Hi, hilus; DG, dentate gyrus. Scale bar, 100 μm.

3.3.6 Neuronal circuitry is affected in the dentate gyrus of Rac1N/Rac3-/- mice

Since mossy cells are part of the circuitry that plays important regulatory functions in the hippocampus (Ratzliff et al., 2002), we investigated the effects of mossy cell-depletion on neuritogenesis and synaptogenesis in the dorsal hippocampus of Rac1N/Rac3-/- mice. During brain development, the axons of mossy cells project to the proximal dendrites of granule cells (Fig. 3.37) in the inner molecular layer of ipsi- and contra-lateral dentate gyrus (Frotscher et al., 1991; Ribak et al., 1985). We found a marked reduction of calretinin-positive axonal projections of mossy cells (Liu et al., 1996) in the inner molecular layer of the dorsal dentate gyrus of double mutant mice (Fig. 3.38), as a consequence of the drastic bilateral reduction of mossy cells. Moreover, we found that the innervation of mossy cells by collaterals of ZnT-3 (zinc transporter protein-3)-positive mossy fibers (Palmiter et al., 1996) within the dorsal hilus of P13 Rac1N/Rac3-/- mice was drastically reduced (Fig. 3.39, right panels). In contrast mossy fiber projections from granule cells to the stratum lucidum of the CA3 pyramidal neurons were normal in the dorsal hilus of P13 Rac1N/Rac3-/- animals (Fig. 3.39, left panels). Therefore, our results showed that both neuritogenesis and synaptogenesis were heavily disrupted in neurons of the dorsal dentate gyrus, which are known to mature postnatally (Ribak et al., 1985).

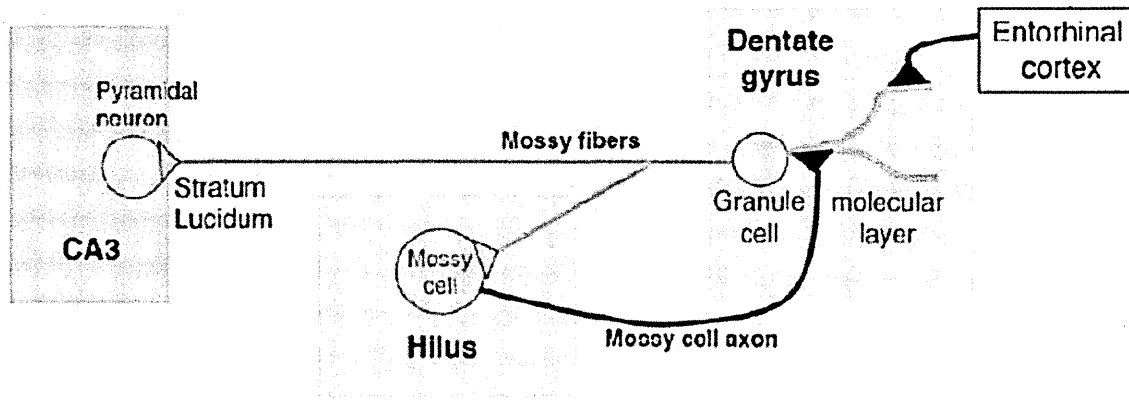

Figure 3.37 Scheme of major connections within the hippocampus involving hilar mossy cells and dentate granule cells. Granule cells send their axons (mossy fibers) both to mossy cells in the hilus and to pyramidal neurons in the CA3. Mossy cells are bi-directionally linked to granule cells by a positive feedback loop that is strategically placed between the entorhinal cortex and the hippocampal CA3 region.

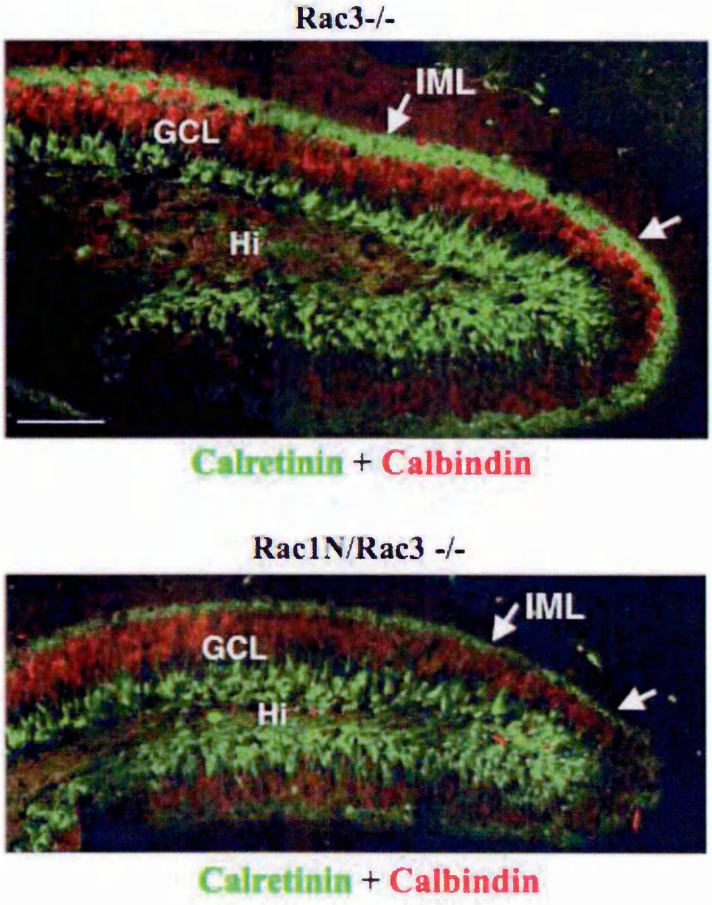

Figure 3.38 Mossy cell axonal projections to dentate granule cells are reduced in the dorsal hilus of P13 double Rac1N/Rac3-/- mice. Immunofluorescence on sections of P13 Rac3-/- and Rac1N/Rac3-/- brains stained with anti-calbindin Ab (red) that labels mature granule cells and with anti-calretinin Ab (green) that stains immature granule cells and mossy cell axonal projections to the inner molecular layer (IML). The calretinin positive projections of mossy cells to the IML of the dorsal dentate gyrus (arrows) are strongly reduced in Rac1N/Rac3-/- mice compared to Rac3-/- mice. GCL, granule cell layer; Hi, hilus. Scale bar, 100 μm.

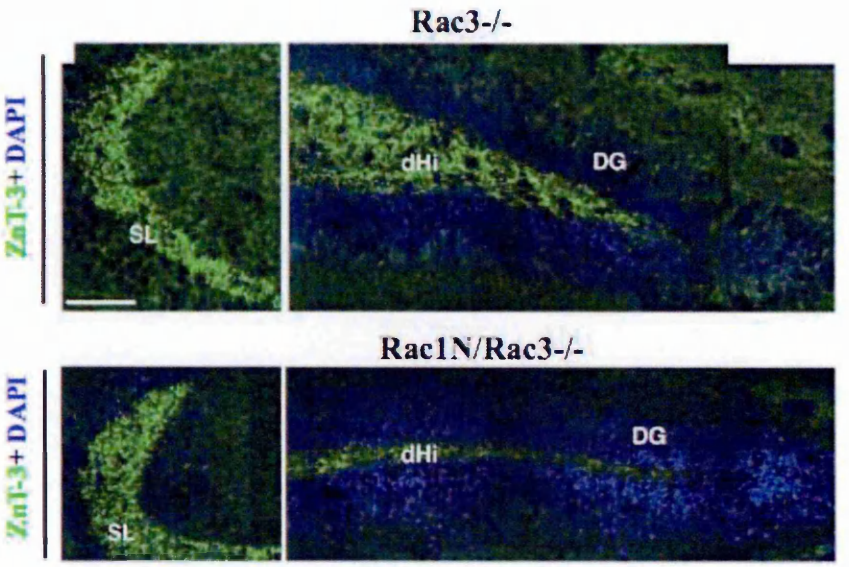

Figure 3.39 Mossy fiber projections from granule cells to mossy cells are strongly reduced in P13 double Rac1N/Rac3-/- mice. Hippocampi from P13 Rac3-/- and Rac1N/Rac3-/- mice were stained with anti-ZnT-3 (green), a marker for granule cell mossy fibers, and with DAPI (blue). The ZnT-3-positive axonal terminals are strongly reduced in the dorsal hilus (dHi) (right panels) of Rac1N/Rac3-/- mice compared to Rac3-/- mice. Axonal projections of granule cells to the stratum lucidum (SL) of the dorsal CA3 subfield are not affected (left panels). Scale bar, 100 μm. DG, dentate gyrus.

3.3.7 Analysis of hippocampal cultures from different knockout mice

Given the severe hippocampal phenotype observed in double Rac1N/Rac3-/- mice, I have used hippocampal cultures to better address the role of Rac1 and Rac3 in late stages of neuronal maturation. It has been previously reported that these events are impaired by the expression of Rac1 mutants. One limitation in the use of these mutants is that they cannot distinguish between the Rac isoforms involved (Luo et al., 1996; Nakayama et al., 2000).

I set up the conditions to culture neurons from single embryos obtained from the following breedings: Rac1F/F/Rac3-/- X Rac1F/+/Syn-Cre/Rac3-/-. Surprisingly, I found that hippocampal neurons from Rac1F/F/Syn-Cre/Rac3-/- embryos grew normally in culture until late stages of neuronal development (Fig. 3.40). Immunofluorescence and PCR analysis on genomic DNA from 15 DIV neurons showed that the Cre-recombinase was very poorly expressed in cultured neurons. There were very few positive cells per culture (Fig. 3.41), although high levels of synapsin-I was detected already at 7 DIV (Fig. 3.42). This might in part be explained by the observation that Synapsin-Cre was not expressed *in vivo* in CA1 pyramidal neurons, and suggests that most of the cultured neurons may derive from this region under our culture conditions. Alternatively, CA3 neurons may not express the transgene *in vitro*. Therefore I could not use this culture system to analyse specific Rac1 and Rac3-dependent mechanisms during late neuronal development.

To study the effects of Rac depletion on synaptogenesis, I then took advantage of the Rac1F/F and Rac1F/F/Rac3-/- mice that I have generated. I obtained cultures from these mice, and transfected with pEGFP-Cre to delete the floxed Rac1 gene *in vitro*, as already published for other genes (Rico et al., 2004).

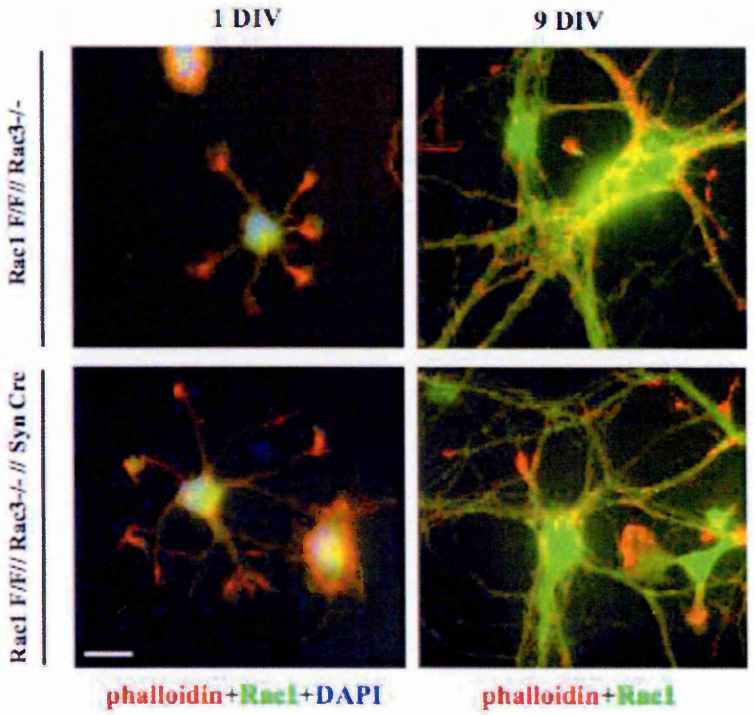

Figure 3.40 Morphological analysis of cultured hippocampal neurons from Rac1F/F/Syn-Cre/Rac3-/- embryos. 1 DIV and 9 DIV hippocampal neurons from Rac1F/F/Rac3-/- (upper panel) and Rac1F/F/Syn-Cre/Rac3-/- (bottom panel) embryos were stained with anti-Rac1 mAb (green), phalloidin (red) and DAPI (blue). Neuritogenesis in neurons from Rac1F/F//SynCre//Rac3-/- is not evidently affected. Scale bar, 20 μm.

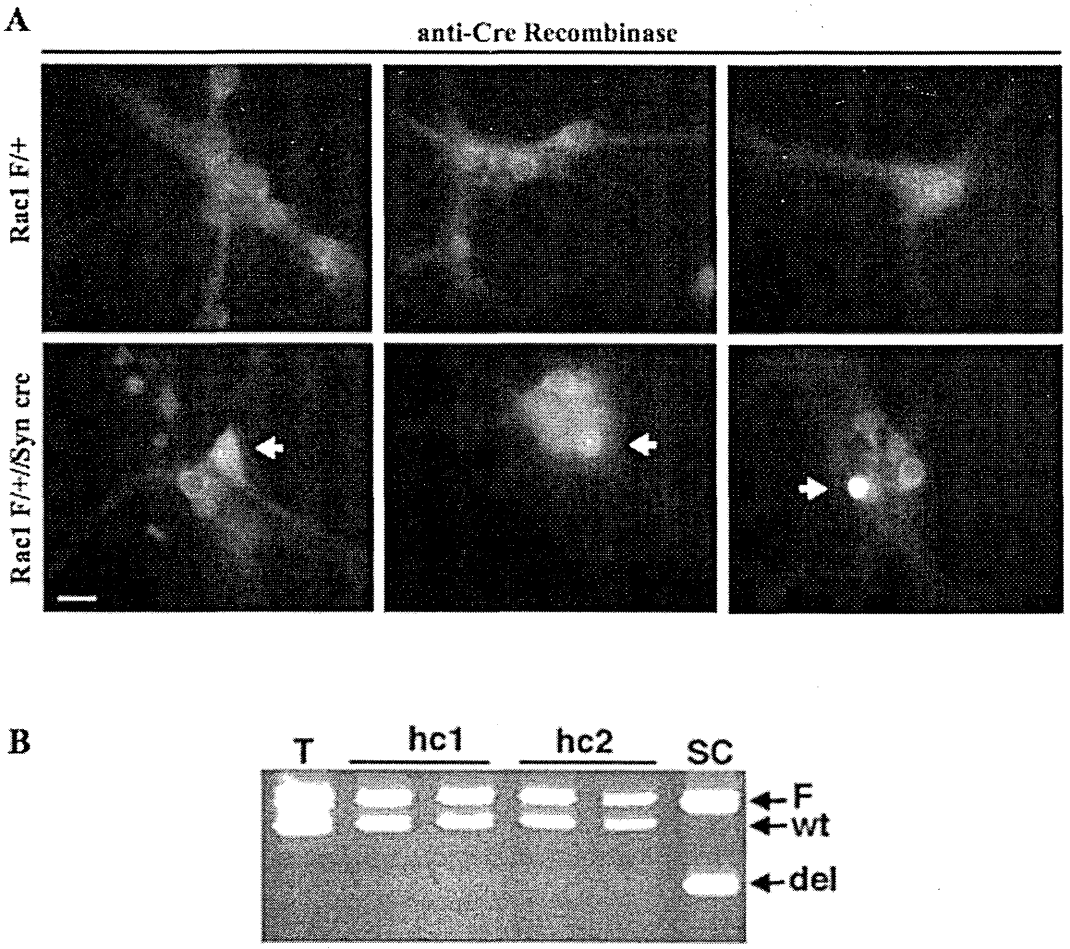

Figure 3.41 Expression and activity of synapsin-Cre-recombinase in cultured hippocampal neurons. (A) Hippocampal neurons from Rac1F/+/SynCre or Rac1F/+ (negative control) embryos were fixed after 15 DIV and stained with anti-Cre mAb to evaluate the expression of the Cre *in vitro*. White arrows indicate Cre-expressing neurons. Very few cells/coverslip are positive. (B) Genomic DNA was extracted from the tail (T) of a Rac1F/+/SynCre mouse (negative control), the spinal cord (SC) of a Rac1F/F/SynCre mouse (positive control), and 15 DIV hippocampal cultures obtained from two different Rac1F/+/SynCre embryos (hc1-hc2). The genomic DNA was analysed by PCR as detailed in fig. 3.24 and in materials and methods. PCR fragments are from floxed (F), wildtype (wt), and deleted alleles (del). The signal for the deleted allele is very weak in 15 DIV hippocampal cultures.

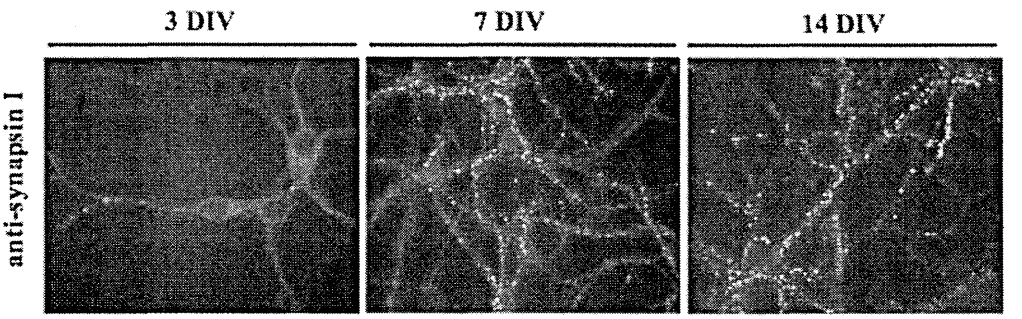

Figure 3.42 Synapsin-I expression in wild-type hippocampal neurons. Hippocampal neurons from wild-type mice were fixed after 3 DIV, 7 DIV and 14 DIV and stained with anti-synapsin-I pAb. Synapsin-I positive vesicles appear first at 3 DIV. After 7 DIV, when synaptogenesis starts, and at 14 DIV the number of synapsin-I positive vesicles is strongly increased.

3.3.8 Rac1 and Rac3 are involved in dendritic spine formation

I evaluated the effects of Rac depletion at later stages of neuronal development, during synaptogenesis. I transfected either pEGFP alone as negative control, or pEGFP together with pEGFP-Cre at 4 DIV in cultures from Rac1F/F and Rac1F/F/Rac3-/- mice. Dendrites at 4 DIV have already extended and they have started to establish the first neuronal connections. The transfected neurons were analysed at 14 DIV. I have considered all the pEGFP transfected neurons in our analysis, since I found that all the pEGFP-positive cells were co-expressing the EGFP-Cre plasmid (Fig. 3.43). I found that the neuritic morphology was similar in EGFP-Cre transfected and EGFP transfected control neurons from both Rac1F/F and Rac1F/F/Rac3-/- mice (Fig. 3.44). Depletion of both Rac1 and Rac3, following expression of EGFP-Cre in Rac1F/F/Rac3-/- neurons affected the process of spinogenesis and spine maturation. In particular, I found that the total number of small dendritic protrusions (including spines, filopodia and lamellipodia) was significantly decreased after deletion of both Rac genes (-21%, $P < 0.00035$). Moreover, the number of postsynaptic dendritic spines, both mushroom-like and stubby, was strongly reduced in double mutant neurons, while the number of long and short dendritic filopodia, and the number of lamellipodia-like protrusions increased significantly in these neurons (Fig. 3.45). The immature protrusions resulted negative to the PSD-95 staining, indicating that they were not active synapses. As mentioned earlier in this thesis, deletion of Rac3 per se had no effects on spine number and spine morphology (Fig. 3.45, 3.46), while deletion of Rac1 by expression of EGFP-Cre in Rac1 F/F neurons had only a weak effect on the number of mushroom-shaped spines (Fig. 3.45, 3.46), indicating a partial compensatory effect mediated by Rac3 during the process of spine formation and maturation. These results show that Rac1 and Rac3 play a synergistic role in the formation of dendritic spines.

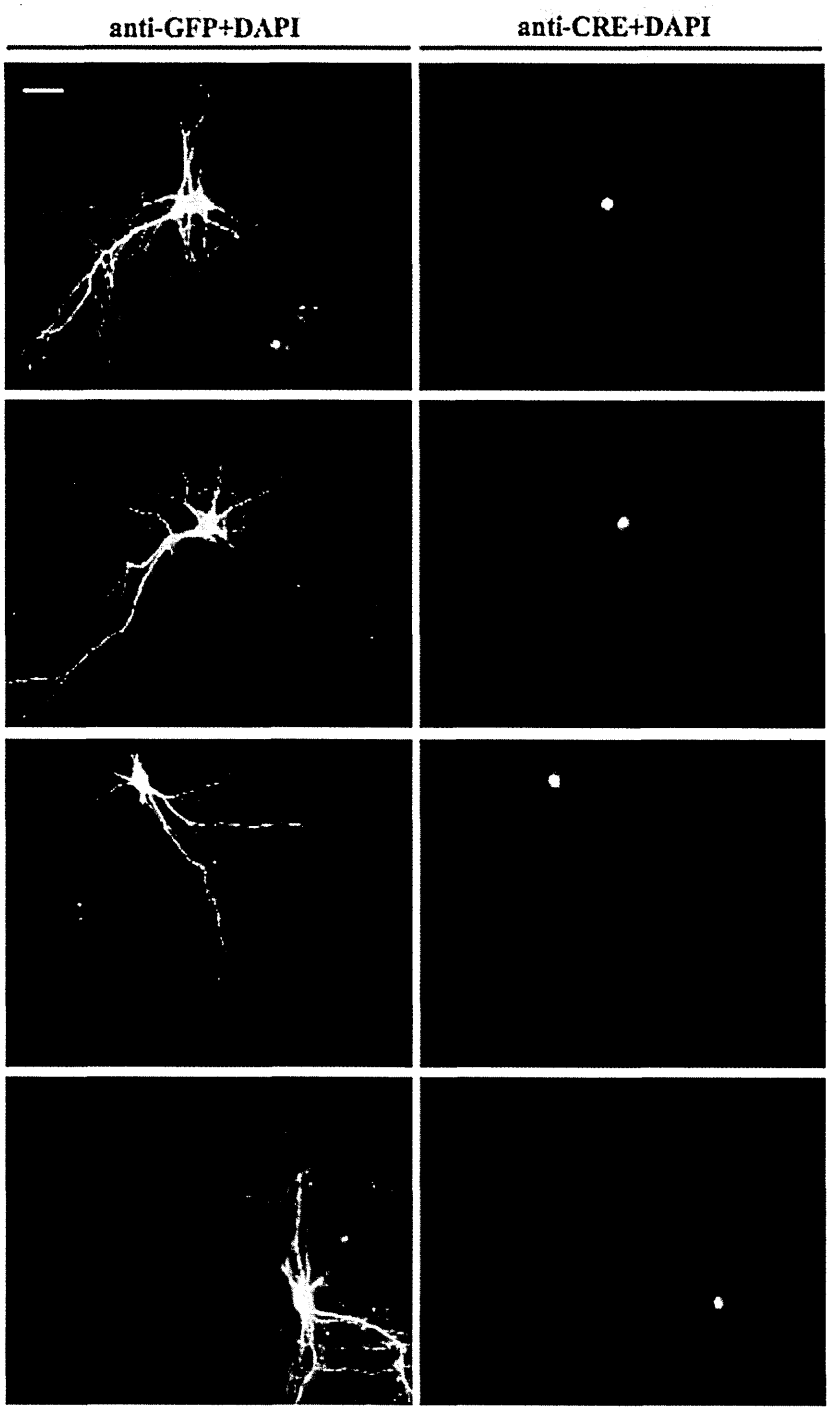

Figure 3.43 Evaluation of pEGFP-Cre and pEGFP cotrasfection in hippocampal neurons cultures. Hippocampal neurons from Rac1F/F embryos were transfected at 4 DIV with 0.5 μg pEGFP-Cre and 0.5 μg of pEGFP plasmids, using Lipofectamine™ 2000. Neurons were fixed at 14DIV and stained with anti-Cre mAb (red), anti-GFP pAb (green) and DAPI (blue). The right and left panels show the same fields. Scale bar, 50 μm. All neurons transfected for pEGFP were co-transfected with pEGFP-Cre.

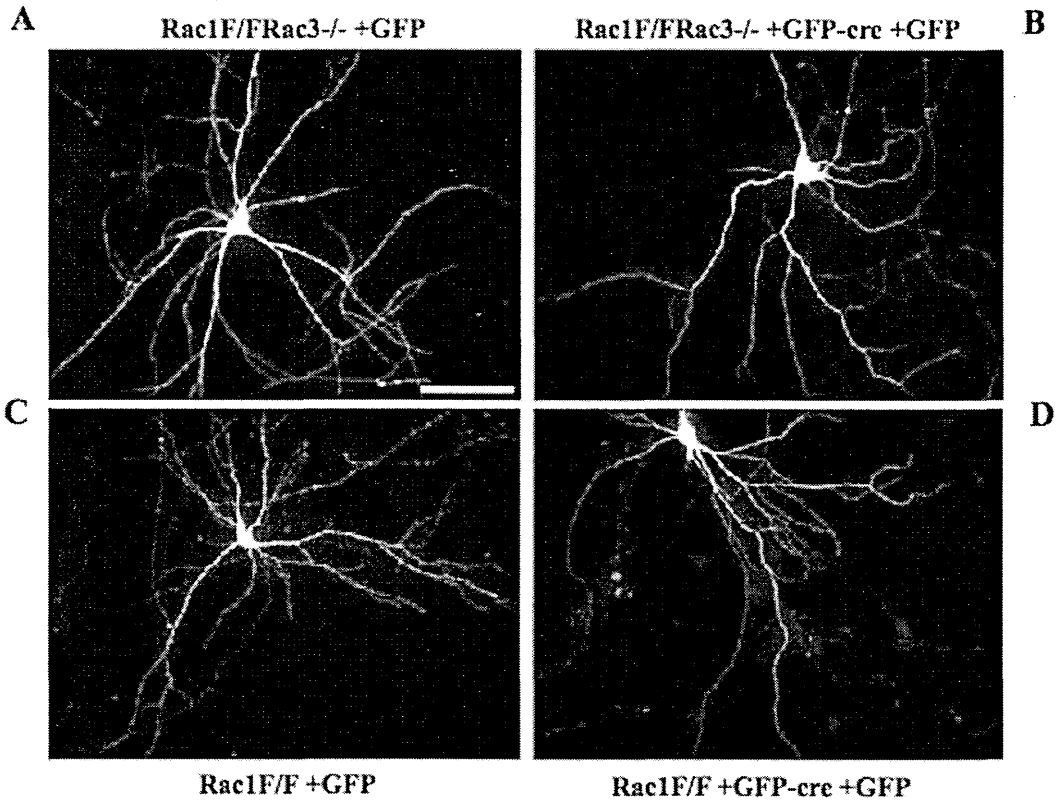

Figure 3.44 Morphology of neurons transfected with GFP and GFP-Cre. Hippocampal neurons from Rac1F/F (C, D) and Rac1F/F/Rac3-/- (A, B) embryos were transfected at 4 DIV with 1 µg pEGFP (A, C) or 0.5 µg pEGFP and 0.5 µg pEGFP-Cre-Recombinase plasmids (B, D), using Lipofectamine™ 2000. Cells were fixed at 14 DIV and stained with anti-GFP pAb. The overall neuritic morphology is not evidently affected in neurons expressing pEGFP-Cre when compared to control neurons transfected with pEGFP. Scale bar, 100 µm.

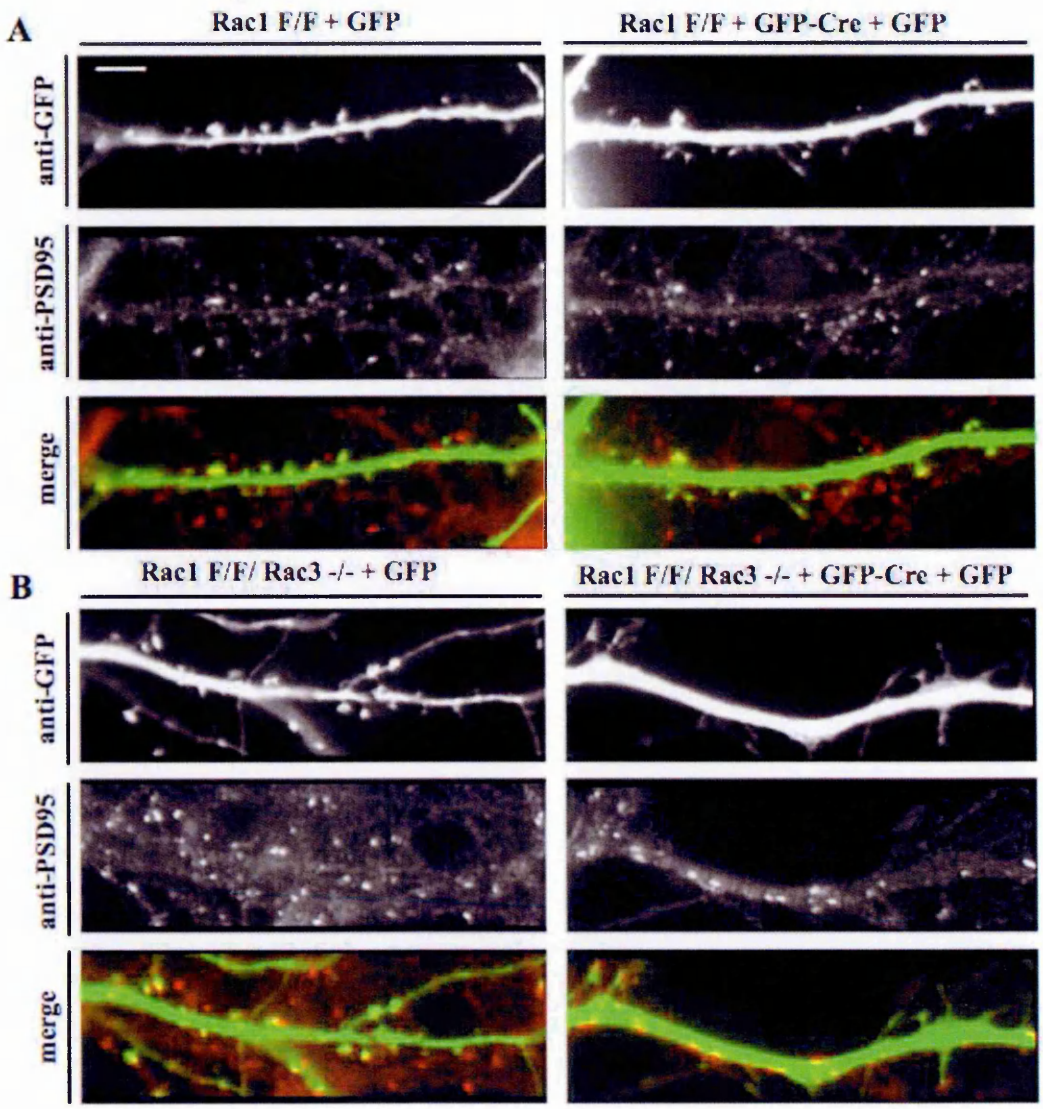

Figure 3.45 Deletion of both Rac1 and Rac3 strongly affects spinogenesis. Hippocampal neurons from Rac1F/F (A) or Rac1F/F/Rac3-/- (B) embryos were transfected at 4 DIV either with 1μg pEGFP alone (left panels), or cotransfected with 0.5 μg pEGFP-Cre and 0.5 μg pEGFP (right panels), using Lipofectamine™ 2000. Neurons were fixed at 14 DIV and stained with anti-GFP pAb (green) and anti-PSD-95 mAb (red). The merged picture is shown for each panel. Scale bar, 5 μm.

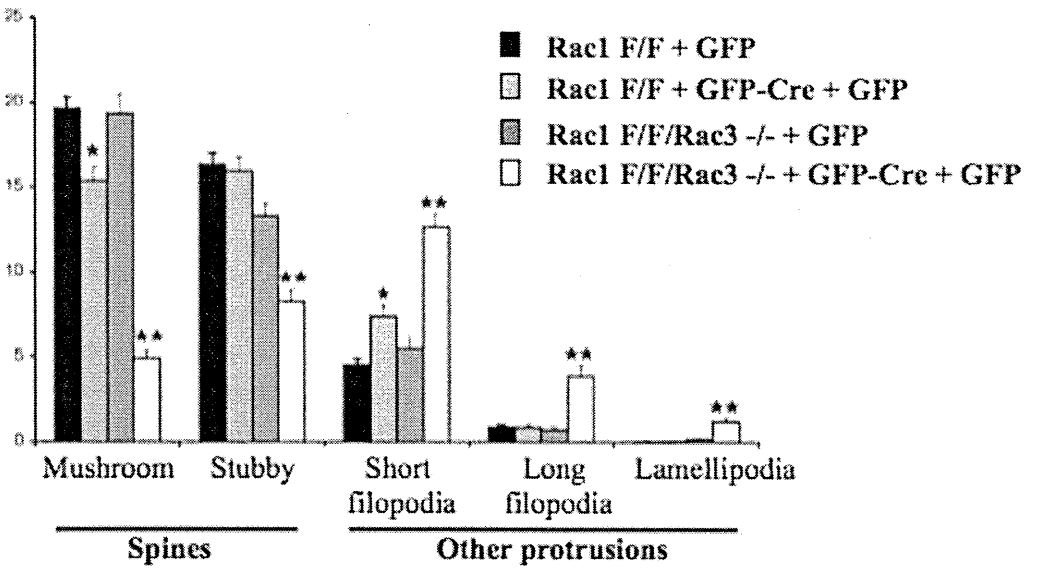

Figure 3.46 Quantification of dendritic spine morphology. The number of mature and immature spines on dendrites of transfected hippocampal neurons (as in Fig. 3.45), shown as average protrusion density (number/100 μm). Quantification was performed on at least 450 protrusions from 7-10 neurons per experiment per conditions. Two independent experiments have been analysed. Dendritic protrusions included: mushroom and stubby spines, short (<4 μm) and long (>4 μm) filopodia, and lamellipodia. *, $P<0.0005$; **, $P<0.00005$ [compared to respective control neurons (Student's *t* test)].

4 DISCUSSION

It is of crucial importance to understand the physiological relevance of two Rac genes expressed in neurons during the nervous system development. Which is their specific function? The majority of previous works studied the role of the Rac proteins in the development of the nervous system by using Rac1 mutants in different systems. This approach cannot distinguish between the specific functions of each Rac isoform. As one example, dominant negative Rac mutants are highly promiscuous in binding and sequestering different exchanging factors that are likely shared by both GTPases (Allen et al., 2000; Lee et al., 2003; Li et al., 2000; Luo et al., 1996; Luo et al., 1994; Nakayama et al., 2000). In this thesis, my goal has been to study the functions of Rac3 and Rac1 proteins during neuronal development, by using both the knockout of these proteins in mice, and the knockdown of the endogenous proteins *in vitro*.

The results obtained in this study, by using both *in vivo* and *in vitro* approaches, give complementarities in the understanding and in the interpretation of the results. Anyway it is of crucial importance to be careful not to directly compare independent results obtained with such different approaches. For example, the effects of Rac1 siRNA at early stages of *in vitro* neuronal development cannot directly be compared with the effects of Rac3 depletion *in vivo*, or with the ones mediated by Cre-recombinase during later phases of *in vitro* neuronal development. Unfortunately I had to study the *in vitro* function of Rac by using such strategies due to different technical problem I encountered in my work. For this reason I consider this, the major limit of this work.

I showed that Rac3-/- hippocampal neurons did not show any defects during neuritogenesis and synaptogenesis under physiological conditions. It would be interesting in the future analyzing the effects of Rac3 depletion under stress conditions, as for example during axonal re-growth after axotomy.

I showed then Rac1 depletion by RNAi in both wild-type and Rac3-/- hippocampal neurons during early stages of neuronal development, specifically affected dendritic development without interfering with axonal outgrowth. Reduced levels of Rac1 impaired growth cone dynamics by decreasing the levels of F-actin in both neurites and growth cones. On the other hand, Rac1 knockdown, by using the Cre-recombinase approach, during later phases of neuronal development did not affect spine morphology, while double depletion of Rac1 and Rac3 induced severe morphological alterations of dendritic spines.

In parallel, while single depletion of Rac1 or Rac3 *in vivo* did not cause a strong phenotype, double knockout mice died around P13, they showed a strong reduction of the body weight and they showed neurological defects. These impairments are correlated to specific alteration of the hippocampal circuits. This work showed for the first time that both Rac1 and Rac3 are important for neuronal development.

4.1 Rac1 is essential for early dendritic development in vitro

My results have indicated that endogenous Rac1 is essential for early dendritic development, whereas normal levels of this GTPase are not required for the initial establishment of neuronal polarity and axonal development, while Rac3 is not essential for early neuronal development.

To explain the different effects of Rac1 down-regulation observed in dendrites and axons, different hypothesis can be formulated. First, as it is often the case when using siRNA, after Rac1 siRNA some residual Rac1 protein may still remain. In my experimental conditions it appears that most of the Rac signal has been eliminated after Rac1 siRNA treatment, although a weak signal is still detected. Therefore, I cannot exclude some residual Rac activity under the experimental conditions used, especially in the very early stages of neuronal development, soon after plating neurons in culture after neuronal transfection, and before maximal down-regulation by siRNA is achieved. On the other

hand, my results showed a dramatic difference between dendritic and axonal development in the same neurons, indicating a clear difference in the sensitivity of the two processes to Rac1 down-regulation. Given the probable incomplete depletion of Rac1 by siRNA, the specific effects on dendrites versus axon may result from different sensitivity to lower Rac levels in the two types of neurites. I showed a correlation between Rac1 down-regulation and reduction of F-actin. This reduction has affected dendrites development specifically. It has been previously shown that a decrease in F-actin, induced by cytochalasin D (actin depolymerizing drug), induced the formation of multiple curved axons per cell (Bradke and Dotti, 1999; Kunda et al., 2001). This has led to suggest that actin instability in growth cones is correlated to axon specification, with the initial steps of axon formation requiring actin cytoskeleton destabilization (Bradke and Dotti, 1999; Da Silva et al., 2005).

Actin depolymerizing drugs destabilize actin filaments by increasing actin turnover and the consequent formation of new actin filaments that promote axonal outgrowth. This could partially explain the Rac1 knock-down phenotype: I found in Rac1 siRNA-treated cells reduced F-actin levels in neurite growth cones, probably due to defects in Rac1-mediated Arp2/3 actin polymerization, with consequent loss of growth cone dynamics. I could assume that Rac1 depletion caused a reduction of F-actin levels, inducing consequent actin instability. Then, spatial-regulation of other activated Rho GTPases in differentiating hippocampal neurons, could explain the effects on dendritic growth. While in the axon the specific activation of other Rho family members, as Cdc42, could trigger actin polymerization and further axonal growth, in dendrites probably only activated Rac1 could induce dendritic outgrowth. This hypothesis is supported by recent data that showed that total depletion of Cdc42 in hippocampal neurons leads striking defects in the formation of axonal tracts, without affecting dendritic development (Garvalov et al., 2007). It would be interesting in the future to investigate *in vivo* the intracellular localization of active Rac and active Cdc42 during neuritic outgrowth.

My results indicate that Rac3 by itself cannot compensate Rac1 function during early neuronal development, since down-regulation of Rac1 by siRNA have led similar inhibition of dendritic development in both wild type and Rac3 knockout neurons.

RhoG may also contribute to differentially control growth-cone motility in axons and dendrites, and help explaining the different response of the two types of neurites to Rac1 down-regulation. Given the co-expression RhoG with Rac1 in hippocampal neurons (O'Kane et al., 2003), it is possible that RhoG plays an important role in the regulation of actin dynamics during early axonal development. RhoG regulates actin dynamics in non-neuronal cells (Gauthier-Rouviere et al., 1998) and is involved in NGF induced neurite outgrowth, together with its GEF Trio (Blangy et al., 2000; Estrach et al., 2002). Accordingly, mice lacking Trio display aberrant organization in several regions of the brain, including the hippocampus (O'Brien et al., 2000).

Analysis of Rac function in *Drosophila* has shown that progressive loss of combined Rac genes activity leads to distinct effects on neuritic development (Ng et al., 2002). The finding that *Drosophila* axons were affected by Rac depletion may be correlated to the use of a different system and/or by the fact that distinct Rac regulators and effectors may be responsible for diverse effects in different neuronal types. In this direction, it has been shown that expression of *Drosophila* dominant-negative N17Rac1 causes axonal outgrowth arrest in sensory neurons (Luo et al., 1994), whereas the same mutant induces guidance defects, but not outgrowth defects, in motor neurons, causing motor axons to extend beyond their normal synaptic partners (Kaufmann et al., 1998). Since inactive Rac mutation compromises the trajectory of axons without inhibiting their extension, a possible role for Rac in some neuronal types may be related to executing specific axonal guidance decisions. In conclusion my results, together with the recent findings regarding the role of Cdc42 in axon formation (Garvalov et al., 2007; Sosa et al., 2006), suggest that Rac1 and Cdc42 play distinct roles in early neuronal development, the first being involved in dendritic, while the latter in axonal development.

On the other hand, it has been interesting to observe that Rac3 depletion by itself does not evidently affect neuronal development, although we cannot exclude compensatory effects produced by Rac1 following long-term Rac3 depletion by gene knockout. We can assume that, the Rac1 compensatory effect observed *in vivo*, may be reproduced during *in vitro* neuronal development. Furthermore, it would be interesting to knockdown Rac3 by siRNA technology in order to compare the effects of the acute down-regulation of both GTPases during early neuronal development.

4.2 Rac1 and Rac3 are essential for dendritic spine morphogenesis

My results have interestingly shown that both Rac1 and Rac3 are essential during later neuronal development *in vitro*. Depletion of Rac1 and Rac3 strongly impaired dendritic spine formation and maturation. So far, Rac1 has been considered the major if not only Rac GTPase required for vertebrate neuronal development. Several studies have indicated the crucial role of Rac GTPases for the correct establishment of functional synapses. For example, Rac specifically activates at the synapses (Zhang et al., 2005), mediates clustering of AMPA receptors during spinogenesis (Wiens et al., 2005), and induces dendritic branching and spine development upon NMDA receptor activation (Tolias et al., 2005). Anyway most evidences are based on studies using constitutively active or dominant negative Rac1 mutants. Rac activation or inactivation by using these mutants, causes severe defects both during spine formation in developing neurons and during spine maintenance in mature neurons (Nakayama et al., 2000; Tashiro and Yuste, 2004; Wiens et al., 2005; Zhang and Macara, 2006). Moreover, various Rac-GEF, including Kalirin7 and Tiam1 play important role during dendritic spine morphogenesis upon the Ephrin B/ EphB receptor activation (Penzes et al., 2003; Penzes et al., 2001; Tolias et al., 2007), supporting the importance of the GTPase correct cycling between the active and the inactive form.

So far nothing was known about the possible role of Rac3 during spinogenesis. I have

shown here that Rac3-/- neurons did not show defects in spine formation and maturation, while Cre-mediated Rac1 depletion causes a slight reduction of the number of mature spines. This effect is not observed upon Rac3 knockout. Anyway, upon single depletion, 14 DIV neurons were able to normally form mature spine with mushroom-like shape, positive for PSD-95, suggesting that they are functional synapses.

These results demonstrated that Rac1 is totally able to compensate the absence of Rac3, while the latter only partially. I believe that the two following hypotheses may explain this result: the first hypothesis is that Rac3 is less abundant than Rac1, therefore not sufficient to totally compensate the absence of Rac1; the second hypothesis is that Rac1 is not only involved in pathways shared with Rac3, but also in Rac1-specific pathways. It would be interesting to measure the expression levels and the activation state of Rac1 and Rac3 in the mature spine head, by using FRET analysis in order to prove or exclude my first hypothesis.

On the other hand, double depletion of Rac1 and Rac3 induces an increase of filopodia-like protrusions and aberrant lamellipodia-like protrusions coupled to a strong reduction of mature spines and number of total protrusions. Interestingly this phenotype resembles the effects induced by both constitutively active and dominant negative mutants, (Nakayama et al., 2000; Tashiro and Yuste, 2004; Wiens et al., 2005; Zhang and Macara, 2006). This again underlies the importance of a correct cycling of these GTPases.

These results indicate for the first time that only double depletion of endogenous Rac1 and Rac3 leads to defects in alteration of the actin cytoskeleton dynamic that is essential for the formation and maturation of dendritic spines.

The *in vitro* analysis presented in this thesis supports the conclusion that Rac3 plays an essential role during later phases of *in vitro* neuronal development, orchestrating together with Rac1 the formation and maturation of post-synaptic specializations. Rac1 depletion alone, for instance, does not lead to the severe impairment in spines maturation observed when double depletion occurs, indicating the Rac3 ability in explicating Rac1 function.

During earlier phases of neuronal development instead, the down-regulation of Rac1 is sufficient to impair dendritic development, indicating that Rac3 does not play a major role during neuritogenesis at these stages. This conclusion is consistent with the expression pattern of Rac3 that shows highest levels during the time of late neuritogenesis and synaptogenesis (Bolis et al., 2003; Corbetta et al., 2005).

4.3 Depletion of Rac GTPases in vivo

We have shown that the GTPases Rac1 and Rac3 are synergistically critical for mammalian brain development, where these proteins may play redundant and yet essential functions. Also *in vivo*, single depletion of Rac3 or Rac1 did not induce a strong phenotype, even though Rac3 depletion was leading to behavioural anomalies (Corbetta et al., 2008), suggesting a crucial role of Rac3 in the correct formation of functional neuronal circuits important for cognitive functions.

Deletion of the two genes in differentiated neurons leads to severe neurological impairments that can be correlated to the morphological defects observed in the development of the dentate gyrus, by hampering the formation of specific circuits connecting hilar neurons and granule cells, two types of neurons that complete their differentiation postnatally (Ribak et al., 1985; Schlessinger et al., 1975). The wiring diagram of the hippocampus is traditionally presented as a trisynaptic loop (Fig. 3.37). Mossy cells are excitatory interneurons believed to be important regulators of the signals arriving to the dentate gyrus from the cortex. During development Rac1 and Rac3 are co-expressed in hilar mossy cells, while only Rac1 is detected in granule cells (Corbetta et al., 2005). Thus, our data indicate that the loss of Rac1 and Rac3 in mossy cells causes a non-cell-autonomous defect in granule cells that reflects defects in the wiring of the hippocampus. This effect may be explained by the drastic decrease of mossy cells found in the dorsal hilus of Rac1-/-/Rac3-/- mice that may therefore underlie the epileptic

phenotype found in the double mutant mice.

It would be interesting in the future to set up the conditions to culture this other population of excitatory neurons alternatively to pyramidal neurons, in order to characterize the endogenous effects of Rac1 and Rac3 depletion on hilar mossy cells maturation and/or migration. This could help correlating the severe defects in the hippocampal wiring.

To investigate the molecular mechanisms through which Rac1 and Rac3 depletion results in the observed phenotype, I have analysed the level of expression of other Rho GTPases and of various Rac effectors or regulators to test if any was affected by the lack of Rac proteins. Interestingly, I found that double depletion of Rac1 and Rac3 induces a decrease of the total levels of RhoA both in synaptosomal fractions and in total brain lysates. RhoA down-regulation can be explained by an autocompensatory effect to the depletion of Rac. Many studies imply that Rac and RhoA activities are antagonistic. Previous studies have also suggested some degree of crosstalk between these two major pathways. Recently for example, it has been shown a functional regulation between these two GTPases in the context of stress fibers maintenance through the complex between the PAK phosphatase POPX2, a negatively regulator of PAK, and the formin mDia, activated by RhoA (Xie et al., 2008). PAK activity has been previously shown to dissolve stress fibers (Manser et al., 1997).

I have also shown that double depletion of Rac1 and Rac3 leads to an increase of PAK phosphorylation on Thr423. Down-regulation of RhoA and increase of PAK activity in double knockout brains could be the result of compensatory mechanisms due to the lack of Rac activity. This would keep the correct balance between actin polymerization mediated by Rac-Arp2/3 signalling and contractility mediated by RhoA-ROCK and RhoA-mDia signalling.

Moreover, another recent work (Sananbenesi et al., 2007), reported that inhibition of Rac1 leads to an increase of PAK1 activity (increase of phopshorylated PAK on Thr 423) and to a reduction of the levels of phosphorylated PAK on Thr 212, a phosphorylation mediated

by p35/cdk5. Previous works have indeed reported that p35/cdk5 interacts with PAK1 upon Rac activation and this interaction has been shown to inhibit PAK activity (Nikolic et al., 1998; Rashid et al., 2001). Sananbenesi showed that upon Rac inhibition, p35/cdk5 dissociated from both the membrane and PAK.

In addition, I found that double depletion of Rac1 and Rac3 cause a strong increase of WAVE1 phosphorylation on Ser 310. It has been reported that phosphorylation of WAVE1 on Ser 310 by Cdk5 inhibits its ability to regulate the Arp2/3-dependent actin polymerization (Kim et al., 2006), suggesting that Arp2/3-WAVE-dependent actin polymerization is altered in the central nervous system of double mutant mice. One interesting hypothesis is that together, the increase of PAK phosphorylation on Thr423 and WAVE1 phosphorilation on Ser310, could be linked by a differently regulated activity of cdk5 in the double Rac1 and Rac3 brains. Specifically, upon Rac down-regulation, the interaction between PAK and p35/cdk5 complex is reduced (Sananbenesi et al., 2007), resulting in an increase of PAK activation. p35/cdk5 is then free to bind and phosphorylate WAVE1 on Ser310 inactivating it. Phosphorylation and dephosphorylation of WAVE1 in neurons has been shown to play crucial roles in the regulation of the actin cytoskeleton and therefore during dendritic spine morphogenesis. For example, neurons in the striatum of WAVE1-/- mice showed a strong reduction of mature spines, coupled to an increase of immature protrusions This phenotype was reversed by expressing a dephosphorylated active form (Kim et al., 2006). Interestingly, this phenotype resembles the one found in double Rac1 and Rac3 knockout hippocampal neurons, suggesting a role of WAVE1 in mediating the effects of Rac during spine morphogenesis. It would be interesting to further investigate the role of WAVE1 phosphorylation, Cdk5 and PAK activation, following Rac down-regulation during spine morphogenesis.

We did not find any consistent differences in the expression levels of other Rac regulators or effectors, including the PIX-GIT1 complex, Kalirin7, Eph, PSD95, vamp2 and Cdc42,

between control and mutant mice, although we cannot exclude that Rac depletion induces changes in the activation form of the protein analysed.

The analysis of Rac3 null mice as well as the *in vivo* and *in vitro* comparative analysis presented in this study suggest that Rac1 and Rac3 are able to at least partially compensate for the lack of the other GTPase, playing both redundant and distinct functions during the neuronal development. Both aspects will need to be considered in future analysis of the function of Rac GTPases in the development of the nervous system. On the other hand, the heavy neurological consequences of the double deletion of Rac1 and Rac3 in neurons show that both proteins contribute to the development of a functional nervous system in vertebrates.

The results reported here are fundamental to future work aiming at defining the role of Rac GTPases in the development of diverse neuronal pathways of the peripheral and central nervous system, in which Rac1 and Rac3 are coexpressed. Moreover, the impairment of hippocampal circuitry and the epileptic phenotype of double mutant animals suggest that these mice may be a valuable model to study the mechanisms of epileptogenesis.

5 REFERENCES

Acebes, A. and Ferrus, A. (2000) Cellular and molecular features of axon collaterals and dendrites. *Trends Neurosci*, **23**, 557-565.

Adamson, P., Marshall, C.J., Hall, A. and Tilbrook, P.A. (1992) Post-translational modifications of p21rho proteins. *J Biol Chem*, **267**, 20033-20038.

Ahmari, S.E., Buchanan, J. and Smith, S.J. (2000) Assembly of presynaptic active zones from cytoplasmic transport packets. *Nat Neurosci*, **3**, 445-451.

Ahnert-Hilger, G., Holtje, M., Grosse, G., Pickert, G., Mucke, C., Nixdorf-Bergweiler, B., Boquet, P., Hofmann, F. and Just, I. (2004) Differential effects of Rho GTPases on axonal and dendritic development in hippocampal neurones. *J Neurochem*, **90**, 9-18.

Albertinazzi, C., Gilardelli, D., Paris, S., Longhi, R. and de Curtis, I. (1998) Overexpression of a neural-specific rho family GTPase, cRac1B, selectively induces enhanced neuritogenesis and neurite branching in primary neurons. *J Cell Biol*, **142**, 815-825.

Allen, M.J., Shan, X. and Murphey, R.K. (2000) A role for Drosophila Drac1 in neurite outgrowth and synaptogenesis in the giant fiber system. *Mol Cell Neurosci*, **16**, 754-765.

Amano, M., Ito, M., Kimura, K., Fukata, Y., Chihara, K., Nakano, T., Matsuura, Y. and Kaibuchi, K. (1996) Phosphorylation and activation of myosin by Rho-associated kinase (Rho-kinase). *J Biol Chem*, **271**, 20246-20249.

Anderson, S.A., Eisenstat, D.D., Shi, L. and Rubenstein, J.L. (1997) Interneuron migration from basal forebrain to neocortex: dependence on Dlx genes. *Science*, **278**, 474-476.

Arakawa, Y., Bito, H., Furuyashiki, T., Tsuji, T., Takemoto-Kimura, S., Kimura, K., Nozaki, K., Hashimoto, N. and Narumiya, S. (2003) Control of axon elongation via an SDF-1alpha/Rho/mDia pathway in cultured cerebellar granule neurons. *J Cell Biol*, **161**, 381-391.

Baas, P.W., Black, M.M. and Banker, G.A. (1989) Changes in microtubule polarity orientation during the development of hippocampal neurons in culture. *J Cell Biol*, **109**, 3085-3094.

Bader, M.F., Doussau, F., Chasserot-Golaz, S., Vitale, N. and Gasman, S. (2004) Coupling actin and membrane dynamics during calcium-regulated exocytosis: a role for Rho and ARF GTPases. *Biochim Biophys Acta*, **1742**, 37-49.

Banker, G.A. and Cowan, W.M. (1977) Rat hippocampal neurons in dispersed cell culture. *Brain Res*, **126**, 397-342.

Bartlett, W.P. and Banker, G.A. (1984a) An electron microscopic study of the development of axons and dendrites by hippocampal neurons in culture. I. Cells which develop without intercellular contacts. *J Neurosci*, **4**, 1944-1953.

Bartlett, W.P. and Banker, G.A. (1984b) An electron microscopic study of the development of axons and dendrites by hippocampal neurons in culture. II. Synaptic relationships. *J Neurosci*, **4**, 1954-1965.

Bellanger, J.M., Astier, C., Sardet, C., Ohta, Y., Stossel, T.P. and Debant, A. (2000) The Rac1- and RhoG-specific GEF domain of Trio targets filamin to remodel cytoskeletal actin. *Nat Cell Biol*, **2**, 888-892.

Bernards, A. and Settleman, J. (2004) GAP control: regulating the regulators of small GTPases. *Trends Cell Biol*, **14**, 377-385.

Blangy, A., Vignal, E., Schmidt, S., Debant, A., Gauthier-Rouviere, C. and Fort, P. (2000) TrioGEF1 controls Rac- and Cdc42-dependent cell structures through the direct activation of rhoG. *J Cell Sci*, **113 (Pt 4)**, 729-739.

Bliss, T.V. and Gardner-Medwin, A.R. (1973) Long-lasting potentiation of synaptic transmission in the dentate area of the unanaestetized rabbit following stimulation of the perforant path. *J Physiol*, **232**, 357-374.

Bliss, T.V. and Lomo, T. (1973) Long-lasting potentiation of synaptic transmission in the dentate area of the anaesthetized rabbit following stimulation of the perforant path. *J Physiol*, **232**, 331-356.

Bokoch, G.M. (2003) Biology of the p21-activated kinases. *Annu Rev Biochem*, **72**, 743-781.

Bolis, A., Corbetta, S., Cioce, A. and de Curtis, I. (2003) Differential distribution of Rac1 and Rac3 GTPases in the developing mouse brain: implications for a role of Rac3 in Purkinje cell differentiation. *Eur J Neurosci*, **18**, 2417-2424.

Bradke, F. and Dotti, C.G. (1999) The role of local actin instability in axon formation. *Science*, **283**, 1931-1934.

Bradke, F. and Dotti, C.G. (2000) Establishment of neuronal polarity: lessons from cultured hippocampal neurons. *Curr Opin Neurobiol*, **10**, 574-581.

Bresler, T., Shapira, M., Boeckers, T., Dresbach, T., Futter, M., Garner, C.C., Rosenblum, K., Gundelfinger, E.D. and Ziv, N.E. (2004) Postsynaptic density assembly is fundamentally different from presynaptic active zone assembly. *J Neurosci*, **24**, 1507-1520.

Brown, M.D., Cornejo, B.J., Kuhn, T.B. and Bamburg, J.R. (2000) Cdc42 stimulates neurite outgrowth and formation of growth cone filopodia and lamellipodia. *J Neurobiol*, **43**, 352-364.

Buchwald, G., Hostinova, E., Rudolph, M.G., Kraemer, A., Sickmann, A., Meyer, H.E., Scheffzek, K. and Wittinghofer, A. (2001) Conformational switch and role of phosphorylation in PAK activation. *Mol Cell Biol*, **21**, 5179-5189.

Bustelo, X.R., Sauzeau, V. and Berenjeno, I.M. (2007) GTP-binding proteins of the Rho/Rac family: regulation, effectors and functions in vivo. *Bioessays*, **29**, 356-370.

Calderon de Anda, F., Gartner, A., Tsai, L.H. and Dotti, C.G. (2008) Pyramidal neuron polarity axis is defined at the bipolar stage. *J Cell Sci*, **121**, 178-185.

Chae, T., Kwon, Y.T., Bronson, R., Dikkes, P., Li, E. and Tsai, L.H. (1997) Mice lacking p35, a neuronal specific activator of Cdk5, display cortical lamination defects, seizures, and adult lethality. *Neuron*, **18**, 29-42.

Chen, L., Liao, G., Waclaw, R.R., Burns, K.A., Linquist, D., Campbell, K., Zheng, Y. and Kuan, C.Y. (2007) Rac1 controls the formation of midline commissures and the competency of tangential migration in ventral telencephalic neurons. *J Neurosci*, **27**, 3884-3893.

Cho, Y.J., Zhang, B., Kaartinen, V., Haataja, L., de Curtis, I., Groffen, J. and Heisterkamp, N. (2005) Generation of rac3 null mutant mice: role of Rac3 in Bcr/Abl-caused lymphoblastic leukemia. *Mol Cell Biol*, **25**, 5777-5785.

Choi, J., Ko, J., Racz, B., Burette, A., Lee, J.R., Kim, S., Na, M., Lee, H.W., Kim, K., Weinberg, R.J. and Kim, E. (2005) Regulation of dendritic spine morphogenesis by insulin receptor substrate 53, a downstream effector of Rac1 and Cdc42 small GTPases. *J Neurosci*, **25**, 869-879.

Cline, H. (2003) Sperry and Hebb: oil and vinegar? *Trends Neurosci*, **26**, 655-661.

Cline, H.T. (2001) Dendritic arbor development and synaptogenesis. *Curr Opin Neurobiol*, **11**, 118-126.

Corbetta, S., D'Adamo, P., Gualdoni, S., Braschi, C., Berardi, N. and de Curtis, I. (2008) Hyperactivity and novelty-induced hyperreactivity in mice lacking Rac3. *Behav Brain Res*, **186**, 246-255.

Corbetta, S., Gualdoni, S., Albertinazzi, C., Paris, S., Croci, L., Consalez, G.G. and de Curtis, I. (2005) Generation and characterization of Rac3 knockout mice. *Mol Cell Biol*, **25**, 5763-5776.

Cory, G.O., Cramer, R., Blanchoin, L. and Ridley, A.J. (2003) Phosphorylation of the WASP-VCA domain increases its affinity for the Arp2/3 complex and enhances actin polymerization by WASP. *Mol Cell*, **11**, 1229-1239.

Czuchra, A., Wu, X., Meyer, H., van Hengel, J., Schroeder, T., Geffers, R., Rottner, K. and Brakebusch, C. (2005) Cdc42 is not essential for filopodium formation, directed migration, cell polarization, and mitosis in fibroblastoid cells. *Mol Biol Cell*, **16**, 4473-4484.

da Silva, J.S. and Dotti, C.G. (2002) Breaking the neuronal sphere: regulation of the actin cytoskeleton in neuritogenesis. *Nat Rev Neurosci*, **3**, 694-704.

Da Silva, J.S., Hasegawa, T., Miyagi, T., Dotti, C.G. and Abad-Rodriguez, J. (2005) Asymmetric membrane ganglioside sialidase activity specifies axonal fate. *Nat Neurosci*, **8**, 606-615.

Dalva, M.B., McClelland, A.C. and Kayser, M.S. (2007) Cell adhesion molecules: signalling functions at the synapse. *Nat Rev Neurosci*, **8**, 206-220.

de Curtis, I. (2001) Cell migration: GAPs between membrane traffic and the cytoskeleton. *EMBO Rep*, **2**, 277-281.

Dehmelt, L. and Halpain, S. (2004) Actin and microtubules in neurite initiation: are MAPs the missing link? *J Neurobiol*, **58**, 18-33.

Dent, E.W. and Gertler, F.B. (2003) Cytoskeletal dynamics and transport in growth cone motility and axon guidance. *Neuron*, **40**, 209-227.

Dent, E.W. and Kalil, K. (2001) Axon branching requires interactions between dynamic microtubules and actin filaments. *J Neurosci*, **21**, 9757-9769.

DerMardirossian, C. and Bokoch, G.M. (2005) GDIs: central regulatory molecules in Rho GTPase activation. *Trends Cell Biol*, **15**, 356-363.

Derry, J.M., Ochs, H.D. and Francke, U. (1994) Isolation of a novel gene mutated in Wiskott-Aldrich syndrome. *Cell*, **79**, following 922.

Desai, A. and Mitchison, T.J. (1997) Microtubule polymerization dynamics. *Annu Rev Cell Dev Biol*, **13**, 83-117.

DesMarais, V., Ghosh, M., Eddy, R. and Condeelis, J. (2005) Cofilin takes the lead. *J Cell Sci*, **118**, 19-26.

Di Cesare, A., Paris, S., Albertinazzi, C., Dariozzi, S., Andersen, J., Mann, M., Longhi, R. and de Curtis, I. (2000) p95-APP1 links membrane transport to Rac-mediated reorganization of actin. *Nat Cell Biol*, **2**, 521-530.

Di Cunto, F., Imarisio, S., Hirsch, E., Broccoli, V., Bulfone, A., Migheli, A., Atzori, C., Turco, E., Triolo, R., Dotto, G.P., Silengo, L. and Altruda, F. (2000) Defective neurogenesis in citron kinase knockout mice by altered cytokinesis and massive apoptosis. *Neuron*, **28**, 115-127.

Didsbury, J., Weber, R.F., Bokoch, G.M., Evans, T. and Snyderman, R. (1989) rac, a novel ras-related family of proteins that are botulinum toxin substrates. *J Biol Chem*, **264**, 16378-16382.

Dillon, C. and Goda, Y. (2005) The actin cytoskeleton: integrating form and function at the synapse. *Annu Rev Neurosci*, **28**, 25-55.

Dotti, C.G., Sullivan, C.A. and Banker, G.A. (1988) The establishment of polarity by hippocampal neurons in culture. *J Neurosci*, **8**, 1454-1468.

Dudek, S.M. and Bear, M.F. (1992) Homosynaptic long-term depression in area CA1 of hippocampus and effects of N-methyl-D-aspartate receptor blockade. *Proc Natl Acad Sci U S A*, **89**, 4363-4367.

Eden, S., Rohatgi, R., Podtelejnikov, A.V., Mann, M. and Kirschner, M.W. (2002) Mechanism of regulation of WAVE1-induced actin nucleation by Rac1 and Nck. *Nature*, **418**, 790-793.

Edwards, D.C., Sanders, L.C., Bokoch, G.M. and Gill, G.N. (1999) Activation of LIM-kinase by Pak1 couples Rac/Cdc42 GTPase signalling to actin cytoskeletal dynamics. *Nat Cell Biol*, **1**, 253-259.

Egea, G., Lazaro-Dieguez, F. and Vilella, M. (2006) Actin dynamics at the Golgi complex in mammalian cells. *Curr Opin Cell Biol*, **18**, 168-178.

Estrach, S., Schmidt, S., Diriong, S., Penna, A., Blangy, A., Fort, P. and Debant, A. (2002) The Human Rho-GEF trio and its target GTPase RhoG are involved in the NGF pathway, leading to neurite outgrowth. *Curr Biol*, **12**, 307-312.

Etienne-Manneville, S. and Hall, A. (2002) Rho GTPases in cell biology. *Nature*, **420**, 629-635.

Evers, E.E., Zondag, G.C., Malliri, A., Price, L.S., ten Klooster, J.P., van der Kammen, R.A. and Collard, J.G. (2000) Rho family proteins in cell adhesion and cell migration. *Eur J Cancer*, **36**, 1269-1274.

Fox, W.M. (1965) Reflex-ontogeny and behavioural development of the mouse. *Anim Behav*, **13**, 234-241.

Frotscher, M., Seress, L., Schwerdtfeger, W.K. and Buhl, E. (1991) The mossy cells of the fascia dentata: a comparative study of their fine structure and synaptic connections in rodents and primates. *J Comp Neurol*, **312**, 145-163.

Fukazawa, Y., Saitoh, Y., Ozawa, F., Ohta, Y., Mizuno, K. and Inokuchi, K. (2003) Hippocampal LTP is accompanied by enhanced F-actin content within the dendritic spine that is essential for late LTP maintenance in vivo. *Neuron*, **38**, 447-460.

Gallo, G. and Letourneau, P.C. (1999) Different contributions of microtubule dynamics and transport to the growth of axons and collateral sprouts. *J Neurosci*, **19**, 3860-3873.

Gallo, G. and Letourneau, P.C. (2004) Regulation of growth cone actin filaments by guidance cues. *J Neurobiol*, **58**, 92-102.

Garrett, M.D., Self, A.J., van Oers, C. and Hall, A. (1989) Identification of distinct cytoplasmic targets for ras/R-ras and rho regulatory proteins. *J Biol Chem*, **264**, 10-13.

Garvalov, B.K., Flynn, K.C., Neukirchen, D., Meyn, L., Teusch, N., Wu, X., Brakebusch, C., Bamburg, J.R. and Bradke, F. (2007) Cdc42 regulates cofilin during the establishment of neuronal polarity. *J Neurosci*, **27**, 13117-13129.

Gauthier-Rouviere, C., Vignal, E., Meriane, M., Roux, P., Montcourier, P. and Fort, P. (1998) RhoG GTPase controls a pathway that independently activates Rac1 and Cdc42Hs. *Mol Biol Cell*, **9**, 1379-1394.

Guthrie, S. (1996) Patterning the hindbrain. *Curr Opin Neurobiol*, **6**, 41-48.

Haataja, L., Groffen, J. and Heisterkamp, N. (1997) Characterization of RAC3, a novel member of the Rho family. *J Biol Chem*, **272**, 20384-20388.

Hajdo-Milasinovic, A., Ellenbroek, S.I., van Es, S., van der Vaart, B. and Collard, J.G. (2007) Rac1 and Rac3 have opposing functions in cell adhesion and differentiation of neuronal cells. *J Cell Sci*, **120**, 555-566.

Hakeda-Suzuki, S., Ng, J., Tzu, J., Dietzl, G., Sun, Y., Harms, M., Nardine, T., Luo, L. and Dickson, B.J. (2002) Rac function and regulation during Drosophila development. *Nature*, **416**, 438-442.

Hall, A. (1998) Rho GTPases and the actin cytoskeleton. *Science*, **279**, 509-514.

Hariharan, I.K., Hu, K.Q., Asha, H., Quintanilla, A., Ezzell, R.M. and Settleman, J. (1995) Characterization of rho GTPase family homologues in Drosophila melanogaster: overexpressing Rho1 in retinal cells causes a late developmental defect. *Embo J*, **14**, 292-302.

Hart, M.J., Eva, A., Evans, T., Aaronson, S.A. and Cerione, R.A. (1991) Catalysis of guanine nucleotide exchange on the CDC42Hs protein by the dbl oncogene product. *Nature*, **354**, 311-314.

Hatten, M.E. (1999) Central nervous system neuronal migration. *Annu Rev Neurosci*, **22**, 511-539.

Hayashi, M.L., Choi, S.Y., Rao, B.S., Jung, H.Y., Lee, H.K., Zhang, D., Chattarji, S., Kirkwood, A. and Tonegawa, S. (2004) Altered cortical synaptic morphology and impaired memory consolidation in forebrain- specific dominant-negative PAK transgenic mice. *Neuron*, **42**, 773-787.

Henkemeyer, M., Itkis, O.S., Ngo, M., Hickmott, P.W. and Ethell, I.M. (2003) Multiple EphB receptor tyrosine kinases shape dendritic spines in the hippocampus. *J Cell Biol*, **163**, 1313-1326.

Heo, W.D. and Meyer, T. (2003) Switch-of-function mutants based on morphology classification of Ras superfamily small GTPases. *Cell*, **113**, 315-328.

Hirokawa, N. (1998) Kinesin and dynein superfamily proteins and the mechanism of organelle transport. *Science*, **279**, 519-526.

Hirokawa, N. and Takemura, R. (2005) Molecular motors and mechanisms of directional transport in neurons. *Nat Rev Neurosci*, **6**, 201-214.

Hirose, M., Ishizaki, T., Watanabe, N., Uehata, M., Kranenburg, O., Moolenaar, W.H., Matsumura, F., Maekawa, M., Bito, H. and Narumiya, S. (1998) Molecular dissection of the Rho-associated protein kinase (p160ROCK)-regulated neurite remodeling in neuroblastoma N1E-115 cells. *J Cell Biol*, **141**, 1625-1636.

Hu, H., Marton, T.F. and Goodman, C.S. (2001) Plexin B mediates axon guidance in Drosophila by simultaneously inhibiting active Rac and enhancing RhoA signaling. *Neuron*, **32**, 39-51.

Huang, T.Y., DerMardirossian, C. and Bokoch, G.M. (2006) Cofilin phosphatases and regulation of actin dynamics. *Curr Opin Cell Biol*, **18**, 26-31.

Innocenti, M., Zucconi, A., Disanza, A., Frittoli, E., Areces, L.B., Steffen, A., Stradal, T.E., Di Fiore, P.P., Carlier, M.F. and Scita, G. (2004) Abi1 is essential for the formation and activation of a WAVE2 signalling complex. *Nat Cell Biol*, **6**, 319-327.

Jaffe, A.B. and Hall, A. (2005) Rho GTPases: biochemistry and biology. *Annu Rev Cell Dev Biol*, **21**, 247-269.

Jiang, S.Y. and Ramachandran, S. (2006) Comparative and evolutionary analysis of genes encoding small GTPases and their activating proteins in eukaryotic genomes. *Physiol Genomics*, **24**, 235-251.

Jourdain, P., Fukunaga, K. and Muller, D. (2003) Calcium/calmodulin-dependent protein kinase II contributes to activity-dependent filopodia growth and spine formation. *J Neurosci*, **23**, 10645-10649.

Joyce, P.L. and Cox, A.D. (2003) Rac1 and Rac3 are targets for geranylgeranyltransferase I inhibitor-mediated inhibition of signaling, transformation, and membrane ruffling. *Cancer Res*, **63**, 7959-7967.

Joyner, A.L. (1996) Engrailed, Wnt and Pax genes regulate midbrain--hindbrain development. *Trends Genet*, **12**, 15-20.

Kaufmann, N., Wills, Z.P. and Van Vactor, D. (1998) Drosophila Rac1 controls motor axon guidance. *Development*, **125**, 453-461.

Kim, A.S., Kakalis, L.T., Abdul-Manan, N., Liu, G.A. and Rosen, M.K. (2000) Autoinhibition and activation mechanisms of the Wiskott-Aldrich syndrome protein. *Nature*, **404**, 151-158.

Kim, S., Ko, J., Shin, H., Lee, J.R., Lim, C., Han, J.H., Altrock, W.D., Garner, C.C., Gundelfinger, E.D., Premont, R.T., Kaang, B.K. and Kim, E. (2003) The GIT family of proteins forms multimers and associates with the presynaptic cytomatrix protein Piccolo. *J Biol Chem*, **278**, 6291-6300.

Kim, Y., Sung, J.Y., Ceglia, I., Lee, K.W., Ahn, J.H., Halford, J.M., Kim, A.M., Kwak, S.P., Park, J.B., Ho Ryu, S., Schenck, A., Bardoni, B., Scott, J.D., Nairn, A.C. and

Greengard, P. (2006) Phosphorylation of WAVE1 regulates actin polymerization and dendritic spine morphology. *Nature*, **442**, 814-817.

Kinsella, B.T., Erdman, R.A. and Maltese, W.A. (1991) Carboxyl-terminal isoprenylation of ras-related GTP-binding proteins encoded by rac1, rac2, and ralA. *J Biol Chem*, **266**, 9786-9794.

Kovar, D.R., Harris, E.S., Mahaffy, R., Higgs, H.N. and Pollard, T.D. (2006) Control of the assembly of ATP- and ADP-actin by formins and profilin. *Cell*, **124**, 423-435.

Kozma, R., Ahmed, S., Best, A. and Lim, L. (1995) The Ras-related protein Cdc42Hs and bradykinin promote formation of peripheral actin microspikes and filopodia in Swiss 3T3 fibroblasts. *Mol Cell Biol*, **15**, 1942-1952.

Kozma, R., Sarner, S., Ahmed, S. and Lim, L. (1997) Rho family GTPases and neuronal growth cone remodelling: relationship between increased complexity induced by Cdc42Hs, Rac1, and acetylcholine and collapse induced by RhoA and lysophosphatidic acid. *Mol Cell Biol*, **17**, 1201-1211.

Kumanogoh, H., Miyata, S., Sokawa, Y. and Maekawa, S. (2001) Biochemical and morphological analysis on the localization of Rac1 in neurons. *Neurosci Res*, **39**, 189-196.

Kunda, P., Paglini, G., Quiroga, S., Kosik, K. and Caceres, A. (2001) Evidence for the involvement of Tiam1 in axon formation. *J Neurosci*, **21**, 2361-2372.

Kurokawa, K. and Matsuda, M. (2005) Localized RhoA activation as a requirement for the induction of membrane ruffling. *Mol Biol Cell*, **16**, 4294-4303.

Lee, A., Li, W., Xu, K., Bogert, B.A., Su, K. and Gao, F.B. (2003) Control of dendritic development by the Drosophila fragile X-related gene involves the small GTPase Rac1. *Development*, **130**, 5543-5552.

Lee, K.J. and Jessell, T.M. (1999) The specification of dorsal cell fates in the vertebrate central nervous system. *Annu Rev Neurosci*, **22**, 261-294.

Lee, T., Winter, C., Marticke, S.S., Lee, A. and Luo, L. (2000) Essential roles of Drosophila RhoA in the regulation of neuroblast proliferation and dendritic but not axonal morphogenesis. *Neuron*, **25**, 307-316.

Leeuwen, F.N., Kain, H.E., Kammen, R.A., Michiels, F., Kranenburg, O.W. and Collard, J.G. (1997) The guanine nucleotide exchange factor Tiam1 affects neuronal morphology; opposing roles for the small GTPases Rac and Rho. *J Cell Biol*, **139**, 797-807.

Lehrach, H., Diamond, D., Wozney, J.M. and Boedtker, H. (1977) RNA molecular weight determinations by gel electrophoresis under denaturing conditions, a critical reexamination. *Biochemistry*, **16**, 4743-4751.

Li, Z., Aizenman, C.D. and Cline, H.T. (2002) Regulation of rho GTPases by crosstalk and neuronal activity in vivo. *Neuron*, **33**, 741-750.

Li, Z., Van Aelst, L. and Cline, H.T. (2000) Rho GTPases regulate distinct aspects of dendritic arbor growth in Xenopus central neurons in vivo. *Nat Neurosci*, **3**, 217-225.

Liu, Y., Fujise, N. and Kosaka, T. (1996) Distribution of calretinin immunoreactivity in the mouse dentate gyrus. I. General description. *Exp Brain Res*, **108**, 389-403.

Lundquist, E.A., Reddien, P.W., Hartwieg, E., Horvitz, H.R. and Bargmann, C.I. (2001) Three C. elegans Rac proteins and several alternative Rac regulators control axon guidance, cell migration and apoptotic cell phagocytosis. *Development*, **128**, 4475-4488.

Luo, L. (2002) Actin cytoskeleton regulation in neuronal morphogenesis and structural plasticity. *Annu Rev Cell Dev Biol*, **18**, 601-635.

Luo, L., Hensch, T.K., Ackerman, L., Barbel, S., Jan, L.Y. and Jan, Y.N. (1996) Differential effects of the Rac GTPase on Purkinje cell axons and dendritic trunks and spines. *Nature*, **379**, 837-840.

Luo, L., Liao, Y.J., Jan, L.Y. and Jan, Y.N. (1994) Distinct morphogenetic functions of similar small GTPases: Drosophila Drac1 is involved in axonal outgrowth and myoblast fusion. *Genes Dev*, **8**, 1787-1802.

Maekawa, M., Ishizaki, T., Boku, S., Watanabe, N., Fujita, A., Iwamatsu, A., Obinata, T., Ohashi, K., Mizuno, K. and Narumiya, S. (1999) Signaling from Rho to the actin cytoskeleton through protein kinases ROCK and LIM-kinase. *Science*, **285**, 895-898.

Malliri, A. and Collard, J.G. (2003) Role of Rho-family proteins in cell adhesion and cancer. *Curr Opin Cell Biol*, **15**, 583-589.

Malosio, M.L., Gilardelli, D., Paris, S., Albertinazzi, C. and de Curtis, I. (1997) Differential expression of distinct members of Rho family GTP-binding proteins during neuronal development: identification of Rac1B, a new neural-specific member of the family. *J Neurosci*, **17**, 6717-6728.

Manser, E., Huang, H.Y., Loo, T.H., Chen, X.Q., Dong, J.M., Leung, T. and Lim, L. (1997) Expression of constitutively active alpha-PAK reveals effects of the kinase on actin and focal complexes. *Mol Cell Biol*, **17**, 1129-1143.

Marston, D.J., Dickinson, S. and Nobes, C.D. (2003) Rac-dependent trans-endocytosis of ephrinBs regulates Eph-ephrin contact repulsion. *Nat Cell Biol*, **5**, 879-888.

Martin, S.J., Grimwood, P.D. and Morris, R.G. (2000) Synaptic plasticity and memory: an evaluation of the hypothesis. *Annu Rev Neurosci*, **23**, 649-711.

Matsuzaki, M., Honkura, N., Ellis-Davies, G.C. and Kasai, H. (2004) Structural basis of long-term potentiation in single dendritic spines. *Nature*, **429**, 761-766.

Matus, A. (2000) Actin-based plasticity in dendritic spines. *Science*, **290**, 754-758.

Matus, A. (2005) Growth of dendritic spines: a continuing story. *Curr Opin Neurobiol*, **15**, 67-72.

Meng, Y., Zhang, Y., Tregoubov, V., Janus, C., Cruz, L., Jackson, M., Lu, W.Y., MacDonald, J.F., Wang, J.Y., Falls, D.L. and Jia, Z. (2002) Abnormal spine morphology and enhanced LTP in LIMK-1 knockout mice. *Neuron*, **35**, 121-133.

Miki, H., Miura, K. and Takenawa, T. (1996) N-WASP, a novel actin-depolymerizing protein, regulates the cortical cytoskeletal rearrangement in a PIP2-dependent manner downstream of tyrosine kinases. *Embo J*, **15**, 5326-5335.

Miki, H., Sasaki, T., Takai, Y. and Takenawa, T. (1998a) Induction of filopodium formation by a WASP-related actin-depolymerizing protein N-WASP. *Nature*, **391**, 93-96.

Miki, H., Suetsugu, S. and Takenawa, T. (1998b) WAVE, a novel WASP-family protein involved in actin reorganization induced by Rac. *Embo J*, **17**, 6932-6941.

Miki, H. and Takenawa, T. (2002) WAVE2 serves a functional partner of IRSp53 by regulating its interaction with Rac. *Biochem Biophys Res Commun*, **293**, 93-99.

Miki, H., Yamaguchi, H., Suetsugu, S. and Takenawa, T. (2000) IRSp53 is an essential intermediate between Rac and WAVE in the regulation of membrane ruffling. *Nature*, **408**, 732-735.

Moll, J., Sansig, G., Fattori, E. and van der Putten, H. (1991) The murine rac1 gene: cDNA cloning, tissue distribution and regulated expression of rac1 mRNA by disassembly of actin microfilaments. *Oncogene*, **6**, 863-866.

Morris, R.G., Anderson, E., Lynch, G.S. and Baudry, M. (1986) Selective impairment of learning and blockade of long-term potentiation by an N-methyl-D-aspartate receptor antagonist, AP5. *Nature*, **319**, 774-776.

Nadarajah, B., Alifragis, P., Wong, R.O. and Parnavelas, J.G. (2002) Ventricle-directed migration in the developing cerebral cortex. *Nat Neurosci*, **5**, 218-224.

Nadarajah, B., Alifragis, P., Wong, R.O. and Parnavelas, J.G. (2003) Neuronal migration in the developing cerebral cortex: observations based on real-time imaging. *Cereb Cortex*, **13**, 607-611.

Nadarajah, B. and Parnavelas, J.G. (2002) Modes of neuronal migration in the developing cerebral cortex. *Nat Rev Neurosci*, **3**, 423-432.

Nakayama, A.Y., Harms, M.B. and Luo, L. (2000) Small GTPases Rac and Rho in the maintenance of dendritic spines and branches in hippocampal pyramidal neurons. *J Neurosci*, **20**, 5329-5338.

Neves, G., Cooke, S.F. and Bliss, T.V. (2008) Synaptic plasticity, memory and the hippocampus: a neural network approach to causality. *Nat Rev Neurosci*, **9**, 65-75.

Ng, J., Nardine, T., Harms, M., Tzu, J., Goldstein, A., Sun, Y., Dietzl, G., Dickson, B.J. and Luo, L. (2002) Rac GTPases control axon growth, guidance and branching. *Nature*, **416**, 442-447.

Nikolic, M., Chou, M.M., Lu, W., Mayer, B.J. and Tsai, L.H. (1998) The p35/Cdk5 kinase is a neuron-specific Rac effector that inhibits Pak1 activity. *Nature*, **395**, 194-198.

Nobes, C.D. and Hall, A. (1995) Rho, rac, and cdc42 GTPases regulate the assembly of multimolecular focal complexes associated with actin stress fibers, lamellipodia, and filopodia. *Cell*, **81**, 53-62.

Nobes, C.D. and Hall, A. (1999) Rho GTPases control polarity, protrusion, and adhesion during cell movement. *J Cell Biol*, **144**, 1235-1244.

O'Brien, S.P., Seipel, K., Medley, Q.G., Bronson, R., Segal, R. and Streuli, M. (2000) Skeletal muscle deformity and neuronal disorder in Trio exchange factor-deficient mouse embryos. *Proc Natl Acad Sci U S A*, **97**, 12074-12078.

O'Kane, E.M., Stone, T.W. and Morris, B.J. (2003) Distribution of Rho family GTPases in the adult rat hippocampus and cerebellum. *Brain Res Mol Brain Res*, **114**, 1-8.

Okamoto, K., Nagai, T., Miyawaki, A. and Hayashi, Y. (2004) Rapid and persistent modulation of actin dynamics regulates postsynaptic reorganization underlying bidirectional plasticity. *Nat Neurosci*, **7**, 1104-1112.

Palmiter, R.D., Cole, T.B., Quaife, C.J. and Findley, S.D. (1996) ZnT-3, a putative transporter of zinc into synaptic vesicles. *Proc Natl Acad Sci U S A*, **93**, 14934-14939.

Pellegrin, S. and Mellor, H. (2007) Actin stress fibres. *J Cell Sci*, **120**, 3491-3499.

Penzes, P., Beeser, A., Chernoff, J., Schiller, M.R., Eipper, B.A., Mains, R.E. and Huganir, R.L. (2003) Rapid induction of dendritic spine morphogenesis by trans-synaptic ephrinB-EphB receptor activation of the Rho-GEF kalirin. *Neuron*, **37**, 263-274.

Penzes, P., Johnson, R.C., Alam, M.R., Kambampati, V., Mains, R.E. and Eipper, B.A. (2000) An isoform of kalirin, a brain-specific GDP/GTP exchange factor, is enriched in the postsynaptic density fraction. *J Biol Chem*, **275**, 6395-6403.

Penzes, P., Johnson, R.C., Sattler, R., Zhang, X., Huganir, R.L., Kambampati, V., Mains, R.E. and Eipper, B.A. (2001) The neuronal Rho-GEF Kalirin-7 interacts with PDZ domain-containing proteins and regulates dendritic morphogenesis. *Neuron*, **29**, 229-242.

Pertz, O., Hodgson, L., Klemke, R.L. and Hahn, K.M. (2006) Spatiotemporal dynamics of RhoA activity in migrating cells. *Nature*, **440**, 1069-1072.

Philips, A., Blein, M., Robert, A., Chambon, J.P., Baghdiguian, S., Weill, M. and Fort, P. (2003) Ascidians as a vertebrate-like model organism for physiological studies of Rho GTPase signaling. *Biol Cell*, **95**, 295-302.

Pollard, T.D. and Borisy, G.G. (2003) Cellular motility driven by assembly and disassembly of actin filaments. *Cell*, **112**, 453-465.

Purpura, D.P. (1974) Dendritic spine "dysgenesis" and mental retardation. *Science*, **186**, 1126-1128.

Raftopoulou, M. and Hall, A. (2004) Cell migration: Rho GTPases lead the way. *Dev Biol*, **265**, 23-32.

Ramakers, G.J. (2002) Rho proteins, mental retardation and the cellular basis of cognition. *Trends Neurosci*, **25**, 191-199.

Rashid, T., Banerjee, M. and Nikolic, M. (2001) Phosphorylation of Pak1 by the p35/Cdk5 kinase affects neuronal morphology. *J Biol Chem*, **276**, 49043-49052.

Ratzliff, A.H., Santhakumar, V., Howard, A. and Soltesz, I. (2002) Mossy cells in epilepsy: rigor mortis or vigor mortis? *Trends Neurosci*, **25**, 140-144.

Ribak, C.E., Seress, L. and Amaral, D.G. (1985) The development, ultrastructure and synaptic connections of the mossy cells of the dentate gyrus. *J Neurocytol*, **14**, 835-857.

Rico, B., Beggs, H.E., Schahin-Reed, D., Kimes, N., Schmidt, A. and Reichardt, L.F. (2004) Control of axonal branching and synapse formation by focal adhesion kinase. *Nat Neurosci*, **7**, 1059-1069.

Ridley, A.J. (2006) Rho GTPases and actin dynamics in membrane protrusions and vesicle trafficking. *Trends Cell Biol*, **16**, 522-529.

Ridley, A.J. and Hall, A. (1992) The small GTP-binding protein rho regulates the assembly of focal adhesions and actin stress fibers in response to growth factors. *Cell*, **70**, 389-399.

Ridley, A.J., Paterson, H.F., Johnston, C.L., Diekmann, D. and Hall, A. (1992) The small GTP-binding protein rac regulates growth factor-induced membrane ruffling. *Cell*, **70**, 401-410.

Riento, K. and Ridley, A.J. (2003) Rocks: multifunctional kinases in cell behaviour. *Nat Rev Mol Cell Biol*, **4**, 446-456.

Roberts, A.W., Kim, C., Zhen, L., Lowe, J.B., Kapur, R., Petryniak, B., Spaetti, A., Pollock, J.D., Borneo, J.B., Bradford, G.B., Atkinson, S.J., Dinauer, M.C. and Williams, D.A. (1999) Deficiency of the hematopoietic cell-specific Rho family GTPase Rac2 is characterized by abnormalities in neutrophil function and host defense. *Immunity*, **10**, 183-196.

Rossman, K.L., Der, C.J. and Sondek, J. (2005) GEF means go: turning on RHO GTPases with guanine nucleotide-exchange factors. *Nat Rev Mol Cell Biol*, **6**, 167-180.

Rossman, K.L., Worthylake, D.K., Snyder, J.T., Siderovski, D.P., Campbell, S.L. and Sondek, J. (2002) A crystallographic view of interactions between Dbs and Cdc42: PH domain-assisted guanine nucleotide exchange. *Embo J*, **21**, 1315-1326.

Rubenstein, J.L. and Beachy, P.A. (1998) Patterning of the embryonic forebrain. *Curr Opin Neurobiol*, **8**, 18-26.

Ruchhoeft, M.L., Ohnuma, S., McNeill, L., Holt, C.E. and Harris, W.A. (1999) The neuronal architecture of Xenopus retinal ganglion cells is sculpted by rho-family GTPases in vivo. *J Neurosci*, **19**, 8454-8463.

Sahai, E. and Marshall, C.J. (2002) RHO-GTPases and cancer. *Nat Rev Cancer*, **2**, 133-142.

Sananbenesi, F., Fischer, A., Wang, X., Schrick, C., Neve, R., Radulovic, J. and Tsai, L.H. (2007) A hippocampal Cdk5 pathway regulates extinction of contextual fear. *Nat Neurosci*, **10**, 1012-1019.

Sander, E.E., van Delft, S., ten Klooster, J.P., Reid, T., van der Kammen, R.A., Michiels, F. and Collard, J.G. (1998) Matrix-dependent Tiam1/Rac signaling in epithelial cells promotes either cell-cell adhesion or cell migration and is regulated by phosphatidylinositol 3-kinase. *J Cell Biol*, **143**, 1385-1398.

Schaefer, A.W., Kabir, N. and Forscher, P. (2002) Filopodia and actin arcs guide the assembly and transport of two populations of microtubules with unique dynamic parameters in neuronal growth cones. *J Cell Biol*, **158**, 139-152.

Schlessinger, A.R., Cowan, W.M. and Gottlieb, D.I. (1975) An autoradiographic study of the time of origin and the pattern of granule cell migration in the dentate gyrus of the rat. *J Comp Neurol*, **159**, 149-175.

Schmidt, A. and Hall, A. (2002) Guanine nucleotide exchange factors for Rho GTPases: turning on the switch. *Genes Dev*, **16**, 1587-1609.

Scott, E.K. and Luo, L. (2001) How do dendrites take their shape? *Nat Neurosci*, **4**, 359-365.

Segura, I., Essmann, C.L., Weinges, S. and Acker-Palmer, A. (2007) Grb4 and GIT1 transduce ephrinB reverse signals modulating spine morphogenesis and synapse formation. *Nat Neurosci*, **10**, 301-310.

Shirsat, N.V., Pignolo, R.J., Kreider, B.L. and Rovera, G. (1990) A member of the ras gene superfamily is expressed specifically in T, B and myeloid hemopoietic cells. *Oncogene*, **5**, 769-772.

Sloviter, R.S. (1987) Decreased hippocampal inhibition and a selective loss of interneurons in experimental epilepsy. *Science*, **235**, 73-76.

Smith, C.L. (1994) The initiation of neurite outgrowth by sympathetic neurons grown in vitro does not depend on assembly of microtubules. *J Cell Biol*, **127**, 1407-1418.

Snyder, J.T., Worthylake, D.K., Rossman, K.L., Betts, L., Pruitt, W.M., Siderovski, D.P., Der, C.J. and Sondek, J. (2002) Structural basis for the selective activation of Rho GTPases by Dbl exchange factors. *Nat Struct Biol*, **9**, 468-475.

Soriano, P. (1999) Generalized lacZ expression with the ROSA26 Cre reporter strain. *Nat Genet*, **21**, 70-71.

Sosa, L., Dupraz, S., Laurino, L., Bollati, F., Bisbal, M., Caceres, A., Pfenninger, K.H. and Quiroga, S. (2006) IGF-1 receptor is essential for the establishment of hippocampal neuronal polarity. *Nat Neurosci*, **9**, 993-995.

Steffen, A., Rottner, K., Ehinger, J., Innocenti, M., Scita, G., Wehland, J. and Stradal, T.E. (2004) Sra-1 and Nap1 link Rac to actin assembly driving lamellipodia formation. *Embo J*, **23**, 749-759.

Stradal, T.E., Rottner, K., Disanza, A., Confalonieri, S., Innocenti, M. and Scita, G. (2004) Regulation of actin dynamics by WASP and WAVE family proteins. *Trends Cell Biol*, **14**, 303-311.

Suetsugu, S., Miki, H. and Takenawa, T. (1999) Identification of two human WAVE/SCAR homologues as general actin regulatory molecules which associate with the Arp2/3 complex. *Biochem Biophys Res Commun*, **260**, 296-302.

Sugihara, K., Nakatsuji, N., Nakamura, K., Nakao, K., Hashimoto, R., Otani, H., Sakagami, H., Kondo, H., Nozawa, S., Aiba, A. and Katsuki, M. (1998) Rac1 is required for the formation of three germ layers during gastrulation. *Oncogene*, **17**, 3427-3433.

Sur, M. and Leamey, C.A. (2001) Development and plasticity of cortical areas and networks. *Nat Rev Neurosci*, **2**, 251-262.

Symons, M. and Rusk, N. (2003) Control of vesicular trafficking by Rho GTPases. *Curr Biol*, **13**, R409-418.

Tada, T. and Sheng, M. (2006) Molecular mechanisms of dendritic spine morphogenesis. *Curr Opin Neurobiol*, **16**, 95-101.

Takenawa, T. and Miki, H. (2001) WASP and WAVE family proteins: key molecules for rapid rearrangement of cortical actin filaments and cell movement. *J Cell Sci*, **114**, 1801-1809.

Tan, S.S., Kalloniatis, M., Sturm, K., Tam, P.P., Reese, B.E. and Faulkner-Jones, B. (1998) Separate progenitors for radial and tangential cell dispersion during development of the cerebral neocortex. *Neuron*, **21**, 295-304.

Tanabe, K., Tachibana, T., Yamashita, T., Che, Y.H., Yoneda, Y., Ochi, T., Tohyama, M., Yoshikawa, H. and Kiyama, H. (2000) The small GTP-binding protein TC10 promotes nerve elongation in neuronal cells, and its expression is induced during nerve regeneration in rats. *J Neurosci*, **20**, 4138-4144.

Tashiro, A., Minden, A. and Yuste, R. (2000) Regulation of dendritic spine morphology by the rho family of small GTPases: antagonistic roles of Rac and Rho. *Cereb Cortex*, **10**, 927-938.

Tashiro, A. and Yuste, R. (2004) Regulation of dendritic spine motility and stability by Rac1 and Rho kinase: evidence for two forms of spine motility. *Mol Cell Neurosci*, **26**, 429-440.

Threadgill, R., Bobb, K. and Ghosh, A. (1997) Regulation of dendritic growth and remodeling by Rho, Rac, and Cdc42. *Neuron*, **19**, 625-634.

Tolias, K.F., Bikoff, J.B., Burette, A., Paradis, S., Harrar, D., Tavazoie, S., Weinberg, R.J. and Greenberg, M.E. (2005) The Rac1-GEF Tiam1 couples the NMDA receptor to the activity-dependent development of dendritic arbors and spines. *Neuron*, **45**, 525-538.

Tolias, K.F., Bikoff, J.B., Kane, C.G., Tolias, C.S., Hu, L. and Greenberg, M.E. (2007) The Rac1 guanine nucleotide exchange factor Tiam1 mediates EphB receptor-dependent dendritic spine development. *Proc Natl Acad Sci U S A*, **104**, 7265-7270.

Tomaselli, K.J., Damsky, C.H. and Reichardt, L.F. (1988) Purification and characterization of mammalian integrins expressed by a rat neuronal cell line (PC12): evidence that they function as alpha/beta heterodimeric receptors for laminin and type IV collagen. *J Cell Biol*, **107**, 1241-1252.

Tsien, J.Z., Huerta, P.T. and Tonegawa, S. (1996) The essential role of hippocampal CA1 NMDA receptor-dependent synaptic plasticity in spatial memory. *Cell*, **87**, 1327-1338.

Valtorta, F., Villa, A., Jahn, R., De Camilli, P., Greengard, P. and Ceccarelli, B. (1988) Localization of synapsin I at the frog neuromuscular junction. *Neuroscience*, **24**, 593-603.

Waites, C.L., Craig, A.M. and Garner, C.C. (2005) Mechanisms of vertebrate synaptogenesis. *Annu Rev Neurosci*, **28**, 251-274.

Walmsley, M.J., Ooi, S.K., Reynolds, L.F., Smith, S.H., Ruf, S., Mathiot, A., Vanes, L., Williams, D.A., Cancro, M.P. and Tybulewicz, V.L. (2003) Critical roles for Rac1 and Rac2 GTPases in B cell development and signaling. *Science*, **302**, 459-462.

Wiens, K.M., Lin, H. and Liao, D. (2005) Rac1 induces the clustering of AMPA receptors during spinogenesis. *J Neurosci*, **25**, 10627-10636.

Wong, R.O. and Ghosh, A. (2002) Activity-dependent regulation of dendritic growth and patterning. *Nat Rev Neurosci*, **3**, 803-812.

Worthylake, D.K., Rossman, K.L. and Sondek, J. (2000) Crystal structure of Rac1 in complex with the guanine nucleotide exchange region of Tiam1. *Nature*, **408**, 682-688.

Wu, K.Y., Hengst, U., Cox, L.J., Macosko, E.Z., Jeromin, A., Urquhart, E.R. and Jaffrey, S.R. (2005) Local translation of RhoA regulates growth cone collapse. *Nature*, **436**, 1020-1024.

Wu, Y.C., Cheng, T.W., Lee, M.C. and Weng, N.Y. (2002) Distinct rac activation pathways control Caenorhabditis elegans cell migration and axon outgrowth. *Dev Biol*, **250**, 145-155.

Xie, Y., Tan, E.J., Wee, S., Manser, E., Lim, L. and Koh, C.G. (2008) Functional interactions between phosphatase POPX2 and mDia modulate RhoA pathways. *J Cell Sci*, **121**, 514-521.

Yang, N., Higuchi, O., Ohashi, K., Nagata, K., Wada, A., Kangawa, K., Nishida, E. and Mizuno, K. (1998) Cofilin phosphorylation by LIM-kinase 1 and its role in Rac-mediated actin reorganization. *Nature*, **393**, 809-812.

Za, L., Albertinazzi, C., Paris, S., Gagliani, M., Tacchetti, C. and de Curtis, I. (2006) betaPIX controls cell motility and neurite extension by regulating the distribution of GIT1. *J Cell Sci*, **119**, 2654-2666.

Zhang, H. and Macara, I.G. (2006) The polarity protein PAR-3 and TIAM1 cooperate in dendritic spine morphogenesis. *Nat Cell Biol*, **8**, 227-237.

Zhang, H., Webb, D.J., Asmussen, H. and Horwitz, A.F. (2003) Synapse formation is regulated by the signaling adaptor GIT1. *J Cell Biol*, **161**, 131-142.

Zhang, H., Webb, D.J., Asmussen, H., Niu, S. and Horwitz, A.F. (2005) A GIT1/PIX/Rac/PAK signaling module regulates spine morphogenesis and synapse formation through MLC. *J Neurosci*, **25**, 3379-3388.

Zhang, L.I. and Poo, M.M. (2001) Electrical activity and development of neural circuits. *Nat Neurosci*, **4 Suppl**, 1207-1214.

Zhang, W. and Benson, D.L. (2001) Stages of synapse development defined by dependence on F-actin. *J Neurosci*, **21**, 5169-5181.

Zhou, F.Q., Waterman-Storer, C.M. and Cohan, C.S. (2002) Focal loss of actin bundles causes microtubule redistribution and growth cone turning. *J Cell Biol*, **157**, 839-849.

Zhu, Y., Romero, M.I., Ghosh, P., Ye, Z., Charnay, P., Rushing, E.J., Marth, J.D. and Parada, L.F. (2001) Ablation of NF1 function in neurons induces abnormal development of cerebral cortex and reactive gliosis in the brain. *Genes Dev*, **15**, 859-876.

Zipkin, I.D., Kindt, R.M. and Kenyon, C.J. (1997) Role of a new Rho family member in cell migration and axon guidance in C. elegans. *Cell*, **90**, 883-894.

ACKNOWLEDGEMENTS

There are lots of people I want to thank for helping me and encouraging me during my time spent in Milan. I don't want to forget anyone!

My first, my absolutely first thought is to you Chris. This would have never been happened without you! Thank you for supporting me day by day, for being super-positive all the time, even though we both know that sometimes it's difficult… thank you so much for having taught me to say "no" whenever it's necessary… thank you for always listening to, and breathing my feelings at the end of each day… thank you for sharing your science with my science… and of course thank you for the antibodies ☺! Thank you for your English and for your Italian… thank you for having waited for my PhD… but most of all thank you for being just as you are! With you everything is easier! Jeg elsker dig til mine dages ende!

Un grazie davvero speciale alla mia famiglia, ai miei genitori che mi hanno sempre amata e che sempre mi ameranno in qualsiasi parte del mondo! Grazie per tutto il supporto che mi date ogni giorno e per aver accettato con serenità e amore la mia scelta! A Laura, per esserci sempre nel momento del bisogno, alle mie due carissime nonne per essere sempre state l'esempio dell'ottimismo. GRAZIE!

I really want to thank my Danish family, thank you all for having opened your arms to me and to have embraced me as a new member of the family.

And my thanks to the Dibit scientists…

I would like to thank my boss Ivan de Curtis for giving me the possibility to work in his lab, for his scientific advice and suggestions. Thank you for letting me becoming an independent researcher.

Thanks to my PhD tutor, Stefano Biffo, for always having listened to me, discussed and given me good suggestions for my future, both during the official meetings and the 925 bus trips!

A big thanks goes to my external supervisor, Vania Braga! Thank you so much for all your help during these 3 years! For being always positive, for being always interested in my project, for helping me also regarding the English scientific community.

And now the hugest thanks go to my lab mates for not only being "fantastic lab mates" but also friends! Un grazie immenso a te "Scorbi" per aver condiviso il bancone e il mio disordine, per ogni tuo piccolo aiuto in stabulario e non solo... per avermi sempre aspettato per pranzo... per le tue correzioni... ma soprattutto per aver lavorato fianco a fianco con me in questo progetto! GRAZIE!

Un grazie molto particolare a Lorena, una grande amica! Grazie per avermi accettata come "flat mate" nonostante fossi già una tua "lab mate"!! Grazie per essere sempre stata stra-disponibile in lab e fuori... per avermi insegnato i trucchi delle IF e del microscopio... per avermi "trasportato" tante volte da Lambrate sulla tua bici!!! Grazie per tutti i nostri momenti insieme!

Un grazie enorme all'altra metà del "lab IdC", Clà e Antò! Grazie per i "soliti" discorsi... per le nostre discussioni scientifiche e tutti i consigli, grazie per esservi sorbiti i miei mattoni!! Grazie per aver voluto usare i neuroni hipp!!!!! Grazie per essere stati fantastici compagni di meeting!

Grazie a Marta per il tuo indispensabile aiuto in stabulario e non....

Un grazie speciale a Simo, il riferimento del lab! Grazie per aver sopportato il mio disordine fin dal primo giorno, e per avermi "leggermente" migliorata! Grazie per avermi insegnato i tuoi trucchi del mestiere per ottenere "gels pennellati"! Grazie per le tue mitiche birre!

Un grazie, anzi due, anzi tre a Gabri Ciceri, il miglior studente! Davvero Gabri, grazie per tutto il tuo entusiasmo, per la tua voglia di fare ricerca, per aver messo corpo e anima in questo progetto, per avere "quasi" concluso i tuoi esami... per il tuo GRANDE aiuto negli esperimenti... per esserti fermato fino alle 11 di venerdì sera con me per caricare i sinaptosomi!!!!!

Grazie a tutti gli "ex" e le "ex" del lab IdC con cui ho trascorso e condiviso davvero bei momenti, Anto, Oronzina, Marzia, Andrea, Laura, Lorena D, Chiara grazie!

Grazie di cuore a Chiara Albertinazzi per aver dedicato tanto tempo ai miei neuroni e per avermi insegnato le tecniche della dissezione..

Grazie alle numerose "new entries" del lab IdC per avermi sopportata in quest'ultimo periodo nel lab, nonostante il mio super-stress!!

Grazie a Cesare, "the master of the microscopes" per l'aiuto nei miei momenti "bui" nelle stanze dell'Alembic.. Grazie per aver esposto la magnifica copertina di Biology of the Cell, August 2007 ☺!

Thanks to all my dear friends I met in these years between Dibit and Ifom....for the wonderful time spent together in Milan, at the seaside and on the mountains, skiing and tracking!! I really loved all these moments! Thank you so much!